Dear Dr. Yool,

Thank you very much for considering our manuscript. We also sincerely thank the three reviewers for their substantial efforts and insightful comments that have helped us improve the manuscript. We have revised the manuscript and modified the model according to the comments. The major revisions we have made include:

1. We have improved the iron cycle by adding a tracer for detrital iron, updated the atmospheric iron deposition data from Luo et al. (2008), and optimized iron-related parameters to the outputs of dissolved iron from Aumont et al. (2003). Accordingly, we also modified the bottom boundary conditions for DIN and dissolved iron (the bottom boundary for dissolved iron cannot be closed since the deposition from the atmosphere continuously adds to the total inventory of iron).
2. We have modified the approach of transporting size variance in diffusion following the work of Bruggeman (2009).
3. As two reviewers suggested, we have added a mesozooplankton compartment and size-selective feeding for two zooplankton compartments.
4. We have modified the codes for parallel computing of the DRAM algorithm to increase its efficiency for optimizing parameter sets.
5. As one reviewer requested, we have expanded the introduction and explanation of the DRAM algorithm to make it easier to follow.

Below are our point-by-point responses to the reviewers' comments.

#=========================================================

Reviewer #1

This paper describes a trait-based continuum plankton model, with size as the principle trait, and successfully uses a parameter optimisation routine to extract the trait characteristics (mean size and variance) at two contrasting study sites.

Major comments. ==========

1. The lack of a size-dependent feeding preference is the single biggest limit to this model. Ideally any plankton web will have a size-range (or a size-trait continuum) for both phytoplankton and zooplankton, as size is such a structuring component of the plankton

across a broad range of sizes and trophic level. Positively, by excluding size-ranges in grazing the model presented does allow a simpler exploration of characteristics of phytoplankton size structuring.

[Response] We agree that adding a size-dependent feeding preference might be useful for investigating the grazing effects on phytoplankton size structure. Accordingly, we have added size-dependent feeding and another zooplankton compartment into the model as also suggested by another reviewer. Please see Section **2.3 Zooplankton size-dependent grazing**.

2. Eq. 7b is missing the detrital remineralisation term, possibly where the two minus signs are.

[Response] Yes, it was a typo in the previous version. We have corrected the equation in the current version (Eq. 3).

3. P15, last paragraph. The use of trait derivatives sounds important, but it was introduced too quickly for me. Could you give a little bit further explanation?

[Response] Here we have modified the text to avoid too much interpretation in the Results section 3.4:

"The values of $\frac{d^2\mu(l)}{dl^2}$ were always negative in all times at both stations, suggesting that without "trait diffusion", size variance would decrease toward zero (Eq. 7c). This highlights the importance of trait diffusion (which can be interpreted as genetic mutation or transgenerational phenotypic plasticity) to sustain diversity."

We added some text in the Discussion section 4.1.1 to explain in more detail on the derivatives:

"In particular, the second derivative of the growth rate at mean size, $\frac{d^2\mu(l)}{dl^2}$, can be conveniently perceived as a proxy for the intensity of resource competition (The more concave is the curve of $\mu(l)$, the more intense is the competition, i.e., the fitness of suboptimal species decreases more steeply with distance from the optimal size).”

4. The first sentence is a turn-off.

[Response] Sorry, we do not understand what exact sentence the reviewer meant.

5. Section 4.2.2. Transport of moments (instead of species) is the biggest issue of this type of trait-based approach. Or is it? This section quantifies through one example for a Gaussian distribution the size of the error. But the particular example chosen seems destined to show a small error, as one community is much smaller than the other. It would be better to show the example with the greatest possible error. Would that be a Gaussian with equal biomass but very different mean size?

[Response] The transport of moments is indeed an issue that bothered us. Fortunately, Jorn Brugemann in his thesis (Brugemann, 2009) has pointed out that the raw moments of the biomass distribution can behave as normal tracers in diffusion and advection. We have followed Jorn’s suggestion to modify the transport of variance in our model (*see* **Sect. 2.1 General description of the 1D ecosystem model**). We have followed the reviewer’s suggestion to test this approach in Fig. 14. It seems clear that when the differences between the two mean sizes or variances are large enough, the mixed community would not follow a Gaussian distribution. But when the two communities differ only moderately in mean size or variance, the approximate should be reasonable.

Minor comments. ===========

P3, L2. Distinguishing between identity and diversity in the first sentence is confusing.

[Response] The “identity” is a term that theoretical ecologists often use (e.g. Tilman et al. PNAS 1997). It means the (dominant) functional traits themselves in contrast to the number of species present. We have added an annotation beside.

P3, L22. I think you mean in practice impossible, rather than almost impossible.

[Response] Yes, we have modified the wording to "which is however impossible in practice due to computational limits".

P4, L15 If trait number = N, trait resolution = D, then difference = N(D-2)-1. The derivative of the difference with trait resolution is N (independent of D). So it is not exponential, it is linear, with a slope N.

[Response] Yes, we have replaced the word "exponential" with "linear".

P6. L16 Do you mean Eq. (4a)?; bimodal?
[Response] Yes. Sorry, it was a typo. We have corrected it to Eq. (10a). It should be unimodal because phytoplankton maximal growth rate usually peaks at nano size range.

P8. Z = depth. [water depth sounds like the bottom depth?]
[Response] Z is the depth of the model grid. We have made it clearer in the revision.

P11, L8 "and both model" – sentence has gone astray?
[Response] Sorry, it was a typo. We have deleted it.

P14, L10 "Large phytoplankton are susceptible to light limitation" I thought it was nutrients?
[Response] Here we meant that because large phytoplankton are susceptible to light limitation, the effect of light limitation offsets the effect of replete nutrients on phytoplankton size at depth, which can explain why the proportion of size-fractionated Chl does not change with depth as predicted based on nutrient effects alone. However, based on the revised modeled results, we have deleted this sentence during revision.

Table 1. Unit of Kchl should be m-2 as written inside the -1 bracket.
[Response] Sorry, it was a typo. We have corrected it.

#===============================================================

Reviewer #2

This is a very nice, well-written paper that describes a continuous trait model and its application to data from two stations. Continuous trait models have some nice advantages over the traditional discrete methods that are typically used, as the authors describe nicely, and this model may provide an interesting and insightful counterpoint to standard methods when applied to 3D models, as the authors state they plan to in the future. I recommend acceptance after minor revisions.

[Response] Thank you for your positive comments on this manuscript!

I have one major criticism of the paper, which could be resolved easily enough in the Discussion section. The criticism is that the model may be sensitive to the lognormal distribution assumed by the authors. The model relies on describing the distribution of traits by the log-mean and the log-variance of volume. Making size the master trait is standard, and discussed by the authors, but they do not even mention the word ‘lognormal’ until page 18. This first of all leads the reader to assume that the authors are using a Gaussian distribution for volume, which would be disastrous, unless one reads carefully that they are considering the log-volume, which cannot be expected of every reader. Readers are likely to get confused without clarifying this earlier) The authors also cite a few papers (the oldest of which is from 2007; what did people think the size distribution of plankton was before 2007?), along with the standard use of Gaussian distributions in continuous-trait models, to justify their use of a lognormal. Arguably, a power-law distribution (sometimes referred to as a Junge distribution in this context) is much more commonly assumed in these situations, yet power laws are not discussed by the authors anywhere in the paper. Additionally, power-law distributions are often not well-described by their lower-order moments, which may in fact be divergent, and are instead better described by their lower cutoff and exponent. The authors do state that the use of a lognormal is a key assumption in their model, but they should also state that they are using a lognormal from the beginning, not just at the end, and they should also state that other size distributions are often used to model phytoplankton, and discuss how e.g. the model might look different if one were using a power-law distribution, and what this means for the authors’ results. Don’t get me wrong; if I had written this paper, I certainly would have started with a lognormal, because this is an easy, defensible place to start. It just merits further discussion that this is perhaps not the size distribution most people think of phytoplankton following, and that this may have (possibly large) implications for the results and how the model is set up.

[Response] The reviewer is entirely correct that phytoplankton size distribution is more commonly assumed to follow a power-law distribution (Sheldon et al. 1972; Gin et al. 1999; Cermeño et al. 2006). The slope of log abundance versus log size (e.g. biovolume) tends to be between –0.7 and –1 (Cermeño et al. 2006), suggesting that the slope of log biomass versus log size should be between 0 and 0.3. However, aside from fact that the power-law distribution is unrealistic in predicting phytoplankton biomass at the limit of either the largest or the smallest size, it is much more inconvenient in terms of mathematical manipulation (e.g. calculating mean and variance) compared to the normal distribution. We have included these points in the discussion in Section 4.2.1.

Relatedly, equations for Gaussian moments cited from other models are not necessarily directly applicable to log-moments of lognormals, because a 1/x can pop out from taking the derivative of a logarithm (e.g. see the equation/definition of the lognormal vs. the Gaussian). I did not check every equation in the paper for this - the authors seem to have been very careful so I do not expect this is a problem - but it is worth mentioning.

[Response] Actually, calculating the derivatives does not involve taking the derivative of a logarithm because the growth rates are directly dependent on log cell volume (see Eqn. 10), not on cell volume itself. In other words, in our model equations, we only have log volume and we do not have any calculations on cell volume directly.

Besides this criticism, the paper scores well for significance, quality, reproducibility, and presentation. I have some specific comments below:

page 3, line 7: What is meant by ‘size’ here? Presumably diameter, but it should be stated, especially given the importance of ‘size’ to the rest of the paper, where size refers to volume.
[Response] Thanks for pointing it out. We have modified it to “ESD”.

page 4, line 27: Might be good to have a reference for the sentence that starts on line 25 and ends on line 27: : :
[Response] We have added the references “(Matsumoto et al., 2014; Wakita et al., 2016)”.

page 5, line 10: The authors sort of 'jump right in' to the terms and equations of the model here; an overview paragraph might be useful. What is the model trying to do? How is this accomplished? This is somewhat described in the abstract and in the Introduction, but a more detailed description of the entire modeling procedure could help some readers follow the paper much better.
[Response] This is really a helpful suggestion to improve the readability and overall organization of the paper. We have added an overall summary at the beginning of Sect. 2 (Model description).

page 5, line 12: What are the units for P (and for 'fer' below)? If they are what I think they should be, doesn't that make it obvious why P^2 v is the term to be considered, rather than P v, so shouldn't the sentence after next be removed?

[Response] We have added the units for P, and fer. However, we do not think that the units themselves can justify the use of P^2 v instead of Pv. We have followed the pioneering work of Bruggeman (2009) to use $P\left(v+\bar{l}^2\right)$ as the tracer for variance to be transported.

page 16, line 20: This is an interesting idea - can the authors flesh it out a bit more?

[Response] Yes, we have explained it in more detail in the Discussion section 4.1.1:
"In particular, the second derivative of the growth rate at mean size, $\frac{d^2\mu(l)}{dl^2}$, can be conveniently perceived as a proxy for the intensity of resource competition (The more concave is the curve of $\mu(l)$, the more intense is the competition since the fitness of suboptimal species decreases more steeply with distance from the optimal size)."

#===========================================================

Reviewer #3

This manuscript presents a newly developed model based on an emergent trait-based approach to simulate phytoplankton traits (size) and associated diversity according to environment factors. The authors chose to construct an adaptative dynamics models that employs moment closure to allow continuous distribution of traits and limit the number of variables. Indeed, the model simulates the characteristics of phytoplankton community in terms of total biomass and mean size while the diversity is approximated by the variance in size. Some important processes for phytoplankton growth, corresponding to physiological adaptation to light and variable C:N ratio are also incorporated. As such, the model described in this paper is of valuable contribution to the scientific understanding of the plankton diversity which has become a central issue of marine ecosystem management. The manuscript is well-written and gives a general overview on the ability of the model to simulate size-structured distribution of phytoplankton in various environmental conditions using two contrasted stations of the Northwest Pacific. However, I have some questions concerning the methodology which has been applied and whether/how this work can be generalized to other stations or a broader oceanic region (e.g. in the context of 3D modeling setup). Indeed, I am not familiar with the use of DRAM-type algorithm to adjust model's parameters value to observational data and it took some time to me to understand exactly the method that is implemented in this study. Therefore, a more detailed description of what is exactly done by the parameters optimization algorithm and how this will be used to apply the model to other regions would be very useful to help the reader to understand the concept behind this model. It would thus significantly raise the likely impact of this paper.

I recommend these questions, detailed in the 'general comments' section below, to be addressed before the manuscript could be considered to be published in 'Geoscientific Model Development'. Some minor and more specific comments are also included at the end of this document.

General comments:

1- Technically, the proposed model setup uses a DRAM algorithm to adjust the targeted parameters values and minimize the differences between model outputs and observational data based on two available dataset for contrasted stations of the Northwest Pacific. In the discussion section (p. 21, l. 3-7), the authors argue that this model would be 'easy to couple with 3D global or regional ocean models' (see also page 5, lines 6-8). As far as I understand, the idea would be to use the single set of parameters which has been found in this study (i.e. the one which gives the highest likelihood with regards to observational data for both stations) to run the model in other oceanic regions (otherwise, I do not see how the method can be applied to large oceanic system while seeking for a single set of parameters that would lead to the best fit to observational data over the considered region). This point is not specify in the manuscript. Could you please add further thoughts on that in your discussion section and describe the preconised method to apply this model to larger oceanic regions?

[Response] This is a good point that we had not explained with sufficient clarity in the previous manuscript. Yes, our intention is to use the single set of parameter values, obtained by fitting the model to the data from the two observation stations, as an initial estimate of parameter values for 3D simulations. As a test of the feasibility of this approach we present an example in which we use the parameter values optimized from the two stations K2 and S1 to model another independent station (the well known station ALOHA) in the North Pacific (Results section 3.5). Although the results are not as satisfactory as we wished, the parameter values obtained in the present study nevertheless provide a useful initial estimate for modeling other stations and for 3D applications. We propose for later studies to combine the “transport matrix” technique with DRAM or other parameter optimization techniques to calibrate 3D models in the discussion (Sect. 4.2.5).

2- In the introduction section (p. 4, l. 16-17), you write that ‘relatively few continuous trait-based models have been validated against oceanic observations’. The comparison that is done in results section 3.3 (p. 13-14) does not constitute a ‘validation analysis’ as you are using the same observational data to contrain the model’s parameters and to ‘validate’ the results. Indeed, the specific aim of the method which is used in this study is to provide the best fit between model outputs and measured data. Therefore, the main outcome of this study is actually the parameters set you obtained after running an ensemble of 10 000 simulations. A validation analysis should involve totally independent data for model parameterization and for validation and could only be carried out if you have runned the model for a different region using the same set of parameters. Here again, a more explicit description of the aim of your method (i.e. seting up a set of parameters which can be subsequently used to run the model in other regions ?) would have been useful to avoid the confusion.

[Response] Yes, we totally agree. We have changed the word “validate” to “calibrate”. We indeed attempted to validate the optimized model against independent datasets at station ALOHA. And we have emphasized our goal is “**CITRATE** is intended to be a starting model for later incorporation into three-dimensional (3D) general ocean circulation models (GCMs) and for further development of more comprehensive trait-based models” at the end of Introduction.

3- How do you convert the mean size and size variance into four size classes fraction? I guess the calculation is done by comparing the occurrence of each size classes from the size distribution (Gaussian distribution of the log biovolume) other time (e.g. seasonal average in fig. 8 and 9?) but this is unclear. Could you please specify the method that has been used in your method section?

[Response] Yes. We have added the method to calculate the four size classes of Chl based on phytoplankton biomass (in terms of nitrogen), mean size, and size variance (after Eq. 11d in Sect. 2.2). Actually, because we assumed lognormal distribution for phytoplankton cell volume, the Chl distribution is no longer a lognormal distribution (because the modeled chlorophyll to carbon ratio depends on cell volume). In order to obtain accurate estimates of the chl distribution, we had to discretize the phytoplankton size spectra to numerically estimate the fractions of size fractionated Chl.

4- In the introduction section, you say that functional groups (PFT) models, representing a defined and limited number of plankton types, generally ’underestimate local diversity’. You argue p.3, l. 24-26 that the main reason for that is their inability to resolve the trait space combined with their failure of representing the appropriate mechanism sustaining high level of diversity. Although these considerations are correct, I think they are not specific to aggregated models but can also apply to the model presented here. Indeed, as you point out in the discussion section, you choose to consider the size as master trait but ignore some other major traits (temperature optima, mixotrophy, grazing resistance etc.) which may also vary among planktonic organisms of same size and enable coexistence by achieving similar fitness between different adaptation strategies (i.e. mechanisms for sustaining diversity). In that sense, I would say that the two techniques have a similar bias of taking into account a limited number of traits and mechanisms to explain the huge plankton diversity. Please modify the introduction to consider this point. Moreover, another difference between the two methods is that the measure of diversity that is provided by moment-closure models corresponds to a relative measure of diversity (variance in size in this case) which only allow a relative and comparative analysis of the phytoplankton diversity (in time and space) but does not provide any absolute measure of diversity (number of taxons or species) to compare with observational data.

[Response] As admitted in the Discussion, we agree that our approach also suffers from lacking some of the important functional traits so that it also underestimates diversity. We also note in Sect. 4.2.1 that a promising approach might be to combine the discrete functional group approach with the continuous trait approach, to include the merits of both approaches. We have added the following text in the Introduction:
"Although this approach might overlook some other important traits that are not related to size and thereby underestimate trait diversity to some extent, it serves as a starting point for later development of more comprehensive diversity models that can include more traits or be integrated with the discrete functional group approach."

Indeed, the diversity metrics of our model cannot be directly comparable to the classic definition of "Richness" as the reviewer mentioned. Maybe other metrics like the Shannon-Wiener index that consider species evenness can be better compared to the trait variance we used in our approach. These metrics can be also calculated from observational data (e.g. size-fractionated Chl.). We have added "The trait variance, treated as a tracer in the model, serves as a measure of trait diversity, although it cannot be simply equated to species richness but may be converted to other diversity metrics like the Shannon-Wiener index (Quintana et al., 2008). The diversity of functional traits is arguably a better diversity index than species richness to relate to ecosystem functioning (Loreau et al., 2001)." in page 4.

p. 4, l. 9, you argue that 'the factors controlling diversity can be directly quantified and better understood' with the continuous trait-based models. This sentence is not unclear. Could you specify how and why are the factors (which factors?) controlling diversity better characterized using the latter method ?

[Response] We meant that from the equations of moment closure, the factors controlling diversity can be directly quantified and better understood because the diversity itself is a tracer, and the sinks (e.g. the second derivative of growth rate indicating resource competition) and sources (e.g. the trait diffusion terms indicating the effects of mutation) are given explicitly. We have revised the sentence to "Thus, the continuous trait-based model has the advantage that the factors controlling diversity can be directly quantified and better understood because the sources (e.g. speciation or immigration) and sinks (e.g. resource competition) for diversity are specified explicitly." to make it clearer.

Specific comments:
Please put 'et al' in italic while citing referenced publications throughout the manuscript.
[Response] Thanks for the comment. But it seems that the GMD format does not require to put 'et al' in italic.

Model description
P5 L12: Add the unit of P
[Response] Added.

P5 L18: Figure 1: What is the inset in the box on the top left (with probability axis)? Please add a description in the figure caption.
[Response] We have added a description in the figure caption.

P5 L22: Please provide more explanations on the role of the trait diffusion parameter
[Response] Yes, we have added a sentence "$u$ is the trait diffusion parameter, which describes the probability of the parental size $l(i)$ changing to adjacent size values $l(i–1)$ or $l(i+1)$ in offspring cells (Merico et al., 2014)." after Eq. 7c.

P6 L7-11: Please provide the references for the growth dependences to light, nutrient concentration and temperature.
[Response] We have added a sentence "Following previous studies (Flynn, 2003; Geider et al., 1997; Follows et al., 2007; Chen and Laws, 2017)," before this sentence.

P6 L17: Eq. (5A) should be Eq. (4A)
[Response] Thanks for pointing it out. We have corrected it (now Eq. (10A)).

Section 2: I would suggest to separate the description of the biogeochemical equations (section 2.2) and the 1D implementation (section 2.3). Therefore the paragraph l. 9-13 on

page 7 should be moved to the section 2.3 and the name of the section 2.2 should mention only ‘Biogeochemical model (nutrient, zooplankton etc.)’
[Response] We have followed the suggestion to separate the description of the ecosystem model (now section 2.1) from that of the 1D implementation (now section 2.4).

P7 L13: The sentence ’the 1D model contains only biological tracers’ is unclear. It should be replaced by ‘the biological model is runned offline’ or something similar

[Response] We have rewritten the sentence to “**For computational efficiency, instead of explicitly solving the complete moment, temperature, and salinity equations, we imported the physics variables that are directly relevant to the ecological processes from external data products.**”.

P8 L5: Please replace ‘water depth’ by ‘the depth of the water column depth’.
[Response] We have changed it to “***z*** **is the depth of the model grid (m)”.**

P8 L11: Please verify the equation for detritus (- -).
[Response] Sorry, it was a typo in the previous version. We have corrected the detritus equation.

P9 L12-14: Do you assume that the surface mixed layer has a depth of 100 m? (the explanation for the use of the threshold of Kv > 10-3 m2.s-1 is unclear).
[Response] Yes. We just tried to use a simple calculation to demonstrate why we use the threshold of Kv > $10^{-3}$ $m^2$ $s^{-1}$.

Why do you use a different parameterization for the MLD calculation for phytoplankton growth and MLD showed on fig. 2 from observational data (page 12, line 15)?
[Response] This is a good question. The definition of MLD based on observed temperature and salinity profiles is because there were no observational data for vertical eddy diffusivity (Kv). In the model, since we have the Kv from 3D model outputs but do not have salinity variables, it is best to define MLD based on Kv.

P11 L8: ’and both model’? Please check the sentence.

[Response] Sorry, it was a typo (although we do not know why it appeared). We have deleted them.

Fig. 2 caption: Add the description of the white scatter plots (MLD) in the legend. Change
': : :at station S1. (f-i) The same for station K2'
[Response] Description of MLD added. The figures indices also corrected.

Fig. 2: Check x-axis thick labels (subplots b, c, f and g).
[Response] Sorry, we did not find problems with x-axis thick labels.

Fig. 3: Add x-axis labels.
[Response] Added.

Results
In general, there is some discussion points that are included in the results section and that should rather be discussed in section 4.

P12 L18-25: This section describes the physical forcing and does not concern a result of the simulation. I would suggest to move this part in section 2.3 (method).
[Response] Yes, it is true. But we think that acquiring physics forcing is also an important component of our modeling work and the physics background should be counted as results although they are not direct results from simulation. So we feel it should better to be put in the results instead of in the method.

P12 L23:
'with the model estimates of MLD consistent with those measured from in situ temperature and salinity profiles': it is not clear what you are comparing exactly. (Please also add a reference to the figure showing that. What are white scatter plots on fig. 2 b and f?).
[Response] As explained above, we were comparing the MLDs from CTD profiles of temp. and salinity with from modeled profiles of Kv. We have added a reference to the figure ("Fig. 2b,f,j") showing this and also descriptions of white scatter boxes in the figure caption.

Fig. 4 caption: Remove the 's' in 'log-likelihood'. Replace (b-j) by (b-i)
[Response] Removed.

P13 L6: The SSqE of the smallest size fraction (fig. 4, q) also increases with time at S1
[Response]  Yes. But in the new simulation results, SSqE of the smallest size fraction decreases with time at S1.

P13 L9: The figure 5 is not commented in the text. Please add a sentence to describe the trend.
[Response] Added in the second paragraph of Sect. 3.2.

P13 L 11-16: The discussion on the value of the trait diffusion parameter should appear in the discussion section.
[Response] We feel that this interpretation on the value of the trait diffusion parameter should immediately follow the results to make the logic smooth and so that readers will easily be able to understand. We have changed the sentence to "The optimized *u* value was much higher than in Acevedo-Trejos et al. (2016). Reducing *u* to 0.05 yielded worse fits to the size-fractionated chlorophyll since lower size variance failed to capture the observed size scatter. It also relates to the limitation of the model that has to assume a lognormal distribution of size (*see* Sect. 4.2.1). However, an abnormally high *u* could drive the model to unstable conditions in which the size variance kept increasing.".  In the Discussion section, we did not present details concerning the parameter values.

Fig. 6 and 8 captions: Complete the caption with the position of the different variables.
[Response] Completed.

P13 L20: 'the higher surface concentrations'
[Response] Yes. Changed to "the higher surface concentrations of DIN during winter than summer".

P13 L22-24: Isn't it in apparent contradiction with the fact that you argued that the modeled MLD is in agreement with observational data (page 12, line 23)?
[Response] Yes, this disappears with the new simulation results.

P13 L22-24: discussion
[Response] This part has been removed during revision.

P14 L5: The observational data on the size fractions are relatively noisy. Could you please provide more details on how these data were obtained (sampling methods, size measurments, sampling frequency) in section 2.5? At station K2, the size distribution in unclear in data and the model overestimate the proportion of 3-10 _m size class. At station S1, observational data show the dominance of smaller cells but do not show the vertical structure of the size distribution that is simulated by the model with smaller cells at the surface. Please add a comment on this.

[Response] We have added a description of how the data of size fractions were obtained. The data did show some seasonal and vertical patterns, and we have described the patterns of the data and comparisons between data and model in Sect. 3.3.

P14 L7-9: ‘At station S1’. Do you mean station ‘K2’?
[Response] We meant at S1. However, we have removed this sentence because there was indeed some vertical pattern at S1 if one looks really carefully.

P14 L10: discussion
[Response] We have moved this sentence to Sect. 3.2 because we feel that the comment of light limitation on large cell size should immediately follow the description of optimized $\alpha_I$.

P14 L19: ‘following stratification which occurs earlier in S1 than K2’
[Response] Yes, we have added ‘which occurs earlier in S1 than K2’.

P14 L24: Show a figure of Chl/C ratio
[Response] The figure of Chl:C ratio shown in Fig. 10 and 11.

Fig. 10, g: High growth rate at the surface at K2 despite low TIN and low Chl a concentrations?
[Response] With the new simulation results, high Chl and growth rate occur at the same timing at surface at K2.

P15 L5-6: discussion
[Response] This sentence has been removed during revision.

P15 L24 – P16 L4: discussion

[Response] We have either moved the text to discussion or deleted it during revision.

P16 L3: The 'dynamic equilibrium theory proposed by Huston is only briefly mentionned (see also page 17, l, 1-2). This hypothesis implies that, under non-equilibrium conditions, the outcomes of the competition depend on the timescale of the competitive displacement and the relative rate of change in competitive abilities of each competing species. This point should be further developed and discussed according to your results on diversity in the discussion part of the manuscript.

[Response] This is a good point. We have added discussions on the 'dynamic equilibrium theory' in Sect. 4.1.1:

"Using 'adaptive dynamics', it is easier to quantify competition intensity (and other ecological quantities), which makes it easier to test ecological theories such as Huston's "general hypothesis of species diversity" (Huston, 1979). For example, the absolute magnitude of $\frac{\mathrm{d}^2\mu(\mathrm{l})}{\mathrm{dl}^2}$ correlates positively with $\mu$ (Fig. 13), indicating that higher growth rates induced greater resource competition. This agrees well with the "dynamic equilibrium theory". Huston (1979) emphasized that in natural environments where equilibrium is rarely achieved, growth rates play a greater role in determining diversity than do steady state competitive abilities as typically quantified by R* values (Tilman, 1982; Litchman et al., 2007). This is because when environmental conditions favour fast growth, it takes less time for the dominant species to predominate, and diversity decreases. The positive correlation between the absolute value of $\frac{d^2\mu(l)}{dl^2}$ and $\mu$ is a mathematical manifestation of the verbal argument in Huston (1979). "

P16 L6-9: As I said above, the role of the trait diffusion in maintaining diversity and the way it is used in the model is a bit tricky to understand. You could perhaps add a paragraph in the method section to clarify this point which is then only discussed briefly page 17, lines 10-14.

[Response] We have expanded the explanations on trait diffusion in Sect. 2.2:

"$u$ is the trait diffusion parameter, which describes the probability of the parental size $l(i)$ changing to adjacent size values $l(i-1)$ or $l(i+1)$ in offspring cells (Merico et al., 2014)."

Also in Sect. 3.4:

"Second, the contributions from the second derivatives of growth and trait diffusion (dominated by $2u\mu(l)$ with the contributions from $\frac{d^4\mu(l)}{dl^4}$ being minor; Eq. 7c) were the two

largest terms, which usually offset against each other. The values of $\frac{d^2\mu(l)}{dl^2}$ were always negative in all times at both stations, suggesting that without "trait diffusion", size variance would decrease toward zero (Eq. 7c). This highlights the importance of trait diffusion (which can be interpreted as genetic mutation or transgenerational phenotypic plasticity) to sustain diversity. The values of $\frac{d^2\mu(l)}{dl^2}$ were more negative when growth rates were higher and it is the margin of these two terms that (partially) drove the changes of size variance. For example, in early April of S1, the decrease of size variance was induced by a more negative $\frac{d^2\mu(l)}{dl^2}$ (*see* also Fig. 11h). Similar situations also occurred at the end of December."
also in Sect. 4.1.1:
"The incorporation of trait diffusion originally developed for continuous trait-based models (Merico et al., 2014) also provides a mechanism similar to speciation (or mutation) for sustaining diversity, linking ecological and evolutionary processes (Rosenzweig, 1995). The increasing effect of trait diffusion with growth rate is consistent with the Metabolic Theory of Ecology that metabolic rates, closely coupled with growth rates and generation time, are expected to correlate with mutation rates and affect speciation (Allen et al., 2006; Dowle et al., 2013). Our results have shown that it can be the largest term to balance competitive exclusion (Fig. 13). Without considering this mechanism, diversity could be underestimated in productive waters due to strong competition. This could also contribute to the latitudinal diversity gradient since in tropical regions (ectothermic) organisms tend to growth fast (i.e. short generation time) due to high temperature and therefore have high mutation and speciation rates (Rohde, 1992; Allen et al., 2006; Dowle et al., 2013). "

Discussion
P17 L22-27: There is no figures showing the N:C and Chl: C ratio patterns at the two stations.
[Response] We have added the figures showing the N:C and Chl: C ratios at the two stations in Fig. 10 and 11.

P18 L3: 'Instead, we employ : : :': The word 'instead' seems unappropriate as you mention a very different process than in the previous sentence: the trade-offs between maximal growth rate and nutrient affinity in the phytoplankton is not related to the size-dependence of the grazing by predators.

[Response] Here actually we meant different mechanisms to control phytoplankton mean size. These two mechanisms are the two most plausible mechanisms (one from bottom-up and the other from top-down) that may affect phytoplankton size structure. We have modified the text to :
“We have provided both bottom-up and top-down mechanisms to affect the size structure of phytoplankton in **CITRATE 1.0**. First, we employ an observation-based unimodal relationship between maximal growth rate and size to give the nanophytoplankton the advantage under nutrient-replete conditions (Chen and Liu, 2010, 2011; Marañón et al., 2013), thus allowing a trade-off between nutrient affinity and maximal growth rate within the pico- and nano-size range.”

As you mention l. 17-19, the role of grazing in shaping phytoplankton community has been shown to be crucial. In order to take into account a various palatability of phytoplankton for zooplankton feeding according to the cell size, the model should ideally involved a larger number of predator size classes (and/or, at least, an additional mesozooplankton size class) which would lead to much more complexity in the model. In addition to the predator-prey size-ratio, the predators’ feeding mode (Mariani et al., 2013) and the formulation that is used to constrain the herbivorous impact on primary producers community composition are also very important. Please add the information on what kind of predation function you are using in your model in ‘Model description’. Also, this points should be mentionned in the discussion section (add other references such as Anderson et al., 2010 ; Prowe et al., 2012).

[Response] We admit that zooplankton feeding including predator-prey size ratio and feeding mode is indeed an important process shaping phytoplankton size structure. We have added a mesozooplankton compartment to allow more subtle effects on phytoplankton size structure and later development of more sophisticated models. However, our parameterizations do not allow zooplankton grazing to play a significant role in affecting phytoplankton size structure because 1) we do not have sufficient data to constrain the zooplankton parameters and 2) following the principle of Occam’s Razor, if bottom-up factors alone can well simulate the patterns of phytoplankton size structure (we feel the bottom-up factors play the dominant role in oligotrophic oceans while top-down factors might be important in coastal waters). Therefore, we feel it unnecessary to add more complications at this time.

We have given the grazing function (Holling-Type III) in the section of 'Model description'. But as we have argued, it is not necessary for our model to contain too many details of zooplankton grazing such as feeding mode without sufficient data.

P20 L12: 'other mecanisms such as vertical migration': I am not sure that vertical migration is a very common process in small phytoplankton populations that are found at the surface of subtropical waters during the summer. What about the nutrient limitation terms? What should be the half-saturation constants for nitrogen/phosphorus uptake in the 1-3 _m size class found in observationnal data?

[Response] Vertical migration is certainly not a common process in small phytoplankton populations. However, some have found that very large phytoplankton that can perform vertical migration in the subtropical oceans (e.g. Villareal et al. Nature 1999; Villareal J. Phycol. 2004). It has been claimed that this vertical migration might be significant for new production and it seems a fair mechanism to provide nutrients to the surface waters.

For the nutrient terms, first we need to clarify that the half-saturation constants for GROWTH ($K_m$) used in the Monod equation should be much smaller than those for nutrient uptake ($K_s$; Laws Ann. Rev. Mar. Sci. 2013). Experimental measurements for $K_m$ are scarce, but generally have very low values, much lower than those used in the model (Laws et al. J. Phycol. 2011). However, we do not believe that using a very small $K_m$ will solve the problem because phytoplankton growth has to be limited by nutrient, and in any case the growth rate in surface waters will be lower than at depth closer to the nutricline. In any case, we do not know any measurements on half-saturation constants of 1-3 µm phytoplankton at our stations.

We hope that our above revisions and discussions could be accepted by the reviewers. Thank you very much.

Best regards,
Bingzhang Chen
S. Lan Smith

# CITRATE 1.0: Phytoplankton continuous trait-distribution model with one-dimensional physical transport applied to the Northwest Pacific

Bingzhang Chen, S. Lan Smith

Research Center for Global Change Research, JAMSTEC (Japan Agency for Marine-Earth Science and Technology), 3173-25 Showa-machi, Kanazawa-ku, Yokohama 236-0001, Japan

*Correspondence to*: Bingzhang Chen (bzchen@jamstec.go.jp)

Chen Bingzhang 2017/10/23 9:59 AM
**Deleted:** 1.1

Bingzhang Chen 2017/9/29 2:46 PM
**Deleted:** 0

Chen Bingzhang 2017/9/13 11:14 AM
**Deleted:** bingzhang.chen@gmail.com

**Abstract.** Diversity plays critical roles in ecosystem functioning, but it remains unclear how best to model phytoplankton diversity in order to better understand those roles and reproduce consistently observed patterns in the ocean. In contrast to the typical approach of resolving distinct species or functional groups, we present a ContInuous TRAiT-basEd phytoplankton model (**CITRATE**) that focuses on macroscopic system properties such as total biomass, mean trait values, and trait variance. This phytoplankton component is embedded within a Nitrogen-Phytoplankton-Zooplankton-Detritus-Iron model that itself is coupled with a simplified one-dimensional ocean model. Size is used as the master trait for phytoplankton. CITRATE also incorporates "trait diffusion" for sustaining diversity, as well as simple representations of physiological acclimation, i.e. flexible chlorophyll-to-carbon and nitrogen-to-carbon ratios. We implemented CITRATE at two contrasting stations in the Northwest Pacific where several years of observational data are available. The model is driven by physical forcing including vertical eddy diffusivity imported from three-dimensional general ocean circulation models (GCMs). One common set of model parameters for the two stations was optimized using the Delayed Rejection Adaptive Metropolis-Hasting Monte Carlo (DRAM) algorithm. The model faithfully reproduced most of the observational patterns and gave robust predictions on phytoplankton mean size and size diversity. CITRATE is a prototype upon which more sophisticated continuous trait-based models and applications within GCMs can be developed.

Bingzhang Chen 2017/9/29 2:46 PM
**Deleted:** 1.0

S. Lan Smith 2017/10/2 11:32 AM
**Deleted:** physics

Bingzhang Chen 2017/9/29 10:31 AM
**Deleted:** With proper physical forcing,

Bingzhang Chen 2017/9/29 2:46 PM
**Deleted:** 1.0

S. Lan Smith 2017/10/2 11:33 AM
**Deleted:** can be applied to any oceanic station where either nitrogen or iron limits phytoplankton growtha starting step

Chen Bingzhang 2017/10/23 4:48 PM
**Deleted:** and couple

S. Lan Smith 2017/10/2 11:36 AM
**Deleted:** d

Chen Bingzhang 2017/10/23 4:48 PM
**Deleted:** for applications within general ocean circulation models

## 1 Introduction

Both species identity (functional traits) and diversity play critical roles in ecosystem functioning (Tilman et al., 1997, 2014). Phytoplankton are a polyphyletic group of oxygenic organisms that account for nearly half of the global primary production (Fields et al., 1998) and also play indispensable roles in other biogeochemical cycles in the Earth system (Falkowski, 2012). They have astonishingly high diversity, with several thousand species already documented and many remaining to be explored (Sournia et al., 1991; Moon-van der Staay et al., 2001). Their equivalent spherical diameter (ESD) can range from less than one micron for cyanobacteria such as *Prochlorococcus* (Chisolmn et al., 1988) to more than 1 mm for some giant diatoms (Villareal, 1993). Furthermore, physiology differs substantially even within the same genera or species and the role of intraspecific variability in population dynamics and biogeochemical cycles remains to be investigated (Strzepek and Harrison, 2004; Johnson et al., 2006; Palenik et al., 2006; Kooistra et al., 2008; Biller et al., 2015).

Although various ocean models have been developed by accounting for different functional groups or categories of phytoplankton such as cyanobacteria, diatoms, diazotrophs, etc. (e.g., Le Quéré et al., 2005; Hashioka et al., 2013), the finite number of such distinct types included limits their ability to resolve the vast diversity of trait values. Some pioneering studies have considered greater numbers of species, each of which is defined by particular set of multivariate trait axes that constitute a hyper-volume niche space (Follows et al., 2007; Barton et al., 2010; Follows and Dutkiewicz, 2011; Matsuda et al., 2016). (It is worth noting that these diversity models usually focus on "functional traits" which are the key to linking phytoplankton diversity, environmental conditions, and ecosystem functioning. Important phytoplankton traits include maximal growth rate, the light absorption and nutrient uptake affinities, optimal growth temperature, and edibility (i.e., susceptibility to grazing), etc (Litchman et al., 2007; Litchman and Klausmeier, 2008; Edwards et al., 2011, 2012, 2015; Merico et al., 2009; Thomas et al., 2012; Chen, 2015)). The total species pool in these modelling studies should ideally cover the entire multi-dimensional trait space constrained by trade-offs (Smith et al. 2011), although computational limits make this impossible in practice. As a compromise, only a limited set of trait combinations is sampled from the entire trait space. Although this approach has effectively generated large-scale patterns of plankton diversity, it generally underestimates local diversity, for two reasons: 1)

Chen Bingzhang 2017/8/5 10:35 PM
**Deleted:** sizes

S. Lan Smith 2017/10/2 11:38 AM
**Deleted:** the

Bingzhang Chen 2017/9/29 10:34 AM
**Deleted:**

S. Lan Smith 2017/10/2 11:38 AM
**Deleted:** various

Bingzhang Chen 2017/9/29 10:50 AM
**Deleted:** has a

Bingzhang Chen 2017/9/29 10:48 AM
**Deleted:** F

Bingzhang Chen 2017/9/29 10:47 AM
**Deleted:** of all possible species

S. Lan Smith 2017/10/2 11:39 AM
**Deleted:** trait

S. Lan Smith 2017/10/2 11:40 AM
**Deleted:** which is however

S. Lan Smith 2017/10/2 11:40 AM
**Deleted:** practically impossible in practice due to

Bingzhang Chen 2017/9/29 10:53 AM
**Deleted:** at

Bingzhang Chen 2017/9/29 10:56 AM
**Deleted:** such models

lack of appropriate mechanisms for sustaining diversity (but *see* Vallina et al., (2014)), and 2) insufficient trait resolution so that fitness differences between species are too large to allow coexistence (i.e. insufficient equalizing effect; *see* Chesson, 2000). In any case, a substantial proportion of the idealized species so modelled cannot survive under realistic oceanic conditions, and therefore the models do not capture the functions associated with many species.

Continuous trait-based models have been developed to address the above questions (Wirtz and Eckhardt, 1996; Norberg et al., 2001; Bruggeman, 2009; Merico et al., 2009, 2014; Terseleer et al., 2014; Acevedo-Trejos et al., 2016; Smith et al., 2016). Instead of modeling the dynamics of individual species, continuous trait-based models or so-called "adaptive dynamics" models focus on macroscopic or aggregate properties of a community such as total biomass, average trait, and trait variance by assuming that phytoplankton traits follow some distribution (usually Gaussian) (Smith et al., 2011). These models do not have the problem of inadequate trait resolution, because they have infinitesimally fine trait resolution. The trait variance, treated as a tracer in the model, serves as a measure of trait diversity; although it cannot be simply equated to species richness, it can be converted to other diversity metrics such as the continuous entropy (Quintana et al., 2008). The diversity of functional traits is arguably a better diversity index than species richness relating to ecosystem functioning (Loreau et al., 2001). Thus, the continuous trait-based model has the advantage that the factors controlling diversity can be directly quantified and better understood because the sources (e.g. speciation or immigration) and sinks (e.g. resource competition) for diversity are specified explicitly. In addition, these models are computationally much more efficient than classic discrete species approaches. For example, assuming two independent traits for the phytoplankton community, a continuous trait-based model only requires 1 (biomass) + 2x2 (trait mean and variance) = 5 tracers for the phytoplankton community, while a discrete species-based model requires 2x10 = 20 tracers if assuming ten discrete values in each trait dimension, which still provides only coarse trait resolution. Furthermore, this difference increases linearly with trait dimension.

Relatively few continuous trait-based models have been coupled with physics transport and calibrated against oceanic observations. Here we describe a new one-dimensional model, **CITRATE 1.0**, built upon the classic nitrogen-phytoplankton-zooplankton-detritus (NPZD) model with a

Bingzhang Chen 2017/9/29 10:57 AM
**Formatted:** Font:Italic

Bingzhang Chen 2017/9/29 10:57 AM
**Deleted:** of the trait space

Bingzhang Chen 2017/9/29 10:57 AM
**Formatted:** Font:Italic

S. Lan Smith 2017/10/2 11:41 AM
**Deleted:** ,

S. Lan Smith 2017/10/2 11:42 AM
**Deleted:** but

Bingzhang Chen 2017/9/30 12:28 PM
**Deleted:** may

S. Lan Smith 2017/10/2 11:42 AM
**Deleted:** like

S. Lan Smith 2017/10/2 11:42 AM
**Deleted:** Shannon-Wiener index

S. Lan Smith 2017/10/2 11:43 AM
**Deleted:** can be

S. Lan Smith 2017/10/2 11:43 AM
**Deleted:** given

Bingzhang Chen 2017/9/29 11:03 AM
**Deleted:** species-based models

Chen Bingzhang 2017/8/12 9:59 AM
**Deleted:** exponentially

Bingzhang Chen 2017/9/29 5:10 PM
**Deleted:** validated

Bingzhang Chen 2017/9/29 2:47 PM
**Deleted:** 1.0

Chen Bingzhang 2017/10/23 9:59 AM
**Deleted:** 1.1

phytoplankton community represented using a continuous distribution of size, taken as a master trait (Fig. 1). In this way, not only total phytoplankton biomass, but also phytoplankton mean size and size variance are explicitly modeled. The distributions of other important functional traits are implicitly modeled via well-established scaling power laws. Although this approach might overlook some other important traits that are not related to size and thereby underestimate trait diversity to some extent, it serves as a starting point for later development of more comprehensive diversity models that can include more traits or be integrated with the discrete functional group approach. For the model to be implemented in the subarctic North Pacific, a well-known high nitrate low chlorophyll (HNLC) region, **CITRATE** also incorporates an iron limitation module. We optimized the model parameters against the extensive observational data at two contrasting stations (K2: 160 ºE, 47 ºN; S1: 145 ºE, 30ºN) in the North Pacific (Fig. 2a). The station K2 is located within the western subarctic North Pacific gyre and is characterized by low temperature, high nitrate, and high carbon export (Matsumoto et al., 2014; Wakita et al., 2016). Iron limitation on phytoplankton growth has been suggested at this station (Fujiki et al., 2014). The station S1 is located within the western subtropical North Pacific and is characterized by high sea surface temperature, low levels of nitrate and carbon export efficiency (Matsumoto et al., 2016; Sasai et al., 2016; Wakita et al., 2016). To independently validate the model, we also use the optimized model parameters from stations K2 and S1 to run the model for station ALOHA (158 ºW, 22.75 ºN) and compare the model outputs with the extensive observational data collected there.

In the following sections, we first describe the details of the model structure and the parameter optimization subroutine. Then we show the results of parameter optimization and modeled patterns of nutrients, phytoplankton biomass, mean size and size diversity. We also discuss the merits and limitations of the model and of the continuous trait-distribution approach. **CITRATE** is intended as a prototype for later incorporation into three-dimensional (3D) general ocean circulation models (GCMs) and for further development of more comprehensive trait-based models.

## 2 Model description

The overall aim of **CITRATE** **1.0** is to implement the continuous trait-based approach for modeling phytoplankton size diversity under realistic environmental conditions at the two representative stations

S. Lan Smith 2017/10/2 11:44 AM
**Deleted:** While we admit that

S. Lan Smith 2017/10/2 11:45 AM
**Deleted:** at

S. Lan Smith 2017/10/2 11:45 AM
**Deleted:** the

Bingzhang Chen 2017/9/29 2:47 PM
**Deleted:** 1.0

S. Lan Smith 2017/10/2 11:46 AM
**Deleted:** to be

S. Lan Smith 2017/10/2 11:46 AM
**Deleted:** starting model

Bingzhang Chen 2017/9/29 2:47 PM
**Deleted:** 1.0

Chen Bingzhang 2017/10/23 9:59 AM
**Deleted:** 1.1

Bingzhang Chen 2017/9/29 11:09 AM
**Deleted:** “adaptive dynamics”

Chen Bingzhang 2017/8/5 10:45 PM
**Formatted:** Normal

in the North Pacific. And our goal is not only to model phytoplankton size structure, but also to faithfully simulate the seasonal and vertical dynamics of other important quantities such as nutrients, Chl *a*, and productivity for later investigations of the roles of phytoplankton diversity in biogeochemical cycles. Hence, **CITRATE 1.0** consists of the following key features:

1) It models the mean and variance of a continuous phytoplankton size (i.e. log cell volume ($\mu$m$^3$)) distribution and incorporates "trait-diffusion" to sustain size diversity (Merico et al., 2014).
2) It contains an iron cycle in addition to the nitrogen cycle because in the subarctic and equatorial Pacific iron instead of nitrogen should be the main limiting nutrient for phytoplankton growth (Behrenfeld et al., 2006; Fujiki et al., 2014).
3) The phytoplankton cells have variable chlorophyll-to-carbon ($\theta$) and nitrogen-to-carbon ($Q_N$) ratios that respond to light and nutrient conditions in a realistic fashion.
4) A single set of model parameters are optimized against field observational data at two time-series stations in the Northwest Pacific.

## 2.1 Description of the ecosystem model

**CITRATE 1.0** contains 9 tracers in total: dissolved inorganic nitrogen (DIN, abbreviated as $\boldsymbol{N}$ in all the equations; unit: $\mu$mol N L$^{-1}$), phytoplankton biomass ($\boldsymbol{P}$; $\mu$mol N L$^{-1}$), microzooplankton biomass ($\boldsymbol{MIC}$; $\mu$mol N L$^{-1}$), mesozooplankton biomass ($\boldsymbol{MES}$; $\mu$mol N L$^{-1}$), detritus in terms of nitrogen ($\boldsymbol{D}$; $\mu$mol N L$^{-1}$) and iron ($\boldsymbol{D_{Fe}}$; nmol Fe L$^{-1}$), dissolved iron ($\boldsymbol{fer}$; nmol Fe L$^{-1}$), the products of $\boldsymbol{P\bar{l}}$ and $\boldsymbol{P(v+\bar{l}^2)}$ where $\boldsymbol{\bar{l}}$ (ln $\mu$m$^3$) is the phytoplankton mean log cell volume and $\boldsymbol{v}$ ((ln $\mu$m$^3$)$^2$) is the log volume variance (Fig. 1).

We assume that phytoplankton size is the master trait that determines all physiological functions (Litchman et al., 2007; Finkel et al., 2010; Edwards et al., 2011, 2012, 2015). We also assume that phytoplankton size follows a lognormal distribution, which is supported by some observational data (Finkel, 2007; Quintana et al., 2008). Since $\boldsymbol{\bar{l}}$ and $\boldsymbol{v}$ are not real standing stocks that can be directly transported in hydrodynamic models but are emergent properties of phytoplankton size structure, we follow Bruggeman (2009) to use the raw moments of biomass probability (i.e. $\boldsymbol{P\bar{l}}$ and $\boldsymbol{P(v+\bar{l}^2)}$ for

Formatted ... [1]

Bingzhang Chen 2017/9/29 11:11 AM
**Deleted:** The constructed model structure a ... [2]

Chen Bingzhang 2017/10/23 9:59 AM
**Deleted:** 1.1

Chen Bingzhang 2017/8/7 10:51 AM
**Formatted** ... [3]

Bingzhang Chen 2017/9/29 11:11 AM
**Formatted** ... [4]

Chen Bingzhang 2017/8/7 10:51 AM
**Formatted** ... [5]

Chen Bingzhang 2017/8/3 12:00 PM
**Deleted:** For simplicity, we assume that ... [6]

Bingzhang Chen 2017/9/29 10:54 AM
**Formatted** ... [7]

Bingzhang Chen 2017/9/29 10:54 AM
**Deleted:** and

Chen Bingzhang 2017/8/3 12:00 PM
**Deleted:** $\boldsymbol{P^2v}$

Bingzhang Chen 2017/9/29 10:54 AM
**Deleted:** , respectively, for the tracers of m ... [8]

Chen Bingzhang 2017/8/3 12:00 PM
**Deleted:** $\boldsymbol{P^2v}$

Bingzhang Chen 2017/9/29 10:55 AM
**Deleted:** over

Chen Bingzhang 2017/8/3 12:00 PM
**Deleted:** $\boldsymbol{Pv}$

Chen Bingzhang 2017/8/3 12:00 PM
**Deleted:** $\boldsymbol{P^2v}$ slightly improved the model ... [9]

Bingzhang Chen 2017/9/29 10:55 AM
**Deleted:** because we found that the use of

Bingzhang Chen 2017/9/30 1:12 PM
**Deleted:** General d…escription of the 1D ... [10]

Chen Bingzhang 2017/8/3 12:01 PM
**Formatted** ... [11]

Chen Bingzhang 2017/10/23 9:28 AM
**Formatted** ... [12]

Bingzhang Chen 2017/9/29 2:47 PM
**Deleted:** 1.0

Chen Bingzhang 2017/10/23 9:59 AM
**Deleted:** 1.1

Chen Bingzhang 2017/8/3 12:07 PM
**Formatted** ... [13]

Chen Bingzhang 2017/8/3 12:11 PM
**Formatted** ... [14]

Bingzhang Chen 2017/9/29 11:12 AM
**Deleted:** size (i.e. …ell volume)…and $\boldsymbol{v}$ (( ... [15]

Chen Bingzhang 2017/8/3 2:02 PM
**Formatted** ... [16]

Chen Bingzhang 2017/8/3 12:12 PM
**Deleted:** For simplicity, w

S. Lan Smith 2017/10/22 10:31 PM
**Formatted** ... [17]

Bingzhang Chen 2017/9/29 11:13 AM

Chen Bingzhang 2017/8/3 12:14 PM
... [18]

Chen Bingzhang 2017/8/3 12:14 PM

mean and variance) as independent tracers involved in transport. All the assumptions made here will be discussed later in **Sect.** 4.

Below we will describe the equations for each tracer. For simplicity, phytoplankton cells are assumed not to excrete inorganic nitrogen or to have any natural mortality to be converted into detritus. Phytoplankton are eaten by both micro- and mesozooplankton:

$$\frac{dP}{dt} = P\mu_{com} - e^{\frac{E_Z}{k}\left(\frac{1}{T_0}-\frac{1}{T}\right)}\left[MICg_{max,1}\frac{{P_{T,1}}^2}{{P_{T,1}}^2+K_{P,1}^2} + MESg_{max,2}\frac{(P_{T,2}+MIC)P}{(P_{T,2}+MIC)^2+K_{P,2}^2}\right] + \frac{d}{dz}\left(K_v\frac{dP}{dz}\right)$$

(1)

Chen Bingzhang 2017/8/3 2:01 PM
**Deleted:** for

Chen Bingzhang 2017/9/5 12:17 PM
**Deleted:** the

Chen Bingzhang 2017/9/5 12:18 PM
**Deleted:** of mean and variance

Chen Bingzhang 2017/8/3 2:01 PM
**Deleted:** diffusion

Chen Bingzhang 2017/8/3 2:18 PM
**Deleted:** .

Chen Bingzhang 2017/8/30 9:43 AM
**Deleted:** Note that we prefer $\boldsymbol{P^2v}$ over $\boldsymbol{Pv}$ because we found that the use of $\boldsymbol{P^2v}$ slightly improved the model fitting.

Chen Bingzhang 2017/8/3 2:02 PM
**Deleted:** Because in certain parts of the North Pacific iron instead of nitrogen is the main limiting nutrient for phytoplankton growth (Fujiki et al., 2014), we also include dissolved iron (***fer***) as another independent tracer. Hence the model includes 7 tracers in total (Fig. 1).

Bingzhang Chen 2017/9/30 1:12 PM
**Deleted:** The 1D model focuses on the upper 1500 meters of the ocean. The vertical grid, a total of 30 layers, follows a stretched vertical coordinate with increasing resolution towards the sea surface (surface stretching parameter = 2.0), similar to that used in the Regional Ocean Modelling System (ROMS) (Shchepetkin and McWilliams, 2005). For computational efficiency, the 1D model contains only biological tracers. The physics variables are imported as external data (*see* Sect. 2.3 for details).

S. Lan Smith 2017/10/2 11:34 AM
**Formatted:** Normal, Right, First line: 0 ch, Line spacing: single

Bingzhang Chen 2017/9/29 11:15 AM
**Deleted:**

Chen Bingzhang 2017/8/3 2:23 PM
**Formatted:** Font:Bold

where $\mu_{com}$ is the phytoplankton specific growth rate ($d^{-1}$) of the whole community (i.e. integrated over the whole size spectra). The equation of $\mu_{com}$, along with those of $\bar{l}$ and $v$, will be described later in Sect. 2.2. $E_z$ is the activation energy (in electron volts [eV], 1 eV = 96.49 kJ $mol^{-1}$) for heterotrophic processes. $g_{max,i}$ ($i$ = 1 for microzooplankton and 2 for mesozooplankton) is zooplankton maximal grazing rate ($d^{-1}$). $K_{P,i}$ is the grazing half-saturation constant of zooplankton. Here we have assumed that zooplankton grazing follows a Holling Type III functional response. $P_{T,i}$ is total palatable prey concentration for zooplankton ($\mu$mol N $L^{-1}$), the details of which will be given later in Sect. 2.3. If zooplankton grazing has no size selectivity on phytoplankton, then $P_T = P$. We assume that microzooplankton preferably feed on small phytoplankton while mesozooplankton prefer large phytoplankton (Table 1). Mesozooplankton also feed on microzooplankton. More descriptions of zooplankton size-dependent grazing will be given later. $z$ is the depth of the model grid (m). $K_v$ is the vertical eddy diffusivity ($m^2$ $s^{-1}$).

The total amount of phytoplankton ingested by zooplankton is divided among three fates: zooplankton net growth, excretion into the inorganic nitrogen pool, and defecation of unassimilated food into the detritus pool (Buitenhuis et al., 2010). Mesozooplankton mortality is set to be proportional to the squares of its biomass and is also converted into detritus pool. As such, the dynamics of micro- and mesozooplankton follow:

$$\frac{dMIC}{dt} = e^{\frac{E_Z}{k}\left(\frac{1}{T_0}-\frac{1}{T}\right)}\left(MICg_{max,1}\frac{{P_{T,1}}^2}{{P_{T,1}}^2+K_{P,1}^2}NGE_1 - MESg_{max,2}\frac{(P_{T,2}+MIC)MIC}{(P_{T,2}+MIC)^2+K_{P,2}^2}\right) + \frac{d}{dz}\left(K_v\frac{dMIC}{dz}\right) \quad (2a)$$

$$\frac{dMES}{dt} = e^{\frac{E_Z}{k}\left(\frac{1}{T_0}-\frac{1}{T}\right)}\left(MESg_{max,2}\frac{(P_{T,2}+MIC)^2}{(P_{T,2}+MIC)^2+K_{P,2}^2}NGE_2 - m_zMES^2\right) + \frac{d}{dz}\left(K_v\frac{dMES}{dz}\right) \quad (2b)$$

Chen Bingzhang 2017/8/3 2:23 PM
**Formatted:** Font:Not Bold

Chen Bingzhang 2017/8/3 2:26 PM
**Formatted:** Superscript

Chen Bingzhang 2017/8/3 2:23 PM
**Formatted:** Font:Not Bold

Chen Bingzhang 2017/8/8 11:59 AM
**Formatted:** Font:Italic

Chen Bingzhang 2017/8/8 11:59 AM
**Formatted:** Font:Italic, Subscript

Chen Bingzhang 2017/8/8 12:01 PM
**Formatted:** Font:Italic

Chen Bingzhang 2017/8/22 12:16 PM
**Formatted:** Font:Bold, English (US)

Chen Bingzhang 2017/8/22 11:11 AM
**Formatted:** Indent: First line: 0 ch

where $NGE_i$ is the net growth efficiency of zooplankton. $m_z$ is the mesozooplankton mortality coefficient (d$^{-1}$ ($\mu$mol N L$^{-1}$)$^{-1}$).

Detritus is converted to DIN at a rate ($R_{dn}$, d$^{-1}$) that has the same temperature sensitivity with zooplankton grazing. Detritus is also assumed to have a constant sinking rate ($W_d$, d$^{-1}$).

$$\frac{dD}{dt} = e^{\frac{E_Z}{k}\left(\frac{1}{T_0}-\frac{1}{T}\right)}\left(MICg_{max,1}\frac{{P_{T,1}}^2}{{P_{T,1}}^2+K_{P,1}^2}unass_1 + MESg_{max,2}\frac{\left(P_{T,2}+MIC\right)^2}{\left(P_{T,2}+MIC\right)^2+K_{P,2}^2}unass_2 + m_z MES^2 - R_{dn}D\right) - W_d\frac{dD}{dz} + \frac{d}{dz}\left(K_v\frac{dD}{dz}\right) \qquad (3)$$

where $unass_i$ represents the fraction of unassimilated food by zooplankton.

DIN is taken up by phytoplankton and is replenished by zooplankton excretion, detritus regeneration and diffusion from the depth:

$$\frac{dN}{dt} = -P\mu_{com} + e^{\frac{E_Z}{k}\left(\frac{1}{T_0}-\frac{1}{T}\right)}\left(MICg_{max,1}\frac{{P_{T,1}}^2}{{P_{T,1}}^2+K_{P,1}^2}(1-NGE_1-unass_1)\right.$$
$$\left.+MESg_{max,2}\frac{\left(P_{T,2}+MIC\right)^2}{\left(P_{T,2}+MIC\right)^2+K_{P,2}^2}(1-NGE_2-unass_2) + DR_{dn}\right) + \frac{d}{dz}\left(K_v\frac{dN}{dz}\right) \qquad (4)$$

The sources and sinks of *fer* largely follow DIN with an additional source (atmospheric deposition; $Fe_{depo}$) and sink (scavenging; $fer_{scav}$) (Aumont et al., 2003; Buitenhuis et al., 2010; Nikelsen et al., 2015):

$$\frac{dfer}{dt} = \begin{bmatrix} -P\mu_{com} + e^{\frac{E_Z}{k}\left(\frac{1}{T_0}-\frac{1}{T}\right)}\left(MICg_{max,1}\frac{{P_{T,1}}^2}{{P_{T,1}}^2+K_{P,1}^2}(1-NGE_1-unass_1)\right. \\ \left.+MESg_{max,2}\frac{\left(P_{T,2}+MIC\right)^2}{\left(P_{T,2}+MIC\right)^2+K_{P,2}^2}(1-NGE_2-unass_2) + DR_{dn}\right) \end{bmatrix} R_{fer_N}$$
$$+Fe_{depo} - fer_{scav} + \frac{d}{dz}\left(K_v\frac{dfer}{dz}\right) \qquad (5a)$$

To translate between nitrogen and iron in phytoplankton and zooplankton, a constant *fer*:*N* ratio ($R_{fer\_N}$) of 0.0265 is assumed. The data of monthly atmospheric deposition of total soluble iron are

Bingzhang Chen 2017/9/29 11:19 AM
**Formatted:** Indent: First line: 0 ch

Chen Bingzhang 2017/8/22 11:16 AM
**Formatted:** Subscript

Chen Bingzhang 2017/8/3 2:39 PM
**Formatted:** Superscript

Chen Bingzhang 2017/8/3 2:39 PM
**Formatted:** Superscript

Chen Bingzhang 2017/8/3 2:34 PM
**Formatted:** Font:Bold, English (US)

Chen Bingzhang 2017/8/3 2:40 PM
**Formatted:** Superscript

Chen Bingzhang 2017/8/22 12:25 PM
**Formatted:** Font:Italic

Chen Bingzhang 2017/8/22 12:25 PM
**Formatted:** Font:Italic, Subscript

Chen Bingzhang 2017/8/22 12:25 PM
**Formatted:** Indent: First line: 0 ch

Chen Bingzhang 2017/8/22 12:39 PM
**Formatted:** Centered

Chen Bingzhang 2017/9/14 3:38 PM
**Formatted:** Font:Times New Roman, Not Italic

Chen Bingzhang 2017/8/3 2:50 PM
**Formatted:** Font:Italic

Chen Bingzhang 2017/8/3 2:52 PM
**Formatted:** Font:Italic, Subscript

Chen Bingzhang 2017/8/3 2:56 PM
**Formatted:** Font:Not Bold

Chen Bingzhang 2017/8/3 2:56 PM
**Formatted:** Font:Italic

Chen Bingzhang 2017/8/3 2:56 PM
**Formatted:** Font:Italic, Subscript

Chen Bingzhang 2017/9/14 3:39 PM
**Formatted:** Font:(Default) Times New Roman, Not Italic

extracted from the Scenario III in Luo et al. (2008). Following Nikelsen et al. (2015), iron scavenging rate ($fer_{scav}$) is composed of both linear scavenging rate ($k_{scm}$) and particle absorption rate ($k_{sc}$):

$$fer_{scav} = \left(k_{scm} + k_{sc}De^{\frac{E_Z}{k}\left(\frac{1}{T_0}-\frac{1}{T}\right)}\right)Fe_{prime} \tag{5b}$$

in which $Fe_{prime}$ is the concentration of free iron:

$$Fe_{prime} = \frac{\left(-A+\sqrt{4ferk_{eq}+A^2}\right)}{2k_{eq}} \tag{5c}$$

$$A = 1 + \left(l_{fe} - fer\right)k_{eq} \tag{5d}$$

where $k_{eq}$ is the equilibrium constant between free iron and ligands and is assumed to depend only on temperature:

$$k_{eq} = 10^{\left(17.27-\frac{1565.7}{T}\right)} \tag{5e}$$

Note that $T$ is in absolute temperature (K). $l_{fe}$ is the total iron ligand concentration that is assumed constant (0.6 nM).

The equation for $D_{Fe}$ is:

$$\frac{dD_{Fe}}{dt} = e^{\frac{E_Z}{k}\left(\frac{1}{T_0}-\frac{1}{T}\right)}\left(MICg_{max,1}\frac{{P_{T,1}}^2}{{P_{T,1}}^2+K_{P,1}^2}unass_1 + MESg_{max,2}\frac{\left(P_{T,2}+MIC\right)^2}{\left(P_{T,2}+MIC\right)^2+K_{P,2}^2}unass_2 + m_zMES^2 - R_{dn}D\right)R_{fe_N} - W_d\frac{dD_{Fe}}{dz} + fer_{scav} + \frac{d}{dz}\left(K_v\frac{dD_{Fe}}{dz}\right) \tag{6}$$

## 2.2 Continuous trait-based phytoplankton model

Following the moment closure techniques in Merico et al. (2009) and the introduction of “trait diffusion” (Merico et al., 2014), the equations for $\mu_{com}$, $l$, and $v$ can be written as:

$$\mu_{com} \approx \left(\mu(l) + \frac{v}{2}\left(\frac{d^2\mu(l)}{dl^2} + u\frac{d^4\mu(l)}{dl^4}\right) - 3u\frac{d^3\mu(l)}{dl^3}\right)\Big|_{l=\bar{l}} \tag{7a}$$

$$\frac{d\bar{l}}{dt} \approx \left[v\left(\frac{d\mu(l)}{dl} - \sum_{i=1}^{2}\frac{dg_i(l)}{dl} + u\frac{d^3\mu(l)}{dl^3}\right) - 3u\frac{d\mu(l)}{dl}\right]\Big|_{l=\bar{l}} \tag{7b}$$

$$\frac{dv}{dt} \approx \left\{v\left[v\left(\frac{d^2\mu(l)}{dl^2} - \sum_{i=1}^{2}\frac{d^2g_i(l)}{dl^2} + u\frac{d^4\mu(l)}{dl^4}\right) - 5u\frac{d^2\mu(l)}{dl^2}\right] + 2u\mu(l)\right\}\Big|_{l=\bar{l}} \tag{7c}$$

Bingzhang Chen 2017/9/29 11:20 AM
**Formatted** ... [19]

Bingzhang Chen 2017/9/29 11:21 AM
**Formatted** ... [20]

Chen Bingzhang 2017/8/3 3:20 PM
**Formatted** ... [21]

Chen Bingzhang 2017/8/3 3:20 PM
**Formatted** ... [22]

Chen Bingzhang 2017/8/3 3:20 PM
**Formatted** ... [23]

Chen Bingzhang 2017/8/8 12:08 PM
**Formatted** ... [24]

Bingzhang Chen 2017/9/30 1:15 PM
**Deleted:** The initial condition of inorganic ... [25]

S. Lan Smith 2017/10/2 11:34 AM
**Formatted** ... [26]

Chen Bingzhang 2017/8/3 5:05 PM
**Formatted** ... [27]

Chen Bingzhang 2017/8/3 11:58 AM
**Formatted** ... [28]

Chen Bingzhang 2017/8/3 11:57 AM
**Deleted:** 1

Chen Bingzhang 2017/8/3 5:00 PM
**Formatted** ... [29]

Chen Bingzhang 2017/8/22 11:47 PM
**Deleted:** ,

Chen Bingzhang 2017/8/3 4:57 PM
**Deleted:** differential

Chen Bingzhang 2017/8/3 5:00 PM
**Deleted:** *P*

Chen Bingzhang 2017/8/3 5:00 PM
**Deleted:** ... [31]

Chen Bingzhang 2017/8/3 11:57 AM
**Deleted:** (1a)

Chen Bingzhang 2017/8/3 5:00 PM
**Formatted** ... [30]

Chen Bingzhang 2017/8/8 2:10 PM
**Deleted:**

Chen Bingzhang 2017/8/3 4:58 PM
**Deleted:** 1

Chen Bingzhang 2017/8/3 12:15 PM
**Deleted:** b

Chen Bingzhang 2017/8/8 2:11 PM
**Deleted:**

Chen Bingzhang 2017/8/3 4:58 PM
**Deleted:** 1c

where $\mu(\boldsymbol{l})$ is the phytoplankton growth rate ($d^{-1}$) at mean size $\boldsymbol{l}$, $u$ is the trait diffusion parameter, which describes the probability of the parental size $l(i)$ changing to adjacent size values $l(i-1)$ or $l(i+1)$ in offspring cells (Merico et al., 2014). Eqs. (7a-c) are approximations because the higher-order moments such as the skewness and kurtosis have been ignored and a Gaussian distribution needs to be assumed for $\boldsymbol{l}$. $\frac{dg_i(l)}{dl}$ and $\frac{d^2g_i(l)}{dl^2}$ are the first and second derivatives of zooplankton clearance rate ($d^{-1}$) against phytoplankton size and will be described in detail in Sect. 2.3.

The equations of $P\bar{l}$ and $P(v+\bar{l}^2)$ follow:

$$\frac{d(P\bar{l})}{dt} = P\frac{d\bar{l}}{dt} + \bar{l}\frac{dP}{dt} + \frac{d}{dz}\left(K_v\frac{d(P\bar{l})}{dz}\right) \tag{7d}$$

$$\frac{d(P(v+\bar{l}^2))}{dt} = P\left(\frac{dv}{dt} + 2\bar{l}\frac{d\bar{l}}{dt}\right) + (v+\bar{l}^2)\frac{dP}{dt} + \frac{d}{dz}\left(K_v\frac{d(P(v+\bar{l}^2))}{dz}\right) \tag{7e}$$

Following previous studies (Flynn, 2003; Geider et al., 1997; Follows et al., 2007; Chen and Laws, 2017), phytoplankton growth rate ($\mu$) depends on temperature ($T$, K), light ($I$, W $m^{-2}$), DIN and *fer*:

$$\mu = \mu_m \min\left(\frac{N}{N+K_N}, \frac{fer}{fer+K_{fer}}\right)\left(1 - e^{-\frac{\alpha_C I}{\mu'_{0,m} e^{\frac{Ep}{k}\left(\frac{1}{T_0}-\frac{1}{T}\right)}}}\right) \tag{8}$$

in which $\mu_m$ is a function of $T$:

$$\mu_m = \mu'_m e^{\frac{Ep}{k}\left(\frac{1}{T_0}-\frac{1}{T}\right)} \tag{9}$$

The trait parameters $\mu'_m$, $K_N$, $K_{fer}$, and $\alpha_c$ are all dependent on cell size $l$:

$$\mu'_m = \mu'_{0,m} e^{\alpha_\mu l + \beta_\mu l^2} \tag{10a}$$

$$K_N = K_{0,N} e^{\alpha_K l} \tag{10b}$$

$$K_{fer} = K_{0,fer} e^{\alpha_{fer} l} \tag{10c}$$

$$\alpha_c = \alpha_{0,c} e^{\alpha_I l} \tag{10d}$$

Eq. (10a) follows that maximal phytoplankton growth rate is a unimodal function of phytoplankton size (Chen et al., 2010, 2011; Marañón et al., 2013). It is worth noting that the light term of phytoplankton growth (the right side of Eq. 8) is usually modelled as $\mathbf{1 - e^{-\frac{\alpha_c I}{\mu_m}}}$ (Flynn, 2003), in which both $\alpha_c$ and $\mu_m$

**Deleted:** ,

Chen Bingzhang 2017/8/22 11:42 PM
**Formatted** ... [32]

Chen Bingzhang 2017/8/3 5:01 PM
**Deleted:** , $K_v$ is the vertical eddy diffusivit ... [33]

Chen Bingzhang 2017/8/8 2:17 PM
**Formatted** ... [34]

Chen Bingzhang 2017/8/8 2:11 PM
**Formatted** ... [35]

Chen Bingzhang 2017/8/3 5:01 PM
**Deleted:** differential

Chen Bingzhang 2017/8/30 9:44 AM
**Deleted:** $P^2$

Chen Bingzhang 2017/8/30 9:45 AM
**Deleted:** … (71 ... [36]

Chen Bingzhang 2017/8/30 9:44 AM
... [37]

Bingzhang Chen 2017/9/30 1:08 PM
**Deleted:** P

Chen Bingzhang 2017/8/3 5:02 PM
**Formatted** ... [38]

Chen Bingzhang 2017/8/3 5:11 PM
**Deleted:** dissolved inorganic nitrogen ($N$, ... [39]

Chen Bingzhang 2017/8/3 5:12 PM
**Formatted** ... [40]

Chen Bingzhang 2017/8/30 9:50 AM
**Deleted:** $e^{-\frac{\alpha_I I}{\mu_m}}$

Chen Bingzhang 2017/8/30 9:57 AM
**Deleted:** … ... [42]

Bingzhang Chen 2017/9/28 12:15 PM
**Formatted** ... [41]

Chen Bingzhang 2017/8/3 5:07 PM
**Deleted:** 3

Chen Bingzhang 2017/8/3 5:06 PM
**Deleted:** $\mu'_m$

Bingzhang Chen 2017/9/28 12:15 PM
**Formatted** ... [43]

Chen Bingzhang 2017/8/22 11:52 PM
**Formatted** ... [44]

Chen Bingzhang 2017/8/3 5:07 PM
**Deleted:** 4

Chen Bingzhang 2017/8/3 5:07 PM
**Deleted:** 4

Chen Bingzhang 2017/8/3 5:07 PM
**Deleted:** 4

Bingzhang Chen 2017/9/29 11:25 AM
**Deleted:** $\frac{\alpha_c}{\mu'_m}$

Chen Bingzhang 2017/8/3 5:07 PM
**Deleted:** 4

Chen Bingzhang 2017/8/3 5:08 PM
**Deleted:** 5

Bingzhang Chen 2017/9/29 11:30 AM
**Formatted** ... [45]

are dependent on size. We use $\alpha_I$ to represent the net effect of size on light-dependent growth for mathematical convenience, which leads to Eq. 8.

Following Flynn (2003), we have derived equations to directly calculate phytoplankton chlorophyll-to-carbon ($\theta$, g Chl (mol C)$^{-1}$) and nitrogen-to-carbon ($Q_N$, mol N (mol C)$^{-1}$) ratios from ambient light and nutrient levels:

$$\theta = \theta_{min} + \frac{\mu}{I\alpha_C}(\theta_{max} - \theta_{min}) \tag{11a}$$

$$Q_N = \frac{Q_{min}}{1-\left(1-\frac{Q_{min}}{Q_{max}}\right)\frac{N}{N+K_N}} \tag{11b}$$

where $\theta_{min}$ and $\theta_{max}$ are minimal and maximal Chl:C ratios, respectively. $Q_{min}$ and $Q_{max}$ are minimal and maximal N:C ratios, respectively. The total Chl *a* concentrations (*Chl*, $\mu$g L$^{-1}$) and net primary production (*NPP*, $\mu$gC L$^{-1}$ d$^{-1}$) integrated over the whole size spectra can be calculated as:

$$Chl = P\left(\frac{\theta}{Q_N} + \frac{v}{2}\frac{d^2\left(\frac{\theta}{Q_N}\right)}{dl^2}\right)\Bigg|_{l=\bar{l}} \tag{11c}$$

$$NPP = P\left(\frac{\mu}{Q_N} + \frac{v}{2}\frac{d^2\left(\frac{\mu}{Q_N}\right)}{dl^2}\right)\Bigg|_{l=\bar{l}} \tag{11d}$$

To calculate the fractions of Chl within a size range (i.e. <1 $\mu$m, 1–3 $\mu$m, 3–10 $\mu$m and > 10 $\mu$m), we had to discretize the size spectra into 60 even size classes between $\bar{l} - 6\sqrt{v}$ and $\bar{l} + 6\sqrt{v}$ and calculated the $\mu$, $\alpha_C$, $K_N$, $Q_N$, $\theta$, and eventually Chl of each size class following Eq. (11a-c). This is because the distributions of Chl do not follow the lognormal distribution of cell volume and an analytic solution is not yet available for calculating only a fraction of Chl. Fortunately, this approach only adds a minor computational cost because we only need to calculate the size-fractionated Chl once per day when saving model outputs.

Bingzhang Chen 2017/9/29 11:31 AM
**Formatted:** English (US)

Chen Bingzhang 2017/8/22 11:53 PM
**Deleted:** are also able…ave derived equat ... [46]

Chen Bingzhang 2017/8/22 11:53 PM
**Deleted:** directly

Bingzhang Chen 2017/9/28 12:15 PM
**Formatted** ... [47]

Bingzhang Chen 2017/9/28 12:15 PM
**Formatted:** English (UK)

Chen Bingzhang 2017/8/3 5:08 PM
**Deleted:** 5

Chen Bingzhang 2017/8/3 5:08 PM
**Deleted:** 5

Chen Bingzhang 2017/8/3 5:12 PM
**Deleted:** 5

Chen Bingzhang 2017/8/3 5:13 PM
**Deleted:** 5

Bingzhang Chen 2017/9/29 5:21 PM
**Formatted** ... [48]

Bingzhang Chen 2017/9/29 5:32 PM
**Formatted** ... [49]

Bingzhang Chen 2017/9/30 1:47 PM
**Deleted:** data

Bingzhang Chen 2017/9/29 5:32 PM
**Formatted:** English (US)

## 2.3 Zooplankton size-dependent grazing

Following Smith et al. (2016), the ingestion rate of zooplankton on size class $l$ can be formulated as:

$$G(l) = g_{max} Z \frac{\rho(l)P(l)}{P_T+\varepsilon} \frac{(P_T+\varepsilon)^2}{(P_T+\varepsilon)^2+K_P^2} = g_{max} Z \rho(l) P(l) \frac{P_T+\varepsilon}{(P_T+\varepsilon)^2+K_P^2} \tag{12a}$$

where $G(l)$ is the zooplankton ingestion rate ($\mu$mol N L$^{-1}$ d$^{-1}$) on the size class $l$. $\rho(l)$ is the relative grazing preference on size class $l$. $Z$ is the biomass of either micro- or mesozooplankton. $\varepsilon$ is the food other than phytoplankton ($\varepsilon = 0$ for microzooplankton and $MIC$ for mesozooplankton). $P_T$ (total palatable phytoplankton food) is formulated as:

$$P_T = \int_{-\infty}^{\infty} \rho(l)P(l)dl \tag{12b}$$

with $P(l)$ is the phytoplankton concentration at size $l$:

$$P(l) = \frac{P}{\sqrt{2\pi v}} e^{-\frac{1}{2}\frac{(l-\bar{l})^2}{v}} \tag{12c}$$

Zooplankton clearance rate ($g$, d$^{-1}$) on size class $l$ can be formulated as:

$$g(l) = g_{max} Z \frac{P_T+\varepsilon}{(P_T+\varepsilon)^2+K_P^2} \rho(l) \tag{12d}$$

For mathematic convenience, we parameterize $\rho(l) = e^{bl+c}$, where $b$ and $c$ are constants. $P_T$ can be approximated as:

$$P_T \approx P\rho(l)\left(1+\frac{v}{2}b^2\right)$$

And:

$$\frac{dP_T}{dl} = bP_T$$

$$\frac{d^2P_T}{dl^2} = b^2P_T$$

Thus, the first derivative of $g(l)$ can then be derived as:

$$\frac{dg(l)}{dl} = bg(l)\left\{\frac{[K_P^2-(P_T+\varepsilon)^2]P_T}{[(P_T+\varepsilon)^2+K_P^2](P_T+\varepsilon)} + 1\right\} \tag{12e}$$

And:

$$\frac{d^2g(l)}{dl^2} = bg(l)\left(\left\{\frac{[K_P^2-(P_T+\varepsilon)^2]P_T}{[(P_T+\varepsilon)^2+K_P^2](P_T+\varepsilon)} + 1\right\}^2 + bP_T\left\{-\frac{4K_P^2P_T}{[(P_T+\varepsilon)^2+K_P^2]^2} + \frac{[K_P^2-(P_T+\varepsilon)^2]}{[(P_T+\varepsilon)^2+K_P^2]}\frac{\varepsilon}{(P_T+\varepsilon)^2}\right\}\right) \tag{12f}$$

Deleted: Light levels ($I_z$) at depth $z$ were ... [50]
Chen Bingzhang 2017/8/3 11:58 AM
Deleted: 2.2 General description of the ... [52]
Bingzhang Chen 2017/9/28 12:15 PM
Formatted ... [51]
Chen Bingzhang 2017/8/8 12:11 PM
Formatted ... [53]
Chen Bingzhang 2017/8/22 11:12 PM
Formatted ... [54]
Chen Bingzhang 2017/8/8 1:44 PM
Formatted ... [55]
Bingzhang Chen 2017/9/30 1:44 PM
Deleted: 3
Chen Bingzhang 2017/8/8 1:45 PM
Formatted ... [56]
Chen Bingzhang 2017/8/8 2:44 PM
Formatted ... [57]
Bingzhang Chen 2017/9/28 12:15 PM
Formatted ... [58]
Chen Bingzhang 2017/8/23 12:05 AM
Formatted ... [59]
Bingzhang Chen 2017/9/28 12:15 PM
Formatted ... [60]
Chen Bingzhang 2017/8/23 12:06 AM
Formatted ... [61]
Bingzhang Chen 2017/9/28 12:15 PM
Formatted ... [62]
Bingzhang Chen 2017/9/30 1:44 PM
Deleted: 3
Chen Bingzhang 2017/8/8 2:05 PM
Formatted ... [63]
Chen Bingzhang 2017/8/8 2:07 PM
Formatted ... [64]
Chen Bingzhang 2017/8/8 2:34 PM
Formatted ... [65]
Chen Bingzhang 2017/8/8 2:45 PM
Formatted ... [66]
Bingzhang Chen 2017/9/30 1:45 PM
Deleted: 3
Chen Bingzhang 2017/8/8 2:07 PM
Formatted ... [67]
Chen Bingzhang 2017/8/8 2:46 PM
Formatted ... [68]
Chen Bingzhang 2017/8/8 2:49 PM
Formatted ... [69]
Bingzhang Chen 2017/9/30 1:45 PM
Deleted: 3
Chen Bingzhang 2017/8/8 2:50 PM
Formatted ... [70]
Bingzhang Chen 2017/9/28 12:16 PM
Formatted ... [71]
Chen Bingzhang 2017/10/23 9:25 AM
Formatted ... [72]
Chen Bingzhang 2017/8/8 2:50 PM
Formatted ... [73]
Chen Bingzhang 2017/8/23 12:25 AM
Formatted ... [74]
Chen Bingzhang 2017/8/8 2:50 PM
Formatted ... [75]
Bingzhang Chen 2017/9/29 11:38 AM
Chen Bingzhang 2017/8/8 2:55 PM
Formatted ... [76]
Chen Bingzhang 2017/8/23 12:12 AM
Formatted ... [77]
Bingzhang Chen 2017/9/30 1:45 PM
Chen Bingzhang 2017/8/23 12:12 AM
Formatted ... [78]
Chen Bingzhang 2017/8/8 5:33 PM
Formatted ... [79]
Chen Bingzhang 2017/8/8 5:38 PM
Formatted ... [80]
Bingzhang Chen 2017/9/30 1:45 PM

Note that we do not optimize the parameters of *b* and *c* because the zooplankton data are insufficient to constrain the parameters (Table 1, 2).

### 2.4 One-dimensional (1D) model

The 1D model focuses on the upper 150 meters of the ocean. The vertical grid, a total of 30 layers, follows a stretched vertical coordinate with increasing resolution towards the sea surface (surface stretching parameter = 2.0), similar to that used in the Regional Ocean Modelling System (ROMS) (Shchepetkin and McWilliams, 2005). For computational efficiency, instead of explicitly solving the complete moment, temperature, and salinity equations, we imported the physics variables that are directly relevant to the ecological processes from external data products.

Four types of external physics forcing data were imported into the 1D model: vertical eddy diffusivity ($K_v$), surface photosynthetic available radiation ($PAR_0$), atmospheric dust deposition, and vertical temperature profiles. Vertical advection of water was neglected, which had been shown relatively unimportant (Fernández-Castro et al., 2016). The most important physics forcing data, $K_v$, determined the upward nutrient flux to the upper euphotic zone and were imported from the output of a three dimensional (3D) eddy-permitting model targeted for North Pacific (Hashioka et al., 2009). This 3D model was able to faithfully simulate the Kuroshio Current and the spatial distributions of the Chl *a* fields. The extracted vertical profiles of $K_v$ were also consistent with the *in situ* estimated mixed layer depths (MLD) at the three stations (Fig. 2). $PAR_0$ were imported from SeaWIFS satellite monthly climatology products. Seasonal temperature vertical profiles were imported from WOA2013 monthly climatology.

Light levels ($I_z$) at depth $z$ were calculated based on $PAR_0$ and Chl *a* concentrations following the Beer-Lambert law:

$$I_z = PAR_0 e^{-z\left(K_w + K_{chl}\int_z^0 Chl(x)dx\right)} \qquad (13)$$

in which $K_w$ and $K_{chl}$ are the attenuation coefficients for seawater and Chl *a*, respectively. To realistically estimate the average light field that a phytoplankton cell should experience in a mixing

Chen Bingzhang 2017/8/8 5:39 PM
**Formatted:** Normal

Chen Bingzhang 2017/8/8 5:46 PM
**Formatted:** Font:Italic

Bingzhang Chen 2017/9/28 12:15 PM
**Formatted:** English (US)

Bingzhang Chen 2017/9/28 12:15 PM
**Formatted:** English (US)

Bingzhang Chen 2017/9/30 1:16 PM
**Deleted:** **External physics data for o**

Bingzhang Chen 2017/9/30 1:16 PM
**Formatted:** Indent: First line: 0 ch

S. Lan Smith 2017/10/2 11:34 AM
**Formatted:** Normal, Indent: First line: 2.36 ch, Line spacing: single

S. Lan Smith 2017/10/2 11:34 AM
**Formatted:** Normal, First line: 0 ch, Line spacing: single

water column (Franks, 2015), the ambient light level for phytoplankton within the surface mixed layer is calculated as the average light throughout the surface mixed layer, which is defined as the deepest depth with $K_v > 10^{-3}$ m$^2$ s$^{-1}$. This calculation is based on eq. (1) in Franks (2015), which gives that the average time for a phytoplankton cell to move 100 m (an approximate estimate of MLD) at the local diffusivity of $10^{-3}$ m$^2$ s$^{-1}$ is roughly half a day. However, to compare with *in situ NPP* estimates that were calculated from incubation bottles without continuous mixing, phytoplankton $\mu$, $\theta$, and $Q_N$ are recalculated from $I_z$ based on the Beer-Lambert law (Eq. 13).

The initial condition of inorganic nitrogen was set to the vertical profile of nitrate in January of the World Ocean Atlas (WOA) 2013 monthly climatology. Initial phytoplankton, zooplankton, and detritus biomass were all set to 0.1 $\mu$mol L$^{-1}$ in each grid. Initial phytoplankton mean log size ($\bar{l}$) and log size variance ($v$) were set to be 1. Initial dissolved iron concentration was set to the vertical profile of iron in January from a 3D global biogeochemical model output (Aumont et al., 2003). The time step of the model was 30 minutes. All the fixed model parameters are shown in Table 1 and the model parameters that are optimized to match observational data are shown in Table 2.

We employed a Dirichlet boundary condition at the bottom for DIN and ***fer*** with the values predefined by the WOA2013 climatology and the model output from Aumont et al. (2003), respectively. For other tracers, we assumed no diffusive flux at the bottom. Detritus was allowed to sink out of the system with the loss of nitrogen and iron replenished by diffusion.

## 2.5 Delayed Rejection Adaptive Metropolis-Hasting Monte Carlo (DRAM) algorithm

The Metropolis-Hasting Monte Carlo (MHMC) algorithm aims to find the posterior distribution (including mean and covariance matrix) of the parameter vectors, given the data provided. The key here is to develop an appropriate proposal covariance matrix ($P_{cvm}$), which determines the magnitude and direction of the proposed perturbations to the parameter values, as the algorithm explores the parameter space. At each iteration of the algorithm the newly proposed parameter set is either accepted or rejected based on the model-data mismatch, as explained below. In the classical random walk MHMC algorithm, the $P_{cvm}$ must be specified by the user to achieve sufficient acceptance rates for the proposed parameters, and this typically requires a great deal of effort and many trials.

Bingzhang Chen 2017/9/30 1:42 PM
**Formatted:** English (US)

Bingzhang Chen 2017/9/30 1:17 PM
**Formatted:** Indent: First line: 2.36 ch

Bingzhang Chen 2017/9/30 1:18 PM
**Deleted:** Four types of external physics forcing data were imported into the 1D model: vertical eddy diffusivity ($K_v$), surface photosynthetic available radiation ($PAR_0$), atmospheric dust deposition, and vertical temperature profiles. Vertical advection of water was neglected, which had been shown relatively unimportant (Fernández-Castro et al., 2016). The most important physics forcing data, $K_v$, determined the upward nutrient flux to the upper euphotic zone and were imported from the output of a three dimensional (3D) eddy-permitting model targeted for North Pacific (Hashioka et al., 2009). This 3D model was able to faithfully simulate the Kuroshio Current and the spatial distributions of the Chl *a* fields. The extracted vertical profiles of $K_v$ were also consistent with the *in situ* estimated mixed layer depths (MLD) at the threewo stations (Fig. 2). Practically, any reasonable outputs of seasonal $K_v$ profiles can be used. $PAR_0$ were imported from SeaWIFS satellite monthly climatology products. Seasonal temperature vertical profiles were imported from WOA2013 monthly climatology.

Chen Bingzhang 2017/8/8 12:10 PM
**Deleted:** 4

S. Lan Smith 2017/10/22 10:33 PM
**Deleted:** with reasonable search efforts

S. Lan Smith 2017/10/22 10:35 PM
**Deleted:** is used to generate a new set of parameters based on current position of the ... [81]

S. Lan Smith 2017/10/22 10:35 PM
**Deleted:** should

Chen Bingzhang 2017/10/23 9:27 AM
**Deleted:** msut

S. Lan Smith 2017/10/22 10:35 PM
**Deleted:** designed

S. Lan Smith 2017/10/22 10:40 PM
**Deleted:** which

S. Lan Smith 2017/10/22 10:38 PM
**Deleted:** however is not

S. Lan Smith 2017/10/22 10:38 PM
**Deleted:** always an easy task and may

S. Lan Smith 2017/10/22 10:38 PM
**Deleted:** need

S. Lan Smith 2017/10/22 10:38 PM
**Deleted:** substantial

S. Lan Smith 2017/10/22 10:38 PM
**Deleted:** s for

The adaptive MHMC (Haario et al. 2001), uses the already accepted parameters to approximate $P_{cvm}$, which it periodically updates as more simulations are conducted. Specifically, the $P_{cvm}$ is tuned based on the covariance matrix ($C_{vm}$) of the already accepted parameter sets after a fixed number of iterations following Gelman et al. (2014) (i.e. $P_{cvm} = C_{vm} \bullet 2.4^2/d$, where $d$ is the length of the target parameter vector). Thus, the algorithm alters the magnitude and direction of proposed 'jumps' in order to efficiently explore the parameter space.

With the delayed rejection MCMC (Mira, 2001), when a newly proposed set of parameters is rejected, $P_{cvm}$ is temporarily downscaled (to 1% of the original $P_{cvm}$ in our case) and a second set of parameters is proposed based on the rejected parameters and the downscaled $P_{cvm}$. This approach is particularly efficient because low acceptance rates typically result when the $P_{cvm}$ is too large (i.e., the parameter jumps are too wide) to find the target distribution of the parameters. Temporarily reducing $P_{cvm}$, can substantially increase the acceptance rate. By using multiple stages of $P_{cvm}$, the algorithm can also effectively deal with the problem of non-Gaussian posteriors, which can reduce the efficiency of the adaptive MHMC (Haario et al., 2006).

The DRAM algorithm, built upon the classic Metropolis-Hasting Monte Carlo (MHMC) algorithm, incorporates the merits of both adaptive and delayed-rejection MHMC algorithm to increase the acceptance rate and thus more efficiently find the target distribution of parameter values (Haario et al., 2006; Laine, 2008). It has been shown to better explore the parameter space compared to other algorithms such as the families of Simulated Annealing, possibly because of its two-stage proposal covariance matrices (Villagran et al., 2008). Compared with the widely used ensemble Kalman filter, DRAM is more suitable for the nonlinear response typically of ecosystems (Annan and Hargreaves, 2007).

Here we briefly outline the DRAM algorithm. For further details and proofs see Haario et al. (2006) and Laine (2008).

1) Initialize the parameter values and $P_{cvm}$, assuming no correlation among parameters, and a standard deviation equal to one sixth the difference between the maximal and minimal value for each parameter, respectively (Table 1).

S. Lan Smith 2017/10/22 10:40 PM
**Deleted:** , developed by …aario et al. (… ... [82]

Chen Bingzhang 2017/8/23 6:58 AM
**Formatted:** Indent: First line: 2.36 ch

S. Lan Smith 2017/10/22 10:44 PM
**Deleted:** usually the main cause for the … ... [83]

S. Lan Smith 2017/10/22 10:46 PM
**Deleted:** DRAM…t has been shown to be ... [84]

Chen Bingzhang 2017/8/27 8:55 PM
**Formatted:** Indent: First line: 1.77 ch

S. Lan Smith 2017/10/22 10:48 PM
**Deleted:** workflow of the …RAM algorith ... [85]

S. Lan Smith 2017/10/22 10:49 PM
**Deleted:** . The initial $P_{cvm}$ is constructed ... [86]

Chen Bingzhang 2017/8/27 9:42 PM
**Formatted:** List Paragraph, Indent: Left: 0 cm, Hanging: 4.26 ch, Numbered + Level: 1 + Numbering Style: 1, 2, 3, … + Start at: 1 + Alignment: Left + Aligned at: 0.75 cm + Indent at: 1.98 cm

Bingzhang Chen 2017/9/29 11:41 AM
**Deleted:**

2) Run the model with the current parameter values ($\theta_{curr}$) and calculate the likelihood ($L$). Note that all the parameter values must be within the boundaries shown in Table 2.

3) Propose a new set of parameters ($\theta_{pro}$) based on $\theta_{curr}$ and $P_{cvm}$, rerun the model, and obtain a new likelihood ($L_1$).

4) If the ratio of $L_1/L$ is larger than a random number between 0 and 1, then accept $\theta_{pro}$ ($\theta_{curr} = \theta_{pro}$) and return to step 2).

5) Otherwise, propose a second set of parameters ($\theta_{pro2}$) based on $\theta_{pro}$ and $P_{cvm2}$ (= $0.01P_{cvm}$), rerun the model, and obtain the second likelihood ($L_2$).

6) If the ratio of $\frac{L_2}{L}\frac{q_1(\theta_{pro2},\theta_{pro1})q_2(\theta_{pro2},\theta_{pro1},\theta_{curr})}{q_1(\theta_{curr},\theta_{pro1})q_2(\theta_{curr},\theta_{pro1},\theta_{pro2})}\frac{1-min\left(1,\frac{L_1}{L_2}\right)}{1-min\left(1,\frac{L_1}{L}\right)}$ is larger than a random number between 0 and 1, then accept $\theta_{pro2}$ ($\theta_{curr} = \theta_{pro2}$) and return to step 2). Otherwise retain the current position, $\theta_{curr}$. Here $q_1(y,x)$ is the probability of proposing $y$ given $x$ and $q_2(z,y,x)$ is the probability of proposing $z$ given $x$ and $y$.

7) After a certain interval, update $P_{cvm}$ based on $C_{vm}$ calculated from the accepted $\theta$.

To increase the computational efficiency and avoid being trapped in local minima because of insufficient chain length, we modified the DRAM algorithm for parallel computing (Calderhead, 2014). That is, we initialize $\theta$ and $P_{cvm}$ simultaneously for $n$ processes. Each process runs the above procedure from 1) to 7) except that at 7) all accepted $\theta$ are consolidated to update the global estimate of $P_{cvm}$, which is then distributed to all sub-processes to propose new $\theta$.

Preliminary model runs suggested that from the third year, the model reached a quasi-steady state, exhibiting regular seasonal cycles under the climatological forcing (Fig. 3). As such, we ran the model for four years and the output of the final year was used for validation against observational data. The model outputs were linearly interpolated to the observational depths and time. To allow fair comparisons among different data types and downplay the effects of extreme values, both the model outputs and observational data were transformed to their 1/4 power and normalized between 0 and 1 to achieve a quasi-normal distribution before calculating sum of squared errors ($SSqE$):

$$SSqE_{k,i} = \sum_{j=1}^{n_{k,i}} \left( \frac{m_{k,i,j}^{0.25} - o_{k,i,min}^{0.25}}{o_{k,i,max}^{0.25} - o_{k,i,min}^{0.25}} - \frac{o_{k,i,j}^{0.25} - o_{k,i,min}^{0.25}}{o_{k,i,max}^{0.25} - o_{k,i,min}^{0.25}} \right)^2 \qquad (14a)$$

Deleted: based on
Chen Bingzhang 2017/8/27 10:00 PM
Formatted ... [87]
Chen Bingzhang 2017/8/27 10:00 PM
Formatted ... [88]
Chen Bingzhang 2017/8/27 10:03 PM
Formatted ... [89]
S. Lan Smith 2017/10/22 10:50 PM
Deleted: go
Chen Bingzhang 2017/8/27 10:07 PM
Formatted ... [90]
S. Lan Smith 2017/10/22 10:51 PM
Deleted: go to
Chen Bingzhang 2017/8/27 11:10 PM
Formatted ... [91]
Chen Bingzhang 2017/8/27 9:42 PM
Formatted ... [92]
S. Lan Smith 2017/10/22 10:51 PM
Deleted: of
Bingzhang Chen 2017/9/28 12:15 PM
Formatted ... [93]
Chen Bingzhang 2017/8/27 11:15 PM
Formatted ... [94]
Chen Bingzhang 2017/8/27 11:15 PM
Formatted ... [95]
S. Lan Smith 2017/10/22 10:52 PM
Deleted: um… due to ... [96]
S. Lan Smith 2017/10/22 10:52 PM
Deleted: from
Bingzhang Chen 2017/9/28 12:15 PM
Formatted ... [97]
Chen Bingzhang 2017/8/27 11:17 PM
Formatted ... [98]
Bingzhang Chen 2017/9/28 12:15 PM
Formatted ... [99]
S. Lan Smith 2017/10/22 10:53 PM
Deleted: at sub-processes
Bingzhang Chen 2017/9/29 11:42 AM
Deleted: transfered
S. Lan Smith 2017/10/22 10:53 PM
Deleted: transferred
Bingzhang Chen 2017/9/28 12:15 PM
Formatted ... [100]
S. Lan Smith 2017/10/22 10:53 PM
Deleted: to the main process
Bingzhang Chen 2017/9/28 12:15 PM
Formatted ... [101]
Chen Bingzhang 2017/8/23 7:05 AM
Deleted: The adaptive component uses ... [102]
Bingzhang Chen 2017/9/29 11:43 AM
Deleted: both model
Chen Bingzhang 2017/8/27 8:53 PM
Deleted: 0

where $SSqE_{k,i}$ is the sum of squared errors of data type $i$ at station $k$. $n_{k,i}$ is the number of observations for data type $i$ at station $k$. $o_{k,i,j}$ is the observed $j^{\text{th}}$ value for data type $i$ at station $k$. $o_{k,i,min}$ and $o_{k,i,max}$ are minimal and maximal observed values for data type $i$ at station $k$, respectively (Note that for all size-fractions of Chl *a*, we intentionally set $o_{k,i,min} = 0$ and $o_{k,i,max} = 1$ to minimize the effects of the large measurement variability). $m_{k,i,j}$ is the value linearly interpolated from model outputs to the same depth and date of $o_{k,i,j}$.

Following Laine (2008), the likelihood function was calculated as the product of the exponential of the sum of squared errors, scaled by a measure of the model-data error for each data type, respectively:

$$L = \prod_{k=1}^{2}\left[\prod_{i=1}^{9}(2\pi)^{-\frac{n_{k,i}}{2}}\sigma_{k,i}^{-n_{k,i}}e^{-\frac{SSqE_{k,i}}{2\sigma_{k,i}^2}}\right] \qquad (14b)$$

in which $\sigma_{k,i}$ is the standard deviation of the Gaussian errors of data type $i$ at station $k$.

Following Laine (2008), we applied Gibbs sampling, which estimates the distribution of each $\sigma_k$, so as to match the ensemble distribution of model output to that of the data. This entails assuming that the prior of $1/\sigma_{k,i}$ follows a gamma distribution, with the prior mean as $S_0^2$ and prior accuracy as $n_0$. At each step the value of $1/\sigma_{k,i}$ was sampled from a conditional gamma distribution $\Gamma\left(\frac{n_0+n_{k,i}}{2}, \frac{n_0S_0^2+SSqE_{k,i}}{2}\right)$. The model parameters were assumed to follow multivariate normal distributions. The likelihood function contributed by the priors of the parameters was:

$$L_{pri} = (2\pi)^{-\frac{n_p}{2}}\left(\prod_{i=1}^{n_p}\eta_i^{-1}\right)e^{-\sum_{i=1}^{n_p}\left(\frac{\theta_i-\gamma_i}{\eta_i}\right)^2} \qquad (14c)$$

in which $n_p$ is the number of parameters to be estimated, $\gamma_i$ and $\eta_i$ are the prior estimates of the $i^{\text{th}}$ parameter and its standard deviation, respectively (Table 2). Values of $\eta_i$ were calculated as one-sixth of the difference between the preset maximal and minimal parameter boundaries. $\theta_i$ is the current parameter value. The MCMC chain was run for an ensemble of 10000 simulations with five processes running in parallel (i.e. a total of 50000 parameter sets were obtained). Although the model contains more than 20 parameters, we only selected 9 parameters for optimization, to minimize the possibility of parameter unidentifiability and avoid optimising highly correlated parameters (e.g. $g_{max}$ and $K_p$) simultaneously (Table 2). The data used are described below.

## 2.6 Observational data

S. Lan Smith 2017/10/22 10:54 PM
**Deleted:** for the nineeight types of observational data (total dissolved inorganic nitrogen (TINDIN), total Chl *a* concentration, *NPP*, particulate organic nitrogen (PON), dissolved inorganic iron (*fer*), and the fractions of four size-fractionated (> 10 µm, 3–10 µm, 1–3 µm, <1 µm) Chl *a*; Table 3) at two stations

Chen Bingzhang 2017/8/27 11:36 PM
**Formatted:** Font:Italic

Chen Bingzhang 2017/10/23 9:33 AM
**Deleted:** is

Chen Bingzhang 2017/8/27 11:31 PM
**Deleted:** *p* = ... [103]

Bingzhang Chen 2017/9/28 12:15 PM
**Formatted:** English (US)

Chen Bingzhang 2017/10/23 9:33 AM
**Deleted:** y…Gibbs sampling, which estir ... [104]

S. Lan Smith 2017/10/22 10:58 PM
**Deleted:** a…suminge ... [105]

Bingzhang Chen 2017/9/28 12:15 PM
**Formatted** ... [106]

Chen Bingzhang 2017/10/23 9:34 AM
**Deleted:** i

Chen Bingzhang 2017/10/23 9:35 AM
**Deleted:** are…assumed to follow multiva ... [107]

Chen Bingzhang 2017/8/27 11:36 PM
... [108]

Bingzhang Chen 2017/9/28 12:15 PM
**Formatted** ... [109]

Chen Bingzhang 2017/9/14 4:45 PM
**Formatted** ... [110]

Bingzhang Chen 2017/9/28 12:15 PM
**Formatted:** English (US)

Chen Bingzhang 2017/8/8 12:10 PM
**Deleted:** 5

For stations K2 and S1, the observations including MLD and nine types of data (DIN, CHL, NPP, PON, Fer, and four size fractions of CHL) were obtained from the K2S1 project (https://ebcrpa.jamstec.go.jp/k2s1/en/index.html; Honda, 2016; Table 3). The observations spanned from 2010 to 2013 at seasonal sampling frequencies. Part of the data have been published in Wakita et al. (2016), Fujiki et al. (2016), Matsumoto et al. (2016), and Sasai et al. (2016). DIN was calculated as the sum of nitrate, nitrite, and ammonia, which were measured with a continuous flow analyzer (QuAAtro 2-HR system, BL-Tech). CHL was measured using the nonacidification method following Welschmeyer (1994). NPP was measured with the technique of NaH$^{13}$CO$_3$ uptake (Matsumoto et al., 2016). PON was measured by an elemental analyser (Wakita et al., 2016). Size fractions of CHL were measured by filtering seawater sequentially through 10 μm, 3 μm, 1 μm polycarbonate membrane filters and finally a GF/F glass-fibre filter. The filters were soaked in N,N-dimethylformamide (DMF) and chlorophyll concentrations retained on the filters were measured with the same protocol as total CHL (Fujiki et al., 2016).

For station ALOHA, the data were downloaded from http://hahana.soest.hawaii.edu/hot/. All the data were pooled together to generate a quasi-climatological seasonal pattern and inter-annual variations were treated as random noise. To improve data coverage, we also included the nitrate data of World Ocean Atlas (WOA) 2013 for observed DIN. Due to the lack of *in situ* observational data, the data of *fer* were obtained from a global biogeochemistry model (Aumont et al., 2003). To calculate MLD from depth profiles of temperature and salinity, MLD was defined as the first depth that the seawater density exceeds surface density by 0.125 kg m$^{-3}$ (Shigemitsu et al., 2012).

## 3 Results

### 3.1 External physics forcing

The validity of external physics forcing data, particularly vertical mixing that determines upward nutrient diffusive supply to the surface mixed layer, is essential for correct results and parameter optimization with the ecosystem model. Here we show in Fig. 2 a representative year of seasonal variations of $K_v$, temperature, surface PAR, and atmospheric iron deposition. Vigorous winter mixing precedes summer water column stratification at K2 and S1, while the seasonal variations of mixing are

Chen Bingzhang 2017/9/14 4:03 PM
**Deleted:** T

S. Lan Smith 2017/10/22 11:00 PM
**Deleted:** nal data

Chen Bingzhang 2017/8/27 11:43 PM
**Deleted:** eight

S. Lan Smith 2017/10/22 11:00 PM
**Deleted:** f

S. Lan Smith 2017/10/22 11:00 PM
**Deleted:** used in DRAM

Bingzhang Chen 2017/9/30 4:10 PM
**Deleted:** (*see* Sect. 2.4)

Bingzhang Chen 2017/9/30 4:28 PM
**Formatted:** Superscript

Bingzhang Chen 2017/9/30 4:28 PM
**Formatted:** Subscript

Chen Bingzhang 2017/9/14 4:10 PM
**Deleted:** Part of the data have been published in Wakita et al. (2016), Fujiki et al. (2016), Matsumoto et al. (2016), and Sasai et al. (2016).

Chen Bingzhang 2017/8/3 12:05 PM
**Deleted:** TIN

Chen Bingzhang 2017/8/27 11:45 PM
**Formatted:** Font:Italic

Chen Bingzhang 2017/8/27 11:44 PM
**Deleted:** calculated

Chen Bingzhang 2017/8/3 11:18 AM
**Deleted:** dust

Chen Bingzhang 2017/9/14 4:15 PM
**Deleted:** d

Chen Bingzhang 2017/9/14 4:12 PM
**Deleted:** both

Chen Bingzhang 2017/9/14 4:12 PM
**Deleted:** stations

less pronounced at ALOHA. At all three stations, the model estimates of mixed layer depths are consistent with those measured from *in situ* temperature and salinity profiles (Fig. 2b,f,j). Water temperatures and surface PAR values at the subarctic station K2 are significantly lower than at the subtropical stations S1 and ALOHA. The station K2 is also characterized by a pronounced spring peak of atmospheric dust deposition.

### 3.2 Parameter optimization and sensitivity analysis

For all the five parallel sub-processes, the log-likelihood continued to increase with the number of model runs and reached a plateau after 1000 iterations (Fig. 4). For most (but not all) types of data, model–data mismatches (*SSqE*) consistently decreased. Comparing the two stations, the model fits to the Chl, and NPP were better at station K2 than S1. The model fits to the size fractions of 1 ~ 3 $\mu$m were better at S1 than K2.

Most values of the optimized parameters fell into reasonable ranges (Table 2; Fig. 5). For example, the estimated $K_{0,N}$ is close to the value (0.2 $\mu$M) given in Ward et al. (2012). For some of the parameters such as $W_d$ and $\mu$, the final optimized value differed substantially from initial estimates, an expected outcome of the algorithm striving to match with the nine different types of observations at both stations with contrasting environments. Below we show some preliminary results of sensitivity analysis particularly on those differing with *a prior* estimates (Table 4).

The mean $\mu'_{0,m}$ estimated from laboratory phytoplankton data is around 0.4 $d^{-1}$, half of the optimized value (Chen and Laws, 2017). Reducing $\mu'_{0,m}$ to 0.4 $d^{-1}$ mainly generated worse fits to the size fractions of <1 $\mu$m fractions of CHL at both stations. This is because the lower phytoplankton growth led to higher nutrient concentrations and lower estimates of <1 $\mu$m fractions.

The estimate of $W_d$ of 20 m $d^{-1}$ is a relatively high sinking speed. Reducing $W_d$ to 10 m $d^{-1}$ only led to slightly worse fits to DIN data at station S1 (but better fits to DIN at K2) and overall did not deteriorate the results substantially.

The estimate of $m_z$ (0.2 ($\mu$M N)$^{-1}$ $d^{-1}$) is also at the high end of those used in the literature. We found that the model results were quite sensitive to the value of the closure term $m_z$. Reducing $m_z$ to 0.1 ($\mu$M N)$^{-1}$ $d^{-1}$ led to higher mesoplankton biomass and generated much worse fits particularly for DIN at K2.

Chen Bingzhang 2017/9/14 4:13 PM
**Deleted:** ,…At all three stations, with … ... [111]

Chen Bingzhang 2017/9/20 3:45 PM
**Deleted:** **O…timization efficiency …nd** ... [112]

Chen Bingzhang 2017/9/14 4:21 PM
**Deleted:** As expected…or all the five par ... [113]

Chen Bingzhang 2017/9/22 2:23 PM
**Formatted** ... [114]

Chen Bingzhang 2017/9/14 4:30 PM
**Deleted:** some

Chen Bingzhang 2017/9/22 2:24 PM
**Formatted** ... [115]

Chen Bingzhang 2017/9/14 4:30 PM
**Deleted:** such as $K_{0,N}$, $W_d$, $\alpha_{0,C}$, and $K_{0,fer}$ ... [116]

Chen Bingzhang 2017/9/22 2:25 PM
**Formatted:** Font:Italic

Chen Bingzhang 2017/9/20 3:41 PM
**Formatted:** Superscript

Chen Bingzhang 2017/9/22 2:34 PM
**Formatted:** Font:Italic

Chen Bingzhang 2017/9/22 3:11 PM
**Formatted:** Superscript

Chen Bingzhang 2017/9/22 3:18 PM
**Formatted** ... [117]

We also tested whether we could assume that the light component of phytoplankton growth is size independent (i.e. $\alpha_I = 0$). The results suggested that with $\alpha_I = 0$, the model predicted much worse fits to the data. An optimized value of –0.26 for $\alpha_I$ is also consistent with the size scaling relationship of light dependent growth in Finkel (2001) and Edwards et al. (2015), suggesting that light limitation could drive phytoplankton being small.

The optimized *u* value was much higher than in Acevedo-Trejos et al. (2016). Reducing *u* to 0.05 led to worse fits to the size-fractionated chlorophyll since lower size variance failed to capture the observed size scatter. It also relates to the limitation of the model that has to assume a lognormal distribution of size (*see* Sect. 4.2.1). However, an abnormally high *u* could drive the model to unstable conditions in which the size variance kept increasing.

### 3.3 Comparison between best model outputs and observation

The best model outputs in terms of the highest likelihood could capture most of the observational patterns quantitatively (Figs. 6–9). At both stations, the model could reproduce the vertical increasing trend of DIN with depth and the higher surface concentrations of DIN during winter than summer and autumn. It is noteworthy that the model could also successfully reproduce the relatively abundant summer DIN concentrations at surface at station K2 due to the incorporation of iron and light limitation. The vertical and seasonal patterns of Chl *a* and NPP could also be well reproduced at station K2. The only problem is that, at station S1, the high NPP at surface could not be well reproduced (Fig. 7).

Validation against observed phytoplankton size data is critical for testing **CITRATE** 1.0 in which phytoplankton size structure is the core component. The model could reproduce most patterns of the proportions of size-fractionated Chl at both stations (Figs. 8, 9). For example, the model correctly reproduced the relative dominance of picophytoplankton (<3 *μ*m) at both stations, although nitrate concentration was high at station K2. The seasonal and vertical fractions of 3–10 *μ*m were generally well simulated at both stations, except for an artificial surface peak at K2. The model could also simulate the relative larger sizes at K2 than at S1.

We also note some deficiencies of the model. At both stations, the fractions of > 10 *μ*m Chl were close to zero at both stations in the model, in contrast to the substantial fractions of > 10 *μ*m during summer at K2 and in the winter at S1. The model also tended to overestimate the 1–3 *μ*m fractions at

Bingzhang Chen 2017/9/29 11:50 AM
**Formatted** ... [118]

Chen Bingzhang 2017/9/20 5:30 PM
**Formatted** ... [119]

Bingzhang Chen 2017/9/29 11:50 AM
**Formatted** ... [120]

Chen Bingzhang 2017/9/20 5:30 PM
**Formatted:** Font:12 pt

Bingzhang Chen 2017/9/29 11:51 AM
**Deleted:** toward

Chen Bingzhang 2017/9/22 2:43 PM
**Formatted:** Font:

Chen Bingzhang 2017/9/20 5:37 PM
**Deleted:** Note that t

Chen Bingzhang 2017/9/22 2:44 PM
**Formatted:** Font:Italic

Chen Bingzhang 2017/9/22 2:44 PM
**Deleted:** , which might be a necessary condition to match with the observed distributions of

Chen Bingzhang 2017/9/14 4:32 PM
**Formatted:** Font:Italic

Bingzhang Chen 2017/9/29 11:51 AM
**Deleted:** We also note that

Chen Bingzhang 2017/9/14 4:31 PM
**Deleted:** increasing *u* beyond some threshold (e.g. 0.2)

Chen Bingzhang 2017/9/14 4:31 PM
**Formatted:** Font:Italic

Chen Bingzhang 2017/9/22 3:29 PM
**Deleted:** .

Chen Bingzhang 2017/8/3 12:05 PM
**Deleted:** TIN…IN with depth and the hig ... [121]

Chen Bingzhang 2017/9/14 5:28 PM
**Formatted:** Font:Italic

Chen Bingzhang 2017/9/14 5:30 PM
**Deleted:** Although with some deviations, ... [122]

Chen Bingzhang 2017/9/16 10:42 PM
**Deleted:** At station S1, the model also reproduced the relatively invariant proportions of size-fractionated Chl with depth during stratified seasons. This is not expected because of a steep vert ... [123]

Chen Bingzhang 2017/9/16 10:43 PM
**Formatted:** Font:Italic

Chen Bingzhang 2017/9/16 10:46 PM
**Deleted:** including the overestimation of ... [124]

Chen Bingzhang 2017/9/16 10:47 PM
**Formatted:** Font:Italic

both stations and underestimate the <1 $\mu$m fractions occasionally. All these problems relate to the assumption of a fixed trait distribution as discussed later.

### 3.4 Modelled seasonal patterns of nutrients, phytoplankton biomass, mean size, and size diversity

At both stations, DIN concentrations were higher during winter in the surface mixed layer due to more vigorous mixing (Figs. 10, 11). Significant drawdown of DIN occurred in surface water following water column stratification which occurs earlier in S1 than K2. At station K2, after an increase during June and July due to the peak of atmospheric deposition, dissolved iron concentration also decreased in the fall due to phytoplankton uptake. By contrast, surface iron concentrations accumulated from late summer to fall due to nitrogen limitation at station S1.

In accordance with the DIN patterns, higher concentrations of Chl *a* were found during winter at station S1, which results from both increased phytoplankton biomass and chlorophyll-to-carbon ratios (Fig. 11). Starting from spring to fall, subsurface maximal layers of Chl *a* formed and progressively deepened with time. By contrast, at station K2, Chl *a* concentrations peaked in summer and subsurface chlorophyll maximum layers were not evident (Fig. 10), suggesting light limitation played a stronger role in limiting phytoplankton growth at K2 than S1.

At both stations, in spite of the nutrient increases in winter, phytoplankton mean size peaked in spring or summer. This is mostly attributed by the light limitation on large cells, which can be reflected by the negative value of $\alpha_I$ (Table 2). At both stations, the main periods of size increases were in spring when light level increased and there were still nutrients left from winter mixing. The increases in light were contributed by both increases in surface PAR and shallower mixing. Nutrient (dissolved iron in the case of K2) depletion together with light decreases led to negative values of $\frac{d\mu(I)}{dI}$ since late spring or summer at both stations, resulting in subsequent decreases in mean size. In general, the modelled mean sizes were significantly larger at station K2 than S1, mainly due to less severe nutrient limitation.

The modelled patterns of size variances (i.e. size diversity) are the focus of **CITRATE**. Within the surface mixed layer, modelled phytoplankton size diversity showed an opposite pattern with mean size, with the peaks in fall at S1 and in winter at K2 (Fig. 10,11). At first glance, we also seemed to find a negative correlation between the growth rate $\mu_{com}$ and size diversity at both stations (Fig. 12a). When growth rates were high, size variances were low, and vice versa. The paired scatterplots between $\mu_{com}$

Chen Bingzhang 2017/9/16 10:48 PM
**Deleted:** K2

Chen Bingzhang 2017/9/16 10:48 PM
**Formatted:** Font:Italic

Chen Bingzhang 2017/9/16 10:48 PM
**Deleted:** The model also tended to underestimate >10 $\mu$m fractions at station S1.

Chen Bingzhang 2017/8/3 12:05 PM
**Deleted:** TIN…IN concentrations were h ... [125]

Chen Bingzhang 2017/8/3 12:05 PM
**Deleted:** TIN…IN patterns, higher conce ... [126]

Chen Bingzhang 2017/9/22 3:40 PM
**Deleted:** around…spring or summer. Thi ... [127]

Chen Bingzhang 2017/9/22 3:48 PM
**Deleted:** the

Chen Bingzhang 2017/9/25 1:58 PM
**Formatted:** Font:Bold

Bingzhang Chen 2017/9/29 11:54 AM
**Deleted:** 1.0

Chen Bingzhang 2017/9/25 1:58 PM
**Formatted:** Font:Not Bold

Chen Bingzhang 2017/9/22 4:01 PM
**Deleted:** M…delled phytoplankton size ... [128]

Chen Bingzhang 2017/9/25 3:32 PM
**Formatted:** Subscript

and size variances in surface waters suggested that these two quantities were not linearly correlated, particularly at S1. Instead, their relationships depended on the timing of the season. At station S1, during the transition from the end of winter to early spring, phytoplankton cells experience a rapid increase in growth rate without much change in size diversity. During the rest of spring, phytoplankton growth rate decreased from the maximum to nearly the minimum; while size diversity first underwent a phase of moderate decrease and then recovered. From the beginning of summer to mid-fall, there were no big changes in growth rate, but size diversity increased dramatically. From mid-fall to the beginning of the winter, phytoplankton growth rate increased, but size diversity decreased to winter values. At station K2, the variability of size diversity was smaller, with high growth rates and low size diversity in summer and the opposite patterns in winter.

We decomposed the different factors in affecting the dynamics of size diversity in surface waters at both stations (Eq. 7c,e; Fig. 12b,c). Three points need to be mentioned. First, the calculated net combined effects, including the second derivatives of growth and grazing ($\frac{d^2\mu(l)}{dl^2}$ and $\frac{d^2g(l)}{dl^2}$), trait diffusion ($\frac{d^4\mu(l)}{dl^4}$ and $\mu(l)$), and vertical mixing (i.e. diffusion), were consistent with the net changes of size variances (some minor differences were because we saved the above quantities at daily interval which could not account for the changes within one day), validating our computation. Second, the contributions from the second derivatives of growth and trait diffusion (dominated by $2\nu\mu(l)$ with the contributions from $\frac{d^4\mu(l)}{dl^4}$ being minor; Eq. 7c) were the two largest terms, which usually offset against each other. The values of $\frac{d^2\mu(l)}{dl^2}$ were always negative in all times at both stations, suggesting that without "trait diffusion", size variance would decrease toward zero (Eq. 7c). This highlights the importance of trait diffusion (which can be interpreted as genetic mutation or transgenerational phenotypic plasticity) to sustain diversity. The values of $\frac{d^2\mu(l)}{dl^2}$ were more negative when growth rates were higher and it is the margin of these two terms that (partially) drove the changes of size variance. For example, in early April of S1, the decrease of size variance was induced by a more negative $\frac{d^2\mu(l)}{dl^2}$ (*see* also Fig. 11h). Similar situations also occurred at the end of December. Third, water column mixing played a significant role in affecting size diversity, which was the main factor leading to the

Chen Bingzhang 2017/9/25 3:28 PM
**Deleted:** peaked during spring and summer at S1 and K2, respectively, due to the improved light condition and high temperature. In other words, although spring or summer blooms can be characterized by high biomass, growth rate, and large size, the size diversity could be higher during winter.

Chen Bingzhang 2017/9/26 12:06 PM
**Formatted:** Indent: First line: 1.18 ch

Chen Bingzhang 2017/9/26 11:41 AM
**Formatted:** Font:Italic

Chen Bingzhang 2017/9/26 11:41 AM
**Formatted:** Font:Italic

Chen Bingzhang 2017/9/26 11:50 AM
**Formatted:** Font:Italic

Chen Bingzhang 2017/8/8 11:11 AM
**Deleted:** ,

Chen Bingzhang 2017/8/8 11:11 AM
**Deleted:** a surrogate for the intensity of competition,

Chen Bingzhang 2017/8/8 11:13 AM
**Deleted:** indicative of the effect of resource competition that reduces diversity

Bingzhang Chen 2017/9/29 11:55 AM
**Deleted:** T

Chen Bingzhang 2017/9/26 12:02 PM
**Formatted:** Font:Not Bold

Chen Bingzhang 2017/9/26 11:58 AM
**Deleted:** less negative in nutrient-replete wintertime and deep waters, suggesting that enhanced nutrient supply relieved the nutrient competition among phytoplankton species, providing a window for large species to thrive, and thus increasing diversity

Chen Bingzhang 2017/9/26 12:06 PM
**Formatted:** Font:Italic

peak of size diversity in fall in surface waters at S1. The effect of mixing became important because at this time, a subsurface maximum of phytoplankton biomass still existed below the surface mixed layer. With the deepening of surface mixed layer, substantial biomass of phytoplankton was entrained into surface waters and these phytoplankton communities had different trait properties with surface ones, thereby enhancing diversity (*see* Sect. 4.1.1 for discussion).

The model also generated reasonable patterns of Chl:C and N:C ratios, which were largely determined by light and nutrient concentrations (Fig. 10i,j; Fig. 11i,j). Both Chl:C and N:C ratios were high in winter when nutrient concentrations were high and light levels were low due to strong mixing. And both ratios were low in surface stratified waters where nutrient supply from below became diminished due to strong stratification and also light levels became strong due to both increased surface PAR and shallow mixing layers.

### 3.5 Validations of the model at station ALOHA

We used the optimal parameter sets obtained at stations S1 and K2 to run the model at station ALOHA. As there were no data of size-fractionated Chl at ALOHA, we only compared the model outputs of DIN, CHL, NPP, and PON with the observational data. While the modelled profiles of DIN matched well with the observed data, the model underestimated CHL, NPP, and PON, although the qualitative patterns could be reproduced (Fig. 13).

## 4 Discussion

### 4.1 Model merits

#### 4.1.1 Facilitating understanding on ecological mechanisms

Besides the improved computational efficiency (Acevedo-Trejos et al., 2016), the most important advantage of the continuous trait-based ‘adaptive dynamics’ approach is expressed well in the following quote from Bak (1996): “If, following traditional scientific methods, we concentrate on an accurate description of the details, we lose perspective.” (p. 10) and “It is a futile endeavour to try to explain most natural phenomena in detail by starting from particle physics and following the trajectories of all particles.” (p. 5). This modelling approach has the potential to make it much easier to understand the mechanisms regulating phytoplankton diversity, because the functional trait diversity itself (quantified

Chen Bingzhang 2017/9/26 11:59 AM
**Deleted:** . The absolute magnitude of $\frac{d^2\mu(l)}{dl^2}$ positively correlated to $\mu$, indicating that higher growth rates induced greater resource competition. This agrees well with the “dynamic equilibrium theory” proposed by Huston (1979). ... [129]

Bingzhang Chen 2017/9/29 11:57 AM
**Formatted:** Font:Italic

Bingzhang Chen 2017/9/28 12:15 PM
**Formatted:** English (US)

Chen Bingzhang 2017/9/25 2:54 PM
**Deleted:**

Chen Bingzhang 2017/9/16 10:50 PM
**Formatted:** Font:Not Bold

Chen Bingzhang 2017/9/16 10:50 PM
**Formatted:** Indent: First line: 1.18 ch

Chen Bingzhang 2017/9/16 10:50 PM
**Formatted:** Font:Not Bold

Chen Bingzhang 2017/9/16 10:49 PM
**Formatted:** Indent: First line: 0 ch

Chen Bingzhang 2017/9/26 4:47 PM
**Deleted:** T

S. Lan Smith 2017/10/22 11:02 PM
**Deleted:** or the

S. Lan Smith 2017/10/22 11:02 PM
**Deleted:**

S. Lan Smith 2017/10/22 11:02 PM
**Deleted:** can be quoted

S. Lan Smith 2017/10/22 11:03 PM
**Deleted:** also

S. Lan Smith 2017/10/22 11:04 PM
**Deleted:** We believe that t

S. Lan Smith 2017/10/22 11:04 PM
**Deleted:** merit

Chen Bingzhang 2017/9/26 4:48 PM
**Deleted:** overweighs other technical adva ... [130]

Chen Bingzhang 2017/9/26 4:48 PM
**Deleted:** s

S. Lan Smith 2017/10/22 11:04 PM
**Deleted:** can

S. Lan Smith 2017/10/22 11:04 PM
**Deleted:** greatly facilitate

S. Lan Smith 2017/10/22 11:04 PM
**Deleted:** ing

Chen Bingzhang 2017/9/26 4:47 PM
**Deleted:** computational efficiency (Acev ... [131]

by the trait variance) is a tracer in the model, and the sources and sinks of diversity are given explicitly (Eq. 7). In particular, the second derivative of the growth rate, $\frac{d^2\mu(l)}{dl^2}$, evaluated at the mean size, is a proxy for the intensity of resource competition. The more concave is the curve of $\mu(l)$, the more intense is the competition, i.e., the fitness of suboptimal species decreases more steeply with distance from the optimal size. In typical NPZD-type models, phytoplankton species compete for the same nutrients, but this competition is not quantified explicitly by any equation or parameter (as it is in the idealized Lotka–Volterra equations). This makes it more difficult to quantify the dynamics of competition using typical approaches that model the trajectories of many species. Using 'adaptive dynamics', it is easier to quantify competition intensity (and other ecological quantities), which makes it easier to test ecological theories such as Huston's "general hypothesis of species diversity" (Huston, 1979). For example, the absolute magnitude of $\frac{d^2\mu(l)}{dl^2}$ correlates positively with $\mu$ (Fig. 13), indicating that higher growth rates induced greater resource competition. This agrees well with the "dynamic equilibrium theory". Huston (1979) emphasized that in natural environments where equilibrium is rarely achieved, growth rates play a greater role in determining diversity than do steady state competitive abilities as typically quantified by R* values (Tilman, 1982; Litchman et al., 2007). This is because when environmental conditions favour fast growth, it takes less time for the dominant species to predominate, and diversity decreases. The positive correlation between the absolute value of $\frac{d^2\mu(l)}{dl^2}$ and $\mu$ is a mathematical manifestation of the verbal argument in Huston (1979).

Similarly, Eq. 7b specifies the sources and sinks of mean size, making it easy to understanding the factors affecting phytoplankton size. In fact, Eqs. 7a-c can be understood as derived from a Taylor expansion representing an infinite number of discrete trait classes. Hence, even if a discrete version of a diversity model is used, it may be also helpful to calculate the terms in Eqs. 7a-c in order to understand the factors affecting species diversity, biomass, and productivity.

The set of Eqs. 7 also provides an excellent platform to investigate the underlying mechanisms for the relationship between biodiversity and ecosystem functioning (productivity, in this case), which have been extensively studied (Loreau et al., 2001; Tilman et al., 2014). While the negative correlation between productivity ($\mu_{com}$) and diversity suggests that enhanced productivity can induce greater

S. Lan Smith 2017/10/22 11:05 PM
**Deleted:** in terms of

Chen Bingzhang 2017/9/26 4:51 PM
**Deleted:** equations themselves (Eq. 1) have already provided the genuine insights for… ... [132]

S. Lan Smith 2017/10/22 11:06 PM
**Deleted:** for…f diversity have been alrea ... [133]

Chen Bingzhang 2017/8/7 11:06 AM
**Deleted:** For example

S. Lan Smith 2017/10/22 11:06 PM
**Deleted:** at mean size

S. Lan Smith 2017/10/22 11:07 PM
**Deleted:** can be…s conveniently perceiv ... [134]

Chen Bingzhang 2017/8/7 11:11 AM
**Formatted** ... [135]

Bingzhang Chen 2017/10/18 11:45 AM
**Deleted:** since …he fitness of suboptima ... [136]

S. Lan Smith 2017/10/22 11:07 PM
**Deleted:** )… In typical NPZD-type mode ... [137]

Chen Bingzhang 2017/8/8 11:22 AM
**Deleted:** T

Unknown
**Field Code Changed**

S. Lan Smith 2017/10/22 11:15 PM
**Deleted:** positively …orrelates positively withd to…$\mu$ (Fig. 13), indicating that higher growth rates induced greater resource competition. This agrees well with the "dynamic equilibrium theory" proposed by Huston (1979). … Huston (1979) emphasized that in natural environments where equilibrium is rarely achieved, the …rowth rates play a greater role instead of competitive ability (e.g. R*; Litchman et al., 2007) of competing species play a central role ... [138]

Chen Bingzhang 2017/10/23 10:06 AM
**Deleted:** ????

S. Lan Smith 2017/10/22 11:19 PM
**Deleted:** When…his is because when environmental conditions favour high…ast growth rates… it takes less time for the dominant species to predominate, thus…nd reducing diversity ... [139]

S. Lan Smith 2017/10/22 11:20 PM
**Deleted:** also gives…pecifies the sources ... [140]

Chen Bingzhang 2017/8/7 11:32 AM
**Deleted:** In typical NPZD-type models in which phytoplankton species compete for the sam ... [141]

Chen Bingzhang 2017/8/7 11:45 AM
**Deleted:** 1

Chen Bingzhang 2017/9/26 4:58 PM
**Formatted** ... [142]

competition and reduce diversity (Huston, 1979), diversity can certainly be affected by other factors besides competition.

The incorporation of trait diffusion originally developed for continuous trait-based models (Merico et al., 2014) provides a means of representing mutation and other processes that sustain diversity, thus linking ecological and evolutionary processes (Rosenzweig, 1995) and allows control of the level of diversity in simulation experiments such as those conducted herein to investigate diversity-productivity relationships. The increasing effect of trait diffusion with growth rate is consistent with the Metabolic Theory of Ecology, in that metabolic rates, closely coupled with growth rates and generation time, are expected to correlate with mutation rates and affect speciation (Allen et al., 2006; Dowle et al., 2013). Our results have shown that it can be the largest term to balance competitive exclusion (Fig. 13). Without considering this mechanism, diversity could be underestimated in productive waters due to strong competition. This could also contribute to the latitudinal diversity gradient because in warm, tropical regions (ectothermic) organisms tend to growth fast (i.e. short generation time) and therefore have high mutation and speciation rates (Rohde, 1992; Allen et al., 2006; Dowle et al., 2013).

The approach of transporting trait moments across spatial grids, originally developed by Bruggeman (2009), also allows water mixing to affect diversity patterns. Although this approach is not perfect (*see* Sect. 4.2.2 and Fig. 14), it does allow that the mixing of two communities with different mean traits can generate a population with trait variance greater than the weighed mean variance of the two original populations. The larger difference of the mean traits, the greater the increase in trait variance upon mixing. Consider the case of mixing two communities with biomass $P_1$ and $P_2$, mean size $l_1$ and $l_2$, size variance $v_1$ and $v_2$. The biomass and mean size of mixed community are $P_1 + P_2$ and $\frac{P_1 l_1+P_2 l_2}{P_1+P_2}$, respectively. After some algebraic manipulation, we can derive the size variance ($v'$) after mixing:

$$v' = \frac{P_1(l_1^2+v_1)+P_2(l_2^2+v_2)}{P_1+P_2} - \left(\frac{P_1 l_1+P_2 l_2}{P_1+P_2}\right)^2 = \frac{P_1 P_2 (l_1-l_2)^2}{(P_1+P_2)^2} + \frac{P_1 v_1+P_2 v_2}{P_1+P_2} \qquad (15)$$

Thus, it is clear from Eq. (15) that the difference between $v'$ and biomass weighed mean variance $\frac{P_1 v_1+P_2 v_2}{P_1+P_2}$ depends on the difference of mean traits. Hence, mixing can enhance diversity to the extent that the traits of the original communities differ. Barton et al. (2010) have shown that the "hotspots" of

Chen Bingzhang 2017/9/26 5:05 PM
**Deleted:** One insight from the results of the temporal decoupling of growth rate and size diversity on the seasonal scale is that productivity and diversity are not necessarily correlated because the productivity can strongly depend on *current* environmental condition, while diversity emerges over time, depending on standing stocks, which themselves are contingent upon *historical* events.

S. Lan Smith 2017/10/22 11:24 PM
**Deleted:** also …rovides a mechanism sin ... [143]

Chen Bingzhang 2017/9/27 10:57 PM
**Deleted:** evolutionary theory…he Metab ... [144]

S. Lan Smith 2017/10/22 11:28 PM
**Deleted:** since…ecause in warm, tropical ... [145]

Chen Bingzhang 2017/10/23 10:10 AM
**Deleted:** This

Bingzhang Chen 2017/9/28 4:50 PM
**Formatted:** Font:Italic

S. Lan Smith 2017/10/22 11:29 PM
**Deleted:** the …rait variance at least ... [146]

Bingzhang Chen 2017/9/28 3:26 PM
**Formatted** ... [147]

Bingzhang Chen 2017/9/28 4:47 PM
**Formatted:** Right

Bingzhang Chen 2017/9/28 4:48 PM
**Formatted:** Font:Italic

S. Lan Smith 2017/10/22 11:30 PM
**Deleted:** the extent that …ixing can enha ... [148]

high phytoplankton diversity were usually located along areas where mixing was strong enough to allow coexistence of multiple populations with different traits. Our simulations are consistent with that view and show that vertical mixing can significantly enhance diversity, specifically during fall in the surface waters at S1.

### **4.1.2 Flexible stoichiometry**

We also consider realistic phytoplankton physiology and optimized model parameters guided by real data. For example, our model has incorporated some features of phytoplankton plasticity (acclimation) such as variable Chl:C ratio and N:C ratios. Although, for the sake of simplicity, these variable ratios do not directly influence phytoplankton specific growth rate as in Geider et al. (1997), they are able to reproduce the high Chl:C ratios in the DCM layer, thus providing a more realistic mechanism for the formation of the DCM layer than with models that assume fixed ratios (Fennel and Boss, 2003). Similarly, the variable N:C ratio also allows phytoplankton cells to achieve higher carbon-based NPP in surface waters compared to models with fixed N:C ratios (Christian, 2005). Although cellular chlorophyll and nitrogen quota are not calculated as independent tracers, model comparisons suggest that more complex models do not yield better fits to the data (Flynn, 2003).

### **4.1.3 Realistic mechanisms for controlling phytoplankton size structure**

We have provided both bottom-up and top-down mechanisms to affect the size structure of phytoplankton in **CITRATE 1.0**. First, we employ an observation-based unimodal relationship between maximal growth rate and size to give the nanophytoplankton the advantage under nutrient-replete conditions (Chen and Liu, 2010, 2011; Marañón et al., 2013), thus allowing a trade-off between nutrient affinity and maximal growth rate within the pico- and nano-size range. Thus, bottom-up factors alone are sufficient to reproduce the observed decrease in the fraction of small phytoplankton with nutrient enrichment (Marañón et al., 2012). We also impose a size-dependent feeding preference of zooplankton based on the general understanding that smaller microzooplankton tend to prefer smaller phytoplankton, whereas larger mesozooplankton tend to prefer larger phytoplankton (Frost, 1972; Hansen and Hansen, 1994; Liu et al., 2005; Ward et al., 2012). These top-down factors have additional effects on phytoplankton size structure. Our assumption of the preference of microzooplankton on small phytoplankton is similar to Terseleer et al., (2014) and Acevedo-Trejos et al., (2015), who assumed a

S. Lan Smith 2017/10/22 11:31 PM
**Deleted:** were…as strong enough to allow ... [149]

Bingzhang Chen 2017/9/28 3:06 PM
**Formatted:** Font:Bold

Bingzhang Chen 2017/9/28 3:06 PM
**Formatted:** Font:Bold

Bingzhang Chen 2017/9/28 3:05 PM
**Formatted:** Indent: First line: 0 ch

Chen Bingzhang 2017/8/7 11:47 AM
**Deleted:** By solving these theoretical differential equations under quasi-realistic ocean conditions, we can evaluate the relative roles of each mechanism that structures the community properties mentioned above.

Bingzhang Chen 2017/9/28 4:58 PM
**Deleted:** Although any model is necessarily an abstraction of the real world, to avoid being too far away from reality, w

Chen Bingzhang 2017/8/29 5:05 PM
**Deleted:** ed

S. Lan Smith 2017/10/22 11:32 PM
**Deleted:** acclimatory …lasticity (acclima ... [150]

Bingzhang Chen 2017/9/28 3:07 PM
**Formatted:** Font:Bold

Bingzhang Chen 2017/9/28 3:06 PM
**Formatted:** Indent: First line: 0 ch

Chen Bingzhang 2017/8/29 5:48 PM
**Formatted:** Font:Bold

Bingzhang Chen 2017/9/29 2:47 PM
**Deleted:** **1.0**

Chen Bingzhang 2017/10/23 9:59 AM
**Deleted:** **1.1….0**. FirstInstead… we empl ... [151]

S. Lan Smith 2017/10/22 11:34 PM
**Deleted:** the …ottom-up factors alone sh ... [152]

Chen Bingzhang 2017/8/29 5:01 PM
**Deleted:** Compared to previous continuous trait-based models (Terseleer et al., 2014; Acevedo-Trejos et al., 2015, 2016), **CITRATE** 1.0. ... [153]

S. Lan Smith 2017/10/22 11:35 PM
**Deleted:** the …maller microzooplankton ... [154]

Chen Bingzhang 2017/8/29 5:35 PM
**Deleted:**

S. Lan Smith 2017/10/22 11:35 PM
**Deleted:** in which they

combination of decreasing maximal phytoplankton growth rate with increasing size and the grazing preference on small phytoplankton in order to offset the growth advantage of small phytoplankton in eutrophic waters. In our case, small phytoplankton lose the advantage in eutrophic waters, where larger phytoplankton grow faster because of the imposed unimodal relationship between maximal growth rate and size. Meanwhile, in eutrophic waters, mesozooplankton dominate and preferentially feed on larger phytoplankton to balance the growth advantages of larger cells.

Interestingly, counter to our intuition, field incubation experiments have often found that microzooplankton feed on diatoms faster than on picophytoplankton, and that diatoms grow faster than picophytoplankton even in oligotrophic waters (Latasa et al., 1997; Zhou et al., 2015). These results raise a paradoxical question: "How can diatoms grow so fast with negligible nutrients in oligotrophic waters, but without accumulating high biomass?" Whether this is because of experimental bias is an open question. Although the feeding preference of mesozooplankton on large prey seems less disputable (Frost, 1972; Liu et al., 2005) (but *see* Terseleer et al., (2014) for an assumption of decreasing feeding preference of copepods on large diatoms), it implies strong top-down control of large phytoplankton in eutrophic waters where mesozooplankton dominate, limiting the biomass of large phytoplankton. This is at odds with the common observation that large phytoplankton dominate total biomass in eutrophic waters (Marañón et al., 2012). Future refinements might include a unimodal feeding preference, similar to the grazing kernel proposed earlier (Hansen and Hansen, 1994; Poulin and Franks, 2010). In any case, more and better zooplankton data are much needed for model calibration and validation.

## 4.2 Model limitations

### 4.2.1 Assumption of trait distribution

To facilitate calculation of trait moments, a certain distribution has to be assumed for the trait (Merico et al., 2009; 2014). In the literature, phytoplankton abundance (and also biomass) is usually modelled as a power-law function of cell size (Gin et al., 1999; Cavender-Bares et al., 2001; Cermeño et al., 2006). The slope of log abundance versus log size (e.g. cell volume) tends to be between –0.7 and –1 (Cermeño et al., 2006), suggesting that the slope of log biomass versus log size should be between 0 and 0.3. However, aside from fact that the power-law distribution is unrealistic in predicting phytoplankton

S. Lan Smith 2017/10/22 11:36 PM
**Deleted:** a …ecreasing maximal phytopla ... [155]

Bingzhang Chen 2017/9/28 5:06 PM
**Deleted:** oligotrophic

S. Lan Smith 2017/10/22 11:37 PM
**Deleted:** the growth superiority of …mal ... [156]

Bingzhang Chen 2017/9/28 5:07 PM
**Deleted:** oligotrophic…utrophic waters, ... [157]

S. Lan Smith 2017/10/22 11:37 PM
**Deleted:** disappears due to the

Bingzhang Chen 2017/9/28 5:09 PM
**Deleted:** so that the grazing preference of microzooplankton on small phytoplankton is necessarily weaker

S. Lan Smith 2017/10/22 11:38 PM
**Deleted:** ….Meanwhile, in eutrophic wat ... [158]

S. Lan Smith 2017/10/22 11:40 PM
**Deleted:** opposite…ounter to our intuitio ... [159]

Bingzhang Chen 2017/9/28 5:22 PM
**Deleted:** fast-growing

S. Lan Smith 2017/10/22 11:40 PM
**Deleted:** also …row faster than picophyt ... [160]

Chen Bingzhang 2017/8/30 10:33 AM
**Formatted:** Font:Italic

S. Lan Smith 2017/10/22 11:43 PM
**Deleted:** will lead to…mplies strong top- ... [161]

Chen Bingzhang 2017/8/30 11:02 AM
**Formatted:** Font:Not Bold

S. Lan Smith 2017/10/22 11:44 PM
**Deleted:** rther

Bingzhang Chen 2017/9/28 5:23 PM
**Deleted:** Another feeling from such modeling exercise is that

S. Lan Smith 2017/10/22 11:44 PM
**Deleted:** addition

Chen Bingzhang 2017/8/29 5:06 PM
**Deleted:** Instead, we employ an observation-based unimodal relationship between maximal growth rate and size to give the large phytoplankton the advantage under nutrient-replete conditions (Chen and Liu, 2010, 2011; Marañón et al., 2013), thus allowing a tradeoff between nutrient affinit ... [162]

Chen Bingzhang 2017/8/29 5:42 PM
**Formatted:** English (US)

Bingzhang Chen 2017/9/28 5:25 PM
**Formatted:** Indent: First line: 0 ch

Bingzhang Chen 2017/9/28 12:16 PM
**Formatted** ... [163]

biomass at the size limits (there must be upper and lower limits of size at which phytoplankton biomass becomes zero, which the power-law cannot reproduce), the power-law distribution is much more inconvenient for mathematical manipulations (e.g. calculating mean and variance) compared to the normal distribution. The lognormal distribution is a much better alternative for phytoplankton size in terms of mathematic properties (e.g., zero probability of negative size) and can be fit well to empirical data (Quintana et al., 2008). Therefore, it is not surprising that the lognormal distribution has been widely used in continuous size models (Terseleer et al., 2014; Acevedo-Trejos et al., 2015, 2016; Smith et al., 2016).

However, this does not guarantee that a fixed probability distribution can hold for all situations (Coutinho et al., 2016). In oligotrophic waters where picophytoplankton, particularly the unicellular cyanobacteria *Prochlorococcus* and *Synechococcus*, dominate (Campbell et al., 1994; Liu et al., 1997), the distribution of phytoplankton log size is more likely right skewed. In other words, abundances of large species are higher than expected from a pure lognormal distribution, which is consistent with the observation that some large diatoms, with significant contributions to new production, can be found in the oligotrophic gyres (Villareal et al., 1999). This is probably one major reason that our model tends to underestimate the fraction of $> 10\ \mu$m size. This is an inevitable consequence of aggregating the description of the entire community into only the three descriptors (i.e. total biomass, mean and variance), which reduces the degrees of freedom, thus sacrificing detailed accuracy for generality and perspective.

One remedy for this problem might be to assign more functional groups in phytoplankton and assume a lognormal distribution for each group, respectively (Terseleer et al., 2014). Having a number of functional groups also circumvents the problem of size-independent functional differences among phytoplankton, such as the different maximal growth rates of diatoms and dinoflagellates despite their similar sizes (Chen and Laws, 2017). We expect that in the near future such a combination of continuous trait distributions and functional groups will likely provide more realistic representations of marine phytoplankton diversity.

**4.2.2 Transport of moments**

Bingzhang Chen 2017/9/28 5:28 PM
**Deleted:** close to

S. Lan Smith 2017/10/22 11:45 PM
**Deleted:** which cannot be predicted by

S. Lan Smith 2017/10/22 11:46 PM
**Deleted:** in terms of

S. Lan Smith 2017/10/22 11:46 PM
**Deleted:** than

Chen Bingzhang 2017/8/7 4:07 PM
**Deleted:** A

Chen Bingzhang 2017/8/7 4:05 PM
**Deleted:** usually appropriate

Chen Bingzhang 2017/8/7 4:07 PM
**Deleted:** Finkel, 2007

Chen Bingzhang 2017/8/7 4:11 PM
**Deleted:** ;

Chen Bingzhang 2017/8/7 4:15 PM
**Formatted:** Indent: First line: 1.18 ch

S. Lan Smith 2017/10/22 11:47 PM
**Deleted:** type of

S. Lan Smith 2017/10/22 11:47 PM
**Deleted:** of the

Chen Bingzhang 2017/8/7 3:42 PM
**Formatted:** English (US)

S. Lan Smith 2017/10/22 11:48 PM
**Deleted:** ces

S. Lan Smith 2017/10/22 11:48 PM
**Deleted:** of

S. Lan Smith 2017/10/22 11:48 PM
**Deleted:** between

S. Lan Smith 2017/10/22 11:48 PM
**Deleted:** that may have

S. Lan Smith 2017/10/22 11:49 PM
**Deleted:** the

S. Lan Smith 2017/10/22 11:49 PM
**Deleted:** (i.e. discrete trait distributions) can

S. Lan Smith 2017/10/22 11:50 PM
**Deleted:** give more

S. Lan Smith 2017/10/22 11:50 PM
**Deleted:** accounts

Another potential problem is the transport of trait moments in ocean circulation models. Unlike nutrients or plankton biomass, trait moments are not real "concentrations" that can be directly involved in advection and diffusion. The immediate summation of two Gaussian curves with different areas (representing the total biomass), mean, and variance is usually not another perfect Gaussian curve (Fig. 14a). Bruggeman (2009) has derived that, if following the assumption of normal distribution of traits, the raw moments of the biomass distribution can behave as normal tracers in GCMs. We have shown a few examples of mixing of communities of different biomass, mean size, and size variance in Fig. 14. These examples demonstrate that when the mean sizes and size variances differ greatly and biomasses are similar, the mixed community may deviate from the assumed normal distribution, making this a poor approximation. For now, we assume that across adjacent grids, phytoplankton communities should be similar enough for this approximation to work reasonably well.

### 4.2.3 Lack of multiple traits

As a first step, we incorporated only size as the master trait that affects all physiological functions of phytoplankton. In reality, many phytoplankton functional traits, such as optimal temperature, $N_2$ fixation, and mixotrophy, are independent of size. For example, the optimal growth temperature of phytoplankton is closely related to environmental temperature, but only weakly relates to size (Thomas et al., 2012; Chen, 2015). The optimal growth temperature and irradiances are certainly function traits that deserve to be incorporated into trait-based models (Follows et al., 2007; Norberg, 2004; Edwards et al., 2015) and are expected to strongly affect phytoplankton functional identity and diversity at large scales.

### 4.2.4 Difficulty in modelling surface peaks of NPP at oligotrophic stations

The near-surface peak of NPP at the oligotrophic stations S1 and ALOHA during summer is not expected if we assume that the source of nutrients comes from below the euphotic zone. Even if variable N:C ratios are used in the model to allow more carbon to be fixed given the same amount of nitrogen near surface waters, surface NPP is still likely to be underestimated even with the presence of $N_2$ fixation because of phosphorus limitation (Christian, 2005). It is possible that other mechanisms such as vertical migration of phytoplankton need to be taken into account (Villareal et al., 1999; Chavez et al., 2012). Therefore, this problem is not only restricted to **CITRATE** 1.0.

Bingzhang Chen 2017/9/28 5:34 PM
**Deleted:** certainly …sually not another p ... [164]

Chen Bingzhang 2017/8/7 4:41 PM
**Deleted:** A schematic diagram is shown in

S. Lan Smith 2017/10/22 11:51 PM
**Deleted:** raw moments

Bingzhang Chen 2017/9/28 5:35 PM
**Deleted:** Fig. 12b shows an to represent one example of such approximationa water mass mixed with a small fraction of an adjacent water mass, which seems to work well to the first order, which seems to work well to the first order. Therefore, the robustness of such approximation depends on the difference of phytoplankton biomass in the present grid and that transported from adjacent grids into the present grid. Since within the mixed layer, the three quantities (*P*,

Bingzhang Chen 2017/9/28 10:31 PM
**Formatted** ... [165]

Unknown
**Field Code Changed**

Bingzhang Chen 2017/9/28 5:35 PM
**Deleted:** $\bar{l}$

S. Lan Smith 2017/10/22 11:51 PM
**Deleted:** From t…hese examples, we cou ... [166]

Bingzhang Chen 2017/9/28 5:35 PM
**Deleted:** , and

Bingzhang Chen 2017/9/28 10:31 PM
**Formatted:** Font:Not Bold

S. Lan Smith 2017/10/22 11:52 PM
**Deleted:**

Bingzhang Chen 2017/9/28 5:35 PM
**Deleted:** $v$) should be similar due to strong mixing, the approximation is not a big concern. The problem mainly lies at the bottom of the mixed layer where there is a sharp gradient of phytoplankton properties particularly biomass (Fig. 12c). We can roughly estimate that, based on the eddy di ... [167]

Chen Bingzhang 2017/8/7 4:50 PM
**Formatted** ... [168]

Bingzhang Chen 2017/9/28 10:40 PM
**Deleted:** should work wellbe reliable in most cases

Chen Bingzhang 2017/8/8 10:58 AM
**Deleted:** and may potentially be a conce ... [169]

Bingzhang Chen 2017/9/28 10:42 PM
**Deleted:** **S1**

Bingzhang Chen 2017/9/29 2:47 PM
**Deleted:** 1.0

Chen Bingzhang 2017/10/23 9:59 AM
**Deleted:** 1.1

### 4.2.5 Optimized parameters for 3D GCM

One purpose of finding a common parameter set optimized to two stations with contrasting environmental conditions is to use this parameter set for 3D GCMs with the expectation that, since this parameter set can work for the two stations, it should work for other stations as well. However, our validation exercise at station ALOHA reveals that the parameter set optimized for stations K2 and S1 only succeeds in matching the DIN data well, but underestimates CHL, NPP and PON at station ALOHA. This suggests that we might be overlooking some unique but important processes at ALOHA. Alternatively, it is also possible that the uneven sampling at K2 and S1 might bias the parameter optimisation to some extent. Similar difficulties in parameter optimisation have been shown previously (Ward et al., 2010). For optimising parameters for 3D GCMs, a better approach might be to use the “Transport Matrix” technique that has been successfully implemented for some biogeochemistry models (Khatiwala, 2007; Kriest et al., 2017). Nonetheless, our optimized parameters can provide a useful initial estimate for modelling other stations and for use in 3D GCMs.

### 4.3 Future directions

Considering the above limitations, one future direction is to increase the number of traits in the model to generate more realistic phytoplankton diversity patterns, which requires both an “envelope” function relating the maximal growth rate with the optimal trait value and a relationship between growth rate and trait value for each species (Norberg, 2004). Another refinement as noted above is to model a continuous trait distribution for each functional group, respectively, thus combining the continuous trait-distribution and functional group approaches to better capture deviations of overall trait distributions from normality.

It is relatively easy to couple the one-dimensional **CITRATE** model with 3D global or regional ocean models, thus providing a means to model the large-scale patterns of phytoplankton size and size diversity. Furthermore, it should be possible in the near future to optimize parameters for such a 3D model using the “transport matrix” technique. In particular, by including both trait diffusion and competitive exclusion it may be possible to begin to untangle the relative roles of ecological versus evolutionary processes in shaping global phytoplankton diversity patterns.

Bingzhang Chen 2017/9/28 10:41 PM
**Deleted:** **Deficiency of the external physics driver**

Bingzhang Chen 2017/9/28 11:08 PM
**Formatted:** Indent: First line: 1.77 ch

Bingzhang Chen 2017/10/18 11:47 AM
**Deleted:** disappointingly

Bingzhang Chen 2017/10/18 11:49 AM
**Formatted:** Font:Not Bold, (Asian) Chinese (PRC), (Other) English (US)

Bingzhang Chen 2017/9/28 10:43 PM
**Deleted:** We note that various aspects of the external environmental drivers such as vertical mixing coefficients ($K_v$) and iron deposition rates may still have some deficiencies that can bias model results and parameter optimization. For example, it is puzzling that although the MLDs derived from $K_v$ seemed consistent with *in situ* temperature and salinity profiles (Fig. 2b), they were usually shallower than the observed nutricline from spring to fall at station S1. It is also possible that this problem arose because certain aspects of phytoplankton biology such as the varying adaptive response to light (Moore et al., 1998) were not included in the model. For example, we expect that including another functional group adapted to low light environments would deepen the nutricline.

S. Lan Smith 2017/10/22 11:55 PM
**Deleted:** each functional group with

S. Lan Smith 2017/10/22 11:55 PM
**Deleted:** -based model

S. Lan Smith 2017/10/22 11:55 PM
**Deleted:** mixing

S. Lan Smith 2017/10/22 11:55 PM
**Deleted:** discrete trait

S. Lan Smith 2017/10/22 11:56 PM
**Deleted:** trait distributions that

S. Lan Smith 2017/10/22 11:56 PM
**Deleted:** e

S. Lan Smith 2017/10/22 11:57 PM
**Deleted:** and later optimising

S. Lan Smith 2017/10/22 11:57 PM
**Deleted:** the

S. Lan Smith 2017/10/22 11:57 PM
**Deleted:** with

## 5. Conclusions

- We present a 1D model with continuous size distribution for phytoplankton (**CITRATE**). The dynamics of phytoplankton mean size and size variance are directly linked to environmental factors and moments of the size distribution (Eq. 7), facilitating understanding of the underlying mechanisms controlling phytoplankton size and diversity. **CITRATE** 1.0 also incorporates "trait diffusion" as an eco-evolutionary process to sustain phytoplankton diversity.
- We optimized the parameters of **CITRATE** using the DRAM algorithm, which revealed that the model can faithfully reproduce observed seasonal patterns of inorganic nitrogen, Chl *a*, and phytoplankton size structure at two contrasting time-series stations. The model structure and associated parameters obtained herein can be useful for 3D regional and global ocean modelling.
- The limitations of **CITRATE** include its assumption of a lognormal distribution for phytoplankton size as the sole master trait, which to some extent limits the precision with which it can reproduce large size classes of phytoplankton. These limitations and others may be overcome in future studies by building on **CITRATE** 1.0 to construct more elaborate continuous trait-distribution models capable of reproducing more realistic patterns of phytoplankton diversity.

## 6. Code and data availability

The code and data of **CITRATE** 1.0 are freely available at: https://github.com/BingzhangChen/citrate under the MIT license.

### 6.1 General instruction

Tutorial: The code for CITRATE 1.0 (DOI: 10.5281/zenodo.1034805) is written in Fortran90 with the Intel Fortran compiler used. We have tested the codes on macOS Sierra 10.12.5 (i386 processor) and also a GNU/Linux cluster with x86-64 architechture. The user is supposed to be familiar with the Fortran language and has some basic knowledge of BASH. Some post-processing scripts are also written in the free software R (version 3.3.2). Before compiling the codes and running the model, the user needs to install the mpi (e.g. openmpi) library for parallel computation. Below we give some instructions and explanations of the codes and how to run the model.

S. Lan Smith 2017/10/22 11:58 PM
**Deleted:** in

S. Lan Smith 2017/10/22 11:58 PM
**Deleted:** (

Chen Bingzhang 2017/9/13 3:41 PM
**Deleted:** 1

Bingzhang Chen 2017/9/29 2:47 PM
**Deleted:** 1.0

Chen Bingzhang 2017/10/23 9:59 AM
**Deleted:** 1.1

S. Lan Smith 2017/10/22 11:59 PM
**Deleted:** .

S. Lan Smith 2017/10/22 11:59 PM
**Deleted:** models

S. Lan Smith 2017/10/23 12:01 AM
**Formatted:** Tabs:Not at 10.04 ch

S. Lan Smith 2017/10/22 11:59 PM
**Deleted:** shortcomings

S. Lan Smith 2017/10/23 12:00 AM
**Deleted:** ... [170]

S. Lan Smith 2017/10/23 12:02 AM
**Deleted:** continuous trait-based models can be built

Bingzhang Chen 2017/9/29 2:47 PM
**Deleted:** 1.0

Chen Bingzhang 2017/10/23 9:59 AM
**Deleted:** 1.1

S. Lan Smith 2017/10/23 12:03 AM
**Deleted:** e

S. Lan Smith 2017/10/23 12:03 AM
**Deleted:** , for example by accounting for multi-dimensional trait distributions

Chen Bingzhang 2017/10/23 9:59 AM
**Deleted:** 1.1

Bingzhang Chen 2017/9/29 2:44 PM
**Deleted:** 0

Chen Bingzhang 2017/9/20 3:19 PM
**Deleted:** NPZDFeCONT

Chen Bingzhang 2017/10/23 9:59 AM
**Deleted:** 1

Bingzhang Chen 2017/9/29 2:44 PM
**Deleted:** 0

Chen Bingzhang 2017/10/23 4:28 PM
**Deleted:** 999151

Bingzhang Chen 2017/9/29 2:45 PM
**Deleted:** 895996

1) Go to the directory you want to run the model (we assume that the root directory is under home directory: ~/).

2) To download the codes, type: "git clone https://github.com/BingzhangChen/citrate.git".

3) Type: "cd DRAM/NPZDcont/BOTH_TD" to go to the working directory.

4) Type: "vi run" to change the setting for model run:

Test = 0 means a fast run, usually for a formal model run for a large number of iterations. Test = 1 means running a model for debugging, which is much slower than the fast run. The user can also modify the compiler flags depending on the purpose in the script. The user needs to confirm the directory where the library of mpifort exists.

5) Type "./run", the model will compile and an executable (CITRATE) will be generated.

6) Type "vi Model.nml", which contains two namelists. The namelist &Model contains the options for station names, the type of ecological model, the type of nutrient uptake function (1 only for CITRATE), and the type for grazing function (four different grazing functions including the three Holling type functions and the Ivlev function). The station name determines the right physics files to be read and the filenames for model output. For now we only allow three possible stations: S1, K2, and HOT. Other station names will generate an error. If the user wants to add more station names, the subroutine Setup_OBSdata within MOD_1D.f90 is the place to be modified. A number of ecological models besides **CITRATE** have been developed. It is beyond the scope of the present study to describe all of them in detail. Just note that the model lists are in the fortran file bio_MOD.f90 and some other details are in choose_model.f90 and MOD_1D.f90.

The namelist &MCMCrun contains the options for defining the total length of the MCMC chain which is at least 2, the number of the ensemble runs, the number of days for each model run, whether the model should start from previous runs (Readfile = 1) or start a new run (Readfile = 0), and the number of runs in the historical files (enssig and enspar).

7) After defining all the model settings, type “mpirun –np 5 citrate” and then the model will run with 5 parallel processes and some outputs will be shown on the screen. Type “mpirun –np 5 citrate > out” to make the model outputs stored in the “out” file. For each model run, the model saves the current parameters into the “enspar” file and the current values of $\sigma$ and $SSqE$ into the ‘enssig’ file. In this way,

Bingzhang Chen 2017/9/28 2:28 PM
**Deleted:** 1. How to run the model:

Chen Bingzhang 2017/9/20 3:22 PM
**Formatted:** Font:Bold

Bingzhang Chen 2017/9/28 2:29 PM
**Deleted:** ./

Bingzhang Chen 2017/9/28 2:30 PM
**Deleted:** ./

Bingzhang Chen 2017/9/28 2:31 PM
**Formatted:** Font:Italic

Bingzhang Chen 2017/9/28 2:30 PM
**Formatted:** Font:Italic

Bingzhang Chen 2017/9/28 2:30 PM
**Deleted:** *s*

even if the model crashes, the user can pick up the current parameter position and updated parameter covariance matrix. The model also generates the files of best parameters, best $\sigma$ and *SSqE* files, best model output files that correspond to observational data, and model output files at daily resolution at each grid after an ensemble run.

For each station, four different physics forcing data including vertical profiles of eddy diffusive coefficients and temperatures, surface PAR and atmospheric dust deposition. We already provided the relevant data for stations S1 and K2. The temporal resolution is one day for the vertical eddy diffusivity and one month for three other types of data.

**6.2 Code structure**

All the source files including the makefile are stored in the *src* folder. Here we briefly describe the functions of the most important source files:

- Main.f90: The main program for DRAM that calls each subroutine in serial.

- MOD_1D.f90: The major module that sets up and runs the 1D model. The module also generates model output that matches with the observational data.

- Interface_MOD.f90: the module that initializes the absolute and normalized parameter vectors, the covariance matrix of the parameters, the prior parameter values, and the upper and lower parameter boundaries.

- SUB_MOD.f90: the module that calculates sum of squared errors (SSqE) between model outputs and observational data. This module also contains the I/O subroutines that save the parameters, $\sigma$, and SSqE for each iteration. It also contains the major subroutine MCMC_adapt that determines whether to accept new parameters, updates covariance matrix, proposes new parameter vectors and calls the subroutine that runs the 1D model with the newly proposed parameters.

- choose_model.f90: the subroutine that defines the number and indices of tracers and the model outputs that need to be written into the output file.

Bingzhang Chen 2017/9/28 2:31 PM
**Formatted:** Font:Italic

Bingzhang Chen 2017/9/28 2:31 PM
**Formatted:** Font:Italic

Bingzhang Chen 2017/9/28 2:31 PM
**Formatted:** Indent: First line: 2.36 ch

Chen Bingzhang 2017/9/20 3:19 PM
**Deleted:** The code for **CITRATE** 1.0 is written in Fortran90 with the Intel Fortran compiler used. The running environment is Linux or Unix. The user is supposed to be familiar with the Fortran lar ... [171]

Bingzhang Chen 2017/9/28 12:16 PM
**Formatted:** English (US)

Bingzhang Chen 2017/9/28 12:16 PM
**Formatted:** English (US)

Bingzhang Chen 2017/9/28 12:16 PM
**Formatted:** English (US)

- NPZD_cont.f90: the major biological subroutine for the CITRATE model.

- bio_MOD.f90: the module that declares most of the model names, indices for model input and output variables and parameters.

Bingzhang Chen 2017/9/29 11:58 AM
**Formatted:** Justified, Line spacing: 1.5

Bingzhang Chen 2017/9/29 11:58 AM
**Deleted:**

Table 1. Fixed parameters of the **CITRATE** 1.0 model.

| Symbol | Description | Value | Unit |
|---|---|---|---|
| $K_w$ | Light attenuation coefficient of seawater | $0.04^{a}$ | $m^{-1}$ |
| $K_{chl}$ | Light attenuation coefficient of chlorophyll | $0.025^{a}$ | $(mg\ Chl\ a\ m^{-2})^{-1}$ |
| $E_p$ | Activation energy of phytoplankton rates | $0.41^{b}$ | eV |
| $E_z$ | Activation energy of heterotrophic rates | $0.65^{b}$ | eV |
| $\theta_{min}$ | Minimal chlorophyll-to-carbon ratio | $0.02^{c}$ | gChl $molC^{-1}$ |
| $\theta_{max}$ | Maximal chlorophyll-to-carbon ratio | 0.47 | gChl $molC^{-1}$ |
| $unass_1$ | Fraction of unassimilated food by microzooplankton | $0.24^{d}$ | dimensionless |
| $unass_2$ | Fraction of unassimilated food by mesozooplankton | $0.31^{e}$ | dimensionless |
| $NGE$ | Net growth efficiency of zooplankton | $0.3^{d}$ | dimensionless |
| $R_{dn}$ | Conversion rate of detritus to inorganic nitrogen | 0.1 | $d^{-1}$ |
| $l_{fe}$ | Total iron ligand concentration | $0.6^{f}$ | nM |
| $K_{scm}$ | Minimal iron scavenging rate | $5 \times 10^{-3\ f}$ | $d^{-1}$ |
| $K_{sc}$ | Particle dependent scavenging rate | $0.03^{f}$ | $(\mu M\ N)^{-1}\ d^{-1}$ |
| $R_{Fe\_N}$ | Plankton iron-to-nitrogen ratio | 0.0265 | nM:$\mu$M |
| $\alpha_\mu$ | First-order size scaling component for $\mu_m$ | $0.2^{b}$ | $(\ln \mu m^3)^{-1}$ |
| $\beta_\mu$ | Second-order size scaling component for $\mu_m$ | $-0.01^{b}$ | $(\ln \mu m^3)^{-2}$ |
| $\alpha_K$ | Size scaling exponent for $K_N$ | $0.27^{g}$ | $(\ln \mu m^3)^{-1}$ |
| $\alpha_{fer}$ | Size scaling exponent for $K_{fer}$ | $0.27^{g}$ | $(\ln \mu m^3)^{-1}$ |
| $Q_{0N}$ | Phytoplankton minimal N:C ratio | 0.06 | mol N: mol C |
| $g_{max,1}$ | Maximal microzooplankton specific ingestion rate for phytoplankton of 1.24 $\mu$m (1 $\mu m^3$) at 15 ºC | $1.35^{h}$ | $d^{-1}$ |
| $g_{max,2}$ | Maximal mesozooplankton specific ingestion rate for phytoplankton of 10 $\mu$m at 15 ºC | $0.53^{h}$ | $d^{-1}$ |
| $K_{p,2}$ | Grazing half-saturation constant of mesozooplankton | $0.5^{h}$ | $\mu$M N |
| $b_1$ | Size-dependent feeding selectivity of microzooplankton | -0.05 | $(\ln \mu m^3)^{-1}$ |
| $b_2$ | Size-dependent feeding selectivity of mesozooplankton | 0.02 | $(\ln \mu m^3)^{-1}$ |

[a]Fennel et al., (2006); [b]Chen and Laws, (2017); [c]Flynn, (2003); [d]Buitenhuis et al., (2010); [e]Buitenhuis et al. (2006); [f]Nickelsen et al., (2015); [g]Ward et al., (2012); [h]Chai et al., (2002).

Chen Bingzhang 2017/9/13 3:02 PM
**Deleted:** including units and values

Bingzhang Chen 2017/9/29 2:47 PM
**Deleted:** 1.0

Chen Bingzhang 2017/10/23 9:59 AM
**Deleted:** 1.1

Chen Bingzhang 2017/9/13 3:02 PM
**Formatted:** Line spacing: 1.5 lines

Chen Bingzhang 2017/9/13 1:51 PM
**Deleted:** 5

Chen Bingzhang 2017/9/13 1:57 PM
**Deleted:** 5

Chen Bingzhang 2017/9/13 2:38 PM
**Deleted:** *Unass*

Chen Bingzhang 2017/9/13 2:40 PM
**Deleted:** $K_p$ ... [172]

Chen Bingzhang 2017/9/13 2:59 PM
**Deleted:**

Chen Bingzhang 2017/9/13 2:59 PM
**Deleted:** $^{d}$

Chen Bingzhang 2017/9/13 1:49 PM
**Deleted:** 3

Chen Bingzhang 2017/9/13 1:49 PM
**Deleted:** $^{5}$

Chen Bingzhang 2017/9/13 2:59 PM
**Deleted:** $^{d}$

Chen Bingzhang 2017/9/13 2:59 PM
**Deleted:** $^{d}$

Chen Bingzhang 2017/9/13 3:04 PM
**Formatted:** Superscript

Chen Bingzhang 2017/9/13 3:02 PM
**Formatted:** Line spacing: 1.5 lines

Chen Bingzhang 2017/9/13 3:06 PM
**Formatted:** Superscript

Chen Bingzhang 2017/9/13 3:06 PM
**Formatted:** Superscript

Table 2. Parameters optimized by the DRAM algorithm. The values inside the parentheses of the initial values indicate the "hard" boundaries for the parameters. The numbers inside the parentheses of the optimized values indicate the standard deviation after the first 10000 iterations have been removed.

| Symbol | Description | Initial | Optimized | Unit |
|---|---|---|---|---|
| $W_d$ | Sinking rate of detritus | 4 (1, 20) | 19.6 (1.0) | m $d^{-1}$ |
| $K_p$ | Grazing half-saturation constant of microzooplankton | 0.5 (0.05, 2) | 0.28 (0.01) | $\mu$M N |
| $m_z$ | Coefficient of mortality rate of mesozooplankton | 0.1 (0.05, 0.2) | 0.20 (0.002) | $(\mu M\ N)^{-1}\ d^{-1}$ |
| $\alpha_{0,c}$ | Initial slope of photosynthesis versus light at 1 $\mu m^3$ | 0.055[a] (0.01, 0.1) | 0.05 (0.004) | $(W\ m^{-2})^{-1}\ d^{-1}$ |
| $\alpha_I$ | Size scaling exponent for $\alpha_c$ | -0.1 (–0.3, 0.1) | -0.26 (0.01) | $(\ln \mu m^3)^{-1}$ |
| $K_{0,N}$ | Growth half-saturation constant for nitrogen for a phytoplankton cell of 1 $\mu m^3$ | 0.2[b] (0.05, 0.5) | 0.29 (0.03) | $\mu$M N |
| $\mu'_{0,m}$ | Phytoplankton maximal growth rate at 1 $\mu m^3$ at 15 ºC | 1.2[c] (0.3, 2.7) | 0.85 (0.05) | $d^{-1}$ |
| $K_{0,fer}$ | Growth half-saturation constant for iron of phytoplankton with 1 $\mu m^3$ | 0.08[d] (0.02, 0.2) | 0.17 (0.02) | nM Fe |
| $u$ | Trait diffusion parameter | 0.08[e] (0, 0.1) | 0.1 (0.0008) | $d^{-1}\ (\ln \mu m^3)^{-2}$ |

[a]Fennel et al., (2006); [b]Ward et al., (2012); [c]Flynn et al., (2016); [d]Gregg et al., (2003); [e]Merico et al., (2014).

**Deleted:** "burn-in" period…(…02…00 ... [173]

Chen Bingzhang 2017/9/13 3:14 PM

**Deleted:** 1…(0.0…, 21 ... [174]

Chen Bingzhang 2017/9/13 3:17 PM

**Deleted:** 3.3…(1.00.3 ... [175]

Chen Bingzhang 2017/9/13 2:36 PM

**Deleted:** $Q_{0N}$ ... [176]

Chen Bingzhang 2017/9/22 2:06 PM

**Deleted:** 3

Chen Bingzhang 2017/9/13 3:20 PM

**Deleted:** 094…(0.00202 ... [177]

Chen Bingzhang 2017/9/13 3:34 PM

**Deleted:** $^b$

Chen Bingzhang 2017/9/13 3:20 PM

**Deleted:** 19…(0.00413 ... [178]

Chen Bingzhang 2017/9/13 3:39 PM

**Deleted:** 0.08…(–0.3, 0.12 ... [179]

Chen Bingzhang 2017/9/13 3:20 PM

**Deleted:** 0.097…(0.01017 ... [180]

Chen Bingzhang 2017/9/13 3:21 PM

**Deleted:** dimensionless

Chen Bingzhang 2017/9/13 3:26 PM

**Deleted:** 5…(0.0501… 0.53 ... [181]

Chen Bingzhang 2017/9/13 3:22 PM

**Deleted:** 0.89…(0.031 ... [182]

Chen Bingzhang 2017/9/13 2:36 PM

**Deleted:** $\alpha_K$ ... [183]

Chen Bingzhang 2017/9/13 3:36 PM

**Deleted:** $^d$…(0.3, 2.73 ... [184]

Chen Bingzhang 2017/9/14 2:56 PM

**Deleted:** 1.34…(0.0518 ... [185]

Chen Bingzhang 2017/9/13 2:36 PM

**Deleted:** $\alpha_\mu$ ... [186]

Chen Bingzhang 2017/9/13 3:36 PM

**Deleted:** $^f$…(0.024 ... [187]

Chen Bingzhang 2017/9/22 11:42 AM

**Deleted:** 058…(0.00…1 ... [188]

Chen Bingzhang 2017/9/13 2:36 PM

**Deleted:** $\alpha_{fer}$ ... [189]

Chen Bingzhang 2017/9/13 3:36 PM

**Deleted:** $^g$…(0.01… 0.12 ... [190]

Chen Bingzhang 2017/9/13 3:25 PM

**Deleted:** 092…(0.00…0816 ... [191]

Chen Bingzhang 2017/9/13 3:33 PM

**Deleted:** dimensionless

Chen Bingzhang 2017/8/7 2:58 PM

**Deleted:** *dustso* ... [192]

Bingzhang Chen 2017/9/28 12:16 PM

**Formatted** ... [193]

Chen Bingzhang 2017/9/13 3:34 PM

**Deleted:** Marañón et al., (2013); $^b$…enne ... [194]

Table 3. Observational data at stations S1 and K2. N: number of observations. Min and Max are minimal and maximal values used in data normalization (*see* Sect. 2.4 for details). DIN: dissolved inorganic nitrogen ($\mu$mol L$^{-1}$). Chl *a*: total chlorophyll a concentration ($\mu$g L$^{-1}$). NPP: net primary production measured by $^{13}$C uptake ($\mu$gC L$^{-1}$ d$^{-1}$). PON: particulate organic nitrogen ($\mu$mol L$^{-1}$). Fer: dissolved iron concentration (nmol L$^{-1}$). SF Chl: percentages of four size fractionated Chl *a*. Note that the data of Fer were from model outputs of Aumont et al., (2003) instead of real observations.

| | K2 | | | S1 | | |
|---|---|---|---|---|---|---|
| Type | N | Min | Max | N | Min | Max |
| DIN | 974 | 4.1 | 45.7 | 902 | 0 | 11.2 |
| Chl *a* | 470 | 0 | 3.4 | 426 | 0 | 1.0 |
| NPP | 112 | 0.1 | 37.1 | 128 | 0.1 | 34.9 |
| PON | 29 | 0.1 | 2.2 | 32 | 0.1 | 1.0 |
| Fer | 168 | 0.02 | 1.12 | 168 | 0.02 | 0.95 |
| SF Chl | 143 x 4 | 0 | 1.0 | 166 x 4 | 0 | 1.0 |

Chen Bingzhang 2017/8/3 12:05 PM
**Deleted:** TIN

Chen Bingzhang 2017/8/3 12:05 PM
**Deleted:** TIN

Table 4. Sum of squared errors between model outputs and observational data for sensitive analysis. The standard run used the optimized parameter values in Table 2. In other runs, only the value of the parameter shown was changed while others were kept constant.

| | Stn | DIN | CHL | NPP | PON | %3–10 µm | %1–3 µm | %<1 µm |
|---|---|---|---|---|---|---|---|---|
| Standard | K2 | 21.5 | 8.1 | 3.0 | 0.92 | 3.6 | 7.3 | 13.3 |
| | S1 | 11.2 | 16.5 | 6.7 | 1.5 | 4.9 | 4.0 | 4.1 |
| $\mu'_{0,m} = 0.4$ | K2 | 19.7 | 11.6 | 5.4 | 0.86 | 6.7 | 7.1 | 23.4 |
| | S1 | 13.2 | 12.8 | 6.6 | 1.3 | 4.4 | 4.3 | 16.3 |
| $W_d = 10$ | K2 | 15.3 | 8.1 | 3.0 | 1.1 | 3.6 | 7.3 | 13.4 |
| | S1 | 17.8 | 12.7 | 4.6 | 1.0 | 2.9 | 4.6 | 6.6 |
| $\alpha_I = 0$ | K2 | 167.3 | 35.8 | 11.8 | 2.0 | 10.4 | 8.6 | 36.4 |
| | S1 | 13.0 | 16.1 | 6.1 | 1.8 | 22.0 | 5.4 | 56.4 |
| $m_z = 0.1$ | K2 | 523.8 | 17.6 | 8.0 | 1.9 | 12.9 | 6.5 | 11.3 |
| | S1 | 11.5 | 17.7 | 7.4 | 1.6 | 9.1 | 2.9 | 3.0 |
| $\mu = 0.05$ | K2 | 22.2 | 8.3 | 3.2 | 0.94 | 4.7 | 8.5 | 15.4 |
| | S1 | 11.1 | 16.9 | 6.8 | 1.6 | 11.0 | 4.2 | 4.0 |

Formatted ... [195]
Chen Bingzhang 2017/9/20 4:04 PM
Formatted ... [196]
Chen Bingzhang 2017/9/20 4:03 PM
Formatted ... [197]
Bingzhang Chen 2017/9/28 11:18 PM
Formatted ... [198]
Bingzhang Chen 2017/9/29 12:05 PM
Formatted ... [199]
Bingzhang Chen 2017/9/29 12:05 PM
Formatted Table ... [200]
Bingzhang Chen 2017/9/28 11:18 PM
Formatted ... [201]
Bingzhang Chen 2017/9/29 12:05 PM
Formatted ... [202]
Bingzhang Chen 2017/9/28 11:18 PM
Formatted ... [203]
Bingzhang Chen 2017/9/29 12:05 PM
Formatted ... [204]
Bingzhang Chen 2017/9/29 12:05 PM
Formatted ... [205]
Bingzhang Chen 2017/9/28 11:18 PM
Formatted ... [206]
Bingzhang Chen 2017/9/29 12:05 PM
Formatted ... [207]
Bingzhang Chen 2017/9/28 11:18 PM
Formatted ... [208]
Bingzhang Chen 2017/9/29 12:05 PM
Formatted ... [209]
Bingzhang Chen 2017/9/28 11:18 PM
Formatted ... [210]
Bingzhang Chen 2017/9/29 12:05 PM
Formatted ... [211]
Bingzhang Chen 2017/9/28 11:18 PM
Formatted ... [212]
Bingzhang Chen 2017/9/29 12:05 PM
Formatted ... [213]
Bingzhang Chen 2017/9/28 11:18 PM
Formatted ... [214]
Bingzhang Chen 2017/9/29 12:05 PM
Formatted ... [215]
Bingzhang Chen 2017/9/28 11:18 PM
Formatted ... [216]
Bingzhang Chen 2017/9/29 12:05 PM
Formatted ... [217]
Bingzhang Chen 2017/9/28 11:18 PM
Formatted ... [218]
Bingzhang Chen 2017/9/29 12:05 PM
Formatted ... [219]
Bingzhang Chen 2017/9/28 11:18 PM
Formatted ... [220]
Bingzhang Chen 2017/9/29 12:05 PM
Formatted ... [221]
Bingzhang Chen 2017/9/28 11:18 PM
Formatted ... [222]
Bingzhang Chen 2017/9/29 12:06 PM
Formatted ... [223]
Bingzhang Chen 2017/9/29 12:08 PM
Formatted ... [224]
Bingzhang Chen 2017/9/28 11:18 PM
Formatted ... [225]
Bingzhang Chen 2017/9/28 11:18 PM
Formatted ... [226]
Bingzhang Chen 2017/9/29 12:06 PM
Formatted ... [227]
Chen Bingzhang 2017/9/21 10:52 AM

## Author contribution

B. Chen and S. L. Smith conceived and designed the study. S. L. Smith wrote the initial MCMC code. B. Chen acquired and organized the observational data, did subsequent coding, and wrote the first draft of the manuscript. Both authors contributed to later revision of the manuscript.

## Competing interests

The authors declare that they have no conflict of interest.

## Acknowledgments

We sincerely thank S. Vallina and C. Carcia-Comas for useful discussions. The comments from the editor and three anonymous reviewers have substantially improved an earlier draft of the manuscript. This study would not be possible without the cruise data shared by the K2S1 project personnel, particularly M. C. Honda, T. Fujiki, and K. Matsumoto. We also sincerely thank T. Hashioka for sharing the data of vertical eddy diffusivity. This study is supported by CREST (Grant Number JPMJCR12A3; P.I. SLS) funded by the Japan Science and Technology (JST) Agency and a Grants-in-Aid for Scientific Research (KAKENHI) (Grant Number JP16K21701; P.I. BC) funded by Japan Society for the Promotion of Science (JSPS).

Chen Bingzhang 2017/9/13 3:11 PM
**Deleted:**

Chen Bingzhang 2017/8/7 2:56 PM
**Deleted:** We sincerely thank

Chen Bingzhang 2017/8/7 2:57 PM
**Deleted:** , for sharing the cruise data

## References

Acevedo-Trejos, E., Brandt, G., Bruggeman, J. and Merico, A., Mechanisms shaping size structure and functional diversity of phytoplankton communities in the ocean, Sci. Rep., 5, 8918, doi: 10.1038/srep08918, 2015.

Acevedo-Trejos, E., Brandt, G., Smith, S. L. and Merico, A., PhytoSFDM version 1.0. 0: Phytoplankton Size and Functional Diversity Model, Geosci. Model Dev., 9, 4071–4085, doi: 10.5194/gmd-9-4071-2016, 2016.

Allen, A.P., Gillooly, J.F., Savage, V.M. and Brown, J.H.: Kinetic effects of temperature on rates of genetic divergence and speciation. Proc. Nat. Acad. Sci., 103, 9130-9135, 2006.

Annan, J. D., and Hargreaves, J. C.: Efficient estimation and ensemble generation in climate modelling. Phil. Trans. R. Soc. A, 365, 2077–2088, 2007.

Aumont, O., Maier-Reimer, E., Blain, S., and Monfray, P.: An ecosystem model of the global ocean including Fe, Si, P colimitations. Global Biogeochem. Cycles, 17, 1060, doi:10.1029/2001GB001745, 2003.

Bak, P.: How nature works: the science of self-organized criticality, New York: Copurnicus, 1996.

Behrenfeld, M. J.: Abandoning Sverdrup's critical depth hypothesis on phytoplankton blooms, Ecology, 91, 977–989, 2010.

Behrenfeld, M. J. and Boss, E. S.: Resurrecting the ecological underpinnings of ocean plankton blooms, Ann. Rev. Mar. Sci., 6, 167–194, 2014.

Behrenfeld, M. J., Worthington, K., Sherrell, R. M., Chavez, F. P., Strutton, P., McPhaden, M., and Shea, D. M.: Controls on tropical Pacific Ocean productivity revealed through nutrient stress diagnostics, Nature, 442, 1025–1028, 2006.

Biller, S. J., Berube, P. M., Lindell, D. and Chisholm, S. W.: *Prochlorococcus*: the structure and function of collective diversity, Nat. Rev. Microb., 13, 13-27, 2015.

Bruggeman, J.: Succession in plankton communities: A trait-based perspective, Ph.D. thesis, 160 pp, 2009.

Chen Bingzhang 2017/8/7 10:44 AM
**Formatted:** Font:Not Italic

Chen Bingzhang 2017/8/7 10:44 AM
**Formatted:** Font:Not Italic

Bingzhang Chen 2017/9/29 10:40 AM
**Formatted:** Font:Italic

Buitenhuis, E., Le Quéré, C., Aumont, O., Beaugrand, G., Bunker, A., Hirst, A., Ikeda, T., O'Brien, T., Piontkovski, S. and Straile, D.: Biogeochemical fluxes through mesozooplankton, Global Biogeochem. Cycles, 20, GB2003, doi:10.1029/2005GB002511, 2006.

Buitenhuis, E. T., Rivkin, R. B., Sailley, S., and Le Quéré, C.: Biogeochemical fluxes through microzooplankton, Global Biogeochem. Cycles, 24, GB4015, doi:10.1029/2009GB003601, 2010.

Calderhead, B.: A general construction for parallelizing Metropolis− Hastings algorithms, Proc. Nat. Acad. Sci., 111, 17408–17413, 2014.

Campbell, L., Nolla, H. A. and Vaulot, D.: The importance of *Prochlorococcus* to community structure in the central North Pacific Ocean, Limnol. Oceanogr., 39, 954–961, 1994.

Cavender-Bares, K. K., Rinaldo, A. and Chisholm, S.W.: Microbial size spectra from natural and nutrient enriched ecosystems, Limnol. Oceanogr., 46, 778–789, 2001.

Cermeño, P., Marañón, E., Harbour, D. and Harris, R. P.: Invariant scaling of phytoplankton abundance and cell size in contrasting marine environments, Ecol. Let., 9, 1210–1215, 2006.

Chai, F., Dugdale, R. C., Peng, T. H., Wilkerson, F. P. and Barber, R. T.: One-dimensional ecosystem model of the equatorial Pacific upwelling system. Part I: model development and silicon and nitrogen cycle, Deep Sea Res. II, 49, 2713–2745, 2002.

Chavez, F. P., Messié, M. and Pennington, J. T.: Marine primary production in relation to climate variability and change, Ann. Rev. Mar. Sci., 3, 227–260, 2011.

Chen, B., and Laws, E. A.: Is there a difference of temperature sensitivity between marine phytoplankton and heterotrophs? Limnol. Oceanogr., 62, 806–817, doi: 10.1002/lno.10462, 2017.

Chen, B., and Liu, H.: Comment: Unimodal relationship between phytoplankton mass–specific growth rate and size: A reply to the comment by Sal and López-Urrutia (2011), Limnol. Oceanogr., 56, 1956–1958, 2011.

Chen, B., and Liu, H.: Relationships between phytoplankton growth and cell size in surface oceans: Interactive effects of temperature, nutrients, and grazing, Limnol. Oceanogr., 55, 965–972, 2010.

Chen, B.: Patterns of thermal limits of phytoplankton, J. Plankton Res., 37, 285–292, 2015.

Chen Bingzhang 2017/8/27 9:01 PM
**Formatted:** Font:Not Italic

Chen Bingzhang 2017/8/27 9:01 PM
**Formatted:** Font:Not Italic

Chen Bingzhang 2017/8/27 9:01 PM
**Formatted:** Font:Not Italic

Chen Bingzhang 2017/8/27 9:01 PM
**Formatted:** Font:Not Italic

Chen Bingzhang 2017/8/7 3:44 PM
**Deleted:** ,

Chen Bingzhang 2017/8/7 3:44 PM
**Deleted:** .

Chen Bingzhang 2017/8/7 3:45 PM
**Formatted:** Font:Not Italic

Chen Bingzhang 2017/8/7 3:47 PM
**Formatted:** Font:Not Italic

Chen Bingzhang 2017/8/7 3:47 PM
**Formatted:** Font:Not Italic

Chen Bingzhang 2017/8/7 3:48 PM
**Formatted:** Font:Not Italic

Chen, B., Liu, H., Landry, M. R., Dai, M., Huang, B. and Sun, J.: Close coupling between phytoplankton growth and microzooplankton grazing in the western South China Sea, Limnol. Oceanog., 54, 1084-1097, 2009.

Chesson, P.: Mechanisms of maintenance of species diversity, Ann. Rev. Ecol. Syst., 31, 343–366, 2000.

Chisholm, S.W., Olson, R. J., Zettler, E. R., Goericke, R., Waterbury, J. B. and Welschmeyer, N.A.: A novel free-living prochlorophyte abundant in the oceanic euphotic zone. Nature, 334, 340–343, 1988.

Christian, J. R.: Biogeochemical cycling in the oligotrophic ocean: Redfield and non-Redfield models, Limnol. Oceanogr., 50, 646–657, 2005.

Coutinho, R.M., Klauschies, T. and Gaedke, U.: Bimodal trait distributions with large variances question the reliability of trait-based aggregate models, Theor. Ecol., 9, 389–408, 2016.

Dowle, E. J., Morgan-Richards, M., and Trewick, S. A.: Molecular evolution and the latitudinal biodiversity gradient, Heredity, 110, 501–510, 2013.

Edwards, K.F., Klausmeier, C.A. and Litchman, E.: Evidence for a three-way trade-off between nitrogen and phosphorus competitive abilities and cell size in phytoplankton. Ecology, 92, 2085–2095, 2011.

Edwards, K. F., Thomas, M. K., Klausmeier, C. A. and Litchman, E.: Light and growth in marine phytoplankton: allometric, taxonomic, and environmental variation, Limnol. Oceanogr., 60, 540–552, 2015.

Edwards, K. F., Thomas, M. K., Klausmeier, C.A. and Litchman, E.: Allometric scaling and taxonomic variation in nutrient utilization traits and maximum growth rate of phytoplankton. Limnol. Oceanogr., 57, 554–566, 2012.

Falkowski, P.: Ocean science: the power of plankton, Nature, 483, S17–S20, 2012.

Fennel, K. and Boss, E.: Subsurface maxima of phytoplankton and chlorophyll: Steady-state solutions from a simple model. Limnol. Oceanogr., 48, 1521–1534, 2003.

Fennel, K., Wilkin, J., Levin, J., Moisan, J., O'Reilly, J. and Haidvogel, D., Nitrogen cycling in the Middle Atlantic Bight: Results from a three-dimensional model and implications for the North

Atlantic nitrogen budget, Global Biogeochem. Cycles, 20, GB3007, doi:10.1029/2005GB002456, 2006.

Fernández-Castro, B., Pahlow, M., Mouriño-Carballido, B., Marañón, E. and Oschlies, A.: Optimality-based *Trichodesmium* diazotrophy in the North Atlantic subtropical gyre, J. Plankton Res., 38, 946–963, doi: 10.1093/plankt/fbw047, 2016.

Finkel, Z. V.: Light absorption and size scaling of light-limited metabolism in marine diatoms, Limnol. Oceanogr., 46, 86–94, 2001.

Finkel, Z. V.: Does phytoplankton cell size matter? The evolution of modern marine food webs (pp. 333-350). Boston, Elsevier, 2007.

Finkel, Z. V., Beardall, J., Flynn, K. J., Quigg, A., Rees, T. A. V. and Raven, J. A.: Phytoplankton in a changing world: cell size and elemental stoichiometry, J. Plankton Res., 32, 119–137, 2010.

Flynn, K. J.: Do we need complex mechanistic photoacclimation models for phytoplankton? Limnol. Oceanogr., 48, 2243–2249, 2003.

Flynn, K.J. and Raven, J.A.: What is the limit for photoautotrophic plankton growth rates? J. Plankton Res., doi:10.1093/plankt/fbw067, 2016.

Franks, P.J.: Has Sverdrup's critical depth hypothesis been tested? Mixed layers vs. turbulent layers. ICES J. Mar. Sci., 72, 1897–1907, 2015.

Follows, M. J., Dutkiewicz, S., Grant, S., and Chisholm, S. W.: Emergent biogeography of microbial communities in a model ocean. Science, 315, 1843–1846, 2007.

Follows, M. J., and Dutkiewicz, S.: Modeling diverse communities of marine microbes, Ann. Rev. Mar. Sci. 3, 427-451, 2011.

Frost, B. W.: Effects of size and concentration of food particles on the feeding behavior of the marine planktonic copepod *Calanus pacificus*. Limnol. Oceanogr., 17, 805–815, 1972.

Fujiki, T., Matsumoto, K., Mino, Y., Sasaoka, K., Wakita, M., Kawakami, H., Honda, M. C., Watanabe, S., and Saino, T.: Seasonal cycle of phytoplankton community structure and photophysiological state in the western subarctic gyre of the North Pacific. Limnol. Oceanogr., 59, 887–900, 2014.

Fujiki, T., Sasaoka, K., Matsumoto, K., Wakita, M., and Mino, Y.: Seasonal variability of phytoplankton community structure in the subtropical western North Pacific, J. Oceanogr., 72, 343–358, 2016.

Gelman, A., Carlin, J. B., Stern, H. S., and Rubin, D. B.: Bayesian data analysis (Vol. 2), Boca Raton, FL, USA, Chapman & Hall/CRC, 2014.

Geider, R. J., MacIntyre, H. L. and Kana, T. M.: Dynamic model of phytoplankton growth and acclimation: responses of the balanced growth rate and the chlorophyll a: carbon ratio to light, nutrient-limitation and temperature, Mar. Ecol. Prog. Ser., 148, 187–200, 1997.

Gin, K. Y., Chisholm, S.W. and Olson, R. J.: Seasonal and depth variation in microbial size spectra at the Bermuda Atlantic time series station, Deep Sea Res. I, 46, 1221–1245, 1999.

Gregg, W. W., Ginoux, P., Schopf, P. S. and Casey, N.W.: Phytoplankton and iron: validation of a global three-dimensional ocean biogeochemical model, Deep Sea Res. II, 50, 3143–3169, 2003.

Haario, H., Saksman, E., and Tamminen, J.: An adaptive Metropolis algorithm, Bernoulli, 7, 223–242, 2001.

Haario, H., Laine, M., Mira, A. and Saksman, E.: DRAM: efficient adaptive MCMC, Stat. Comput., 16, 339–354, 2006.

Hansen, B., Bjornsen, P. K. and Hansen, P. J.: The size ratio between planktonic predators and their prey, Limnol. Oceanogr., 39, 395-403, 1994.

Hashioka, T., Sakamoto, T.T., and Yamanaka, Y.: Potential impact of global warming on North Pacific spring blooms projected by an eddy-permitting 3-D ocean ecosystem model. Geophys. Res. Let., 36, L20604, doi:10.1029/2009GL038912, 2009.

Hashioka, T., Vogt, M., Yamanaka, Y., Le Quere, C., Buitenhuis, E.T., Aita, M.N., Alvain, S., Bopp, L., Hirata, T., Lima, I.D. and Sailley, S. F.: Phytoplankton competition during the spring bloom in four plankton functional type models, Biogeosciences, 10, 6833–6850, doi: 10.5194/bg-10-6833-2013, 2013.

Honda, M. C.: Short introduction to the K2S1 project, J. Oceanogr., 72, 341–342, 2016.

Huston, M.: A general hypothesis of species diversity, Am. Nat., 113, 81–101, 1979.

Chen Bingzhang 2017/8/7 3:49 PM
**Deleted:** .

Chen Bingzhang 2017/8/7 3:49 PM
**Formatted:** Font:Not Italic

Chen Bingzhang 2017/8/7 3:49 PM
**Formatted:** Font:Not Italic

Chen Bingzhang 2017/8/7 3:49 PM
**Formatted:** Font:Not Italic

Chen Bingzhang 2017/8/23 7:03 AM
**Formatted:** Font:Not Italic

Chen Bingzhang 2017/8/23 7:03 AM
**Formatted:** Font:Not Italic

Chen Bingzhang 2017/8/23 7:09 AM
**Deleted:** .

Bingzhang Chen 2017/9/28 11:26 PM
**Deleted:** .

Johnson, Z. I., Zinser, E. R., Coe, A., McNulty, N. P., Woodward, E. M. S., and Chisholm, S. W.: Niche partitioning among *Prochlorococcus* ecotypes along ocean-scale environmental gradients, Science 311, 1737–1740, 2006.

Khatiwala, S.: A computational framework for simulation of biogeochemical tracers in the ocean, Global Biogeochem. Cycles, 21, GB3001, doi:10.1029/2007GB002923, 2007.

Kriest, I., Sauerland, V., Khatiwala, S., Srivastav, A. and Oschlies, A.: Calibrating a global three-dimensional biogeochemical ocean model (MOPS-1.0), Geosc. Model Dev., 10, 127-154, 2017.

Kooistra, W. H., Sarno, D., Balzano, S., Gu, H., Andersen, R. A., and Zingone, A.: Global diversity and biogeography of *Skeletonema* species (Bacillariophyta), Protist, 159, 177-193, 2008.

Laine, M.: Adaptive MCMC methods with applications in environmental and geophysical models, Ph.D. thesis, 48 pp, Finnish Meteorological Institute, 2008.

Latasa, M., Landry, M. R., Louise, S. and Bidigare, R. R.: Pigment specific growth and grazing rates of phytoplankton in the central equatorial Pacific, Limnol. Oceanogr., 42, 289–298, 1997.

Large, W. G., McWilliams, J. C., and Doney, S. C., Oceanic vertical mixing: A review and a model with a nonlocal boundary layer parameterization, Rev. Geophys., 32, 363–403, 1994.

Le Quéré, C., Harrison, S. P., Prentice, I. C., Buitenhuis, E. T., Aumont, O., Bopp, L., Claustre, H., et al.: Ecosystem dynamics based on plankton functional types for global ocean biogeochemistry models, Global Change Biol., 11, 2016–2040, 2005.

Litchman, E., and Klausmeier, C.A.: Trait-based community ecology of phytoplankton, Ann. Rev. Ecol. Evol. Syst., 39, 615–639, 2008.

Liu, H., Nolla, H. A., and Campbell, L.: *Prochlorococcus* growth rate and contribution to primary production in the equatorial and subtropical North Pacific Ocean, Aquat. Microb. Ecol., 12, 39–47, 1997.

Liu, H., Dagg, M. J., and Strom, S.: Grazing by the calanoid copepod Neocalanus cristatus on the microbial food web in the coastal Gulf of Alaska, J. Plankton Res., 27, 647–662, 2005.

Loreau, M., Naeem, S., Inchausti, P., Bengtsson, J., Grime, J. P., Hector, A., Hooper, D. U., Huston, M. A., Raffaelli, D., Schmid, B. and Tilman, D.: Biodiversity and ecosystem functioning: current knowledge and future challenges, Science, 294, 804-808, 2001.

Bingzhang Chen 2017/9/28 11:24 PM
**Formatted:** Font:Not Italic

Bingzhang Chen 2017/9/28 11:24 PM
**Formatted:** Font:Not Italic

Bingzhang Chen 2017/9/28 11:24 PM
**Formatted:** Font:Not Italic

Chen Bingzhang 2017/8/2 2:59 PM
**Deleted:** .

Chen Bingzhang 2017/8/2 2:59 PM
**Deleted:** .

Chen Bingzhang 2017/8/30 10:07 AM
**Formatted:** Font:Not Italic

Chen Bingzhang 2017/8/30 10:07 AM
**Formatted:** Font:Not Italic

Chen Bingzhang 2017/8/30 10:07 AM
**Formatted:** Font:Not Italic

Bingzhang Chen 2017/9/30 12:32 PM
**Formatted:** Font:Not Italic

Bingzhang Chen 2017/9/30 12:32 PM
**Formatted:** Font:Not Italic

Luo, C., Mahowald, N., Bond, T., Chuang, P. Y., Artaxo, P., Siefert, R., Chen, Y., and Schauer, J.: Combustion iron distribution and deposition, Global Biogeochem. Cycles, 22, GB1012, doi:10.1029/2007GB002964, 2008.

Maranón, E., Cermeño, P., Latasa, M., and Tadonléké, R.D.: Temperature, resources, and phytoplankton size structure in the ocean, Limnol. Oceanogr., 57, 1266–1278, 2012.

Marañón, E., Cermeño, P., López-Sandoval, D. C., Rodríguez-Ramos, T., Sobrino, C., Huete-Ortega, M., Blanco, J. M., and Rodríguez, J.: Unimodal size scaling of phytoplankton growth and the size dependence of nutrient uptake and use, Ecol. Let., 16, 371–379, 2013.

Masuda, Y., Yamanaka, Y., Hirata, T. and Nakano, H.: Competition and community assemblage dynamics within a phytoplankton functional group: Simulation using an eddy-resolving model to disentangle deterministic and random effects, Ecol. Mod., 343, 1–14, 2017.

Matsumoto, K., Honda, M. C., Sasaoka, K., Wakita, M., Kawakami, H., and Watanabe, S., Seasonal variability of primary production and phytoplankton biomass in the western Pacific subarctic gyre: control by light availability within the mixed layer, J. Geophys. Res. Oceans, 119, 6523–6534, 2014.

Matsumoto, K., Abe, O., Fujiki, T., Sukigara, C. and Mino, Y., Primary productivity at the time-series stations in the northwestern Pacific Ocean: is the subtropical station unproductive? J. Oceanogr., 72, 359–371, 2016.

Merico, A., Brandt, G., Smith, S. L., and Oliver, M.: Sustaining diversity in trait-based models of phytoplankton communities, Front. Ecol. Evol., 2, 59, doi: 10.3389/fevo.2014.00059, 2014.

Merico, A., Bruggeman, J., and Wirtz, K.: A trait-based approach for downscaling complexity in plankton ecosystem models, Ecol. Mod., 220, 3001–3010, 2009.

Mira, A.: On Metropolis-Hastings algorithms with delayed rejection, Metron, 59, 231–241, 2001.

Moon-van der Staay, S. Y., De Wachter, R., and Vaulot, D.: Oceanic 18S rDNA sequences from picoplankton reveal unsuspected eukaryotic diversity, Nature, 409, 607–610, 2001.

Moore, L. R., Rocap, G., Chisholm, S. W.: Physiology and molecular phylogeny of coexisting *Prochlorococcus* ecotypes, Nature, 393, 464–467, 1998.

Chen Bingzhang 2017/8/30 11:04 AM
**Formatted:** Font:Not Italic

Chen Bingzhang 2017/8/30 11:04 AM
**Formatted:** Font:Not Italic

Chen Bingzhang 2017/8/30 11:04 AM
**Formatted:** Font:Not Italic

Chen Bingzhang 2017/8/2 2:58 PM
**Deleted:** .

Chen Bingzhang 2017/8/5 10:43 PM
**Formatted:** Font:Not Italic

Chen Bingzhang 2017/8/5 10:43 PM
**Formatted:** Font:Not Italic

Chen Bingzhang 2017/8/5 10:43 PM
**Formatted:** Font:Not Italic

Chen Bingzhang 2017/8/5 10:43 PM
**Formatted:** Font:Not Italic

Chen Bingzhang 2017/8/5 10:43 PM
**Formatted:** Font:Not Italic

Chen Bingzhang 2017/8/23 7:08 AM
**Formatted:** Font:Not Italic

Chen Bingzhang 2017/8/23 7:08 AM
**Formatted:** Font:Not Italic

Nickelsen, L., Keller, D. and Oschlies, A.: A dynamic marine iron cycle module coupled to the University of Victoria Earth System Model: the Kiel Marine Biogeochemical Model 2 for UVic 2.9, Geosci. Model Dev., 8, 1357–1381, doi:10.5194/gmd-8-1357-2015, 2015.

Norberg, J., Swaney, D. P., Dushoff, J., Lin, J., Casagrandi, R., and Levin, S. A.: Phenotypic diversity and ecosystem functioning in changing environments: a theoretical framework, Proc. Nat. Acad. Sci., 98, 11376–11381, 2001.

Norberg, J.: Biodiversity and ecosystem functioning: a complex adaptive systems approach, Limnol. Oceanogr., 49, 1269–1277, 2004.

Palenik, B., Ren, Q., Dupont, C. L., Myers, G. S., Heidelberg, J. F., Badger, J. H., Madupu, R., et al.: Genome sequence of *Synechococcus* CC9311: insights into adaptation to a coastal environment, Proc. Nat. Acad. Sci., 103, 13555–13559, 2006.

Poulin, F. J. and Franks, P. J.: Size-structured planktonic ecosystems: constraints, controls and assembly instructions, J. Plankton Res., 32, 1121–1130, 2010.

Quintana, X. D., Brucet, S., Boix, D., López - Flores, R., Gascón, S., Badosa, A., Sala, J., Moreno− Amich, R. and Egozcue, J. J.: A nonparametric method for the measurement of size diversity with emphasis on data standardization, Limnol. Oceanogr. Methods, 6, 75–86, 2008.

Rohde, K.: Latitudinal gradients in species diversity: the search for the primary cause, Oikos, 65, 514–527, 1992.

Rosenzweig, M. L.: Species diversity in space and time, Cambridge University Press, 1995.

Sasai, Y., Yoshikawa, C., Smith, S. L., Hashioka, T., Matsumoto, K., Wakita, M., Sasaoka, K. and Honda, M. C., Coupled 1-D physical–biological model study of phytoplankton production at two contrasting time-series stations in the western North Pacific, J. Oceanogr., 72, 509–526, 2016.

Shchepetkin, A. F., and McWilliams, J. C., The regional oceanic modeling system (ROMS): a split-explicit, free-surface, topography-following-coordinate oceanic model, Ocean Mod., 9, 347–404, 2005.

Shigemitsu, M., Okunishi, T., Nishioka, J., Sumata, H., Hashioka, T., Aita, M. N., Smith, S. L., Yoshie, N., Okada, N. and Yamanaka, Y., Development of a one-dimensional ecosystem model including

Chen Bingzhang 2017/8/30 11:10 AM
**Formatted:** Font:Not Italic

Chen Bingzhang 2017/8/30 11:10 AM
**Formatted:** Font:Not Italic

Chen Bingzhang 2017/8/30 11:10 AM
**Formatted:** Font:Not Italic

Chen Bingzhang 2017/8/7 4:10 PM
**Formatted:** Font:Not Italic

Chen Bingzhang 2017/8/7 4:10 PM
**Formatted:** Font:Not Italic

Chen Bingzhang 2017/8/7 4:10 PM
**Formatted:** Font:Not Italic

Chen Bingzhang 2017/8/7 4:10 PM
**Formatted:** Font:Not Italic

the iron cycle applied to the Oyashio region, western subarctic Pacific, J. Geophys. Res., 117, C06021, doi:10.1029/2011JC007689, 2012.

Smith, S. L., Vallina, S. M., and Merico, A.: Phytoplankton size-diversity mediates an emergent trade-off in ecosystem functioning for rare versus frequent disturbances. Sci. Rep., 6, 34170, doi: 10.1038/srep34170, 2016.

Sournia, A., Chrdtiennot-Dinet, M-J., Ricard, M.: Marine phytoplankton: how many species in the world ocean? J. Plankton Res. 13, 1093–1099, 1991.

Strzepek, R. F., and Harrison, P. J.: Photosynthetic architecture differs in coastal and oceanic diatoms, Nature, 431, 689–692, 2004.

Terseleer, N., Bruggeman, J., Lancelot, C. and Gypens, N.: Trait-based representation of diatom functional diversity in a plankton functional type model of the eutrophied southern North Sea. Limnol. Oceanogr., 59, 1958–1972, 2014.

Thomas, M. K., Kremer, C. T., Klausmeier, C. A., and Litchman, E.: A global pattern of thermal adaptation in marine phytoplankton, Science, 338, 1085–1088, 2012.

Tilman, D.: Resource competition and community structure, Princeton university press, 1982.

Tilman, D., Isbell, F., and Cowles, J. M., Biodiversity and ecosystem functioning. Ann. Rev. Ecol. Evol. Syst., 45, 471–493, 2014.

Tilman, D., Lehman, C. L., and Thomson, K. T.: Plant diversity and ecosystem productivity: theoretical considerations. Proc. Nat. Acad. Sci., 94, 1857–1861, 1997.

Vallina, S. M., Follows, M. J., Dutkiewicz, S., Montoya, J. M., Cermeno, P. and Loreau, M.: Global relationship between phytoplankton diversity and productivity in the ocean, Nat. Commun., 5, 4299, doi: 10.1038/ncomms5299, 2014.

Villagran, A., Huerta, G., Jackson, C. S. and Sen, M. K.: Computational methods for parameter estimation in climate models, Bayesian Analysis, 3, 823-850, 2008.

Villareal, T. A.: Abundance of the giant diatom *Ethmodiscus* in the southwest Atlantic Ocean and central Pacific gyre, Diatom Res., 8, 171–177, 1993.

Villareal, T.A., Pilskaln, C., Brzezinski, M., Lipschultz, F., Dennett, M. and Gardner, G.B.: Upward transport of oceanic nitrate by migrating diatom mats, Nature, 397, 423–425, 1999.

Chen Bingzhang 2017/10/23 10:08 AM
**Deleted:** Tegen, I., and Fung, I., Contribution to the atmospheric mineral aerosol load from land surface modification, J. Geophys. Res.: Atmospheres, 100(D9), 18707-18726, 1995.

Chen Bingzhang 2017/10/23 10:08 AM
**Formatted:** Font:Not Italic

Bingzhang Chen 2017/9/29 11:00 AM
**Formatted:** Font:Not Italic

Bingzhang Chen 2017/9/29 11:01 AM
**Formatted:** Font:Not Italic

Wakita, M., Honda, M. C., Matsumoto, K., Fujiki, T., Kawakami, H., Yasunaka, S., Sasai, Y., Sukigara, C., Uchimiya, M., Kitamura, M. and Kobari, T.: Biological organic carbon export estimated from the annual carbon budget observed in the surface waters of the western subarctic and subtropical North Pacific Ocean from 2004 to 2013, J. Oceanogr., 72, 665-685, 2016.

Ward, B.A., Friedrichs, M.A., Anderson, T.R. and Oschlies, A.: Parameter optimisation techniques and the problem of underdetermination in marine biogeochemical models, J. Mar. Sys., 81, 34-43, 2010.

Ward, B.A., Dutkiewicz, S., Jahn, O. and Follows, M.J.: A size-structured food-web model for the global ocean, Limnol. Oceanogr., 57, 1877-1891, 2012.

Welschmeyer, N. A.: Fluorometric analysis of chlorophyll a in the presence of chlorophyll b and pheopigments, Limnol. Oceanogr., 39, 1985–1992, 1994.

Wirtz, K. W., and Eckhardt, B.: Effective variables in ecosystem models with an application to phytoplankton succession, Ecol. Mod., 92, 33–53, 1996.

Zhou, L., Tan, Y., Huang, L. and Li, G.: Does microzooplankton grazing contribute to the pico-phytoplankton dominance in subtropical and tropical oligotrophic waters? Acta Ecol. Sin., 35, 29–38, 2015.

Bingzhang Chen 2017/9/30 4:20 PM
**Formatted:** English (US)

Figure captions

Fig. 1. Schematic description of the CITRATE model. Thick arrows indicate nitrogen flows and dashed lines indicate the simplified iron cycle. The inset denotes an example of phytoplankton community with a lognormal distribution for cell volume.

Fig. 2. (a) Locations of the three stations, K2, S1 and ALOHA, overlaid on annual Chl *a* climatology of the North Pacific. (b-e) Seasonal forcing of vertical eddy diffusivity ($K_v$), temperature, surface PAR, and atmospheric dust deposition, respectively, at station S1. The white squares are measured mixed layer depths from *in situ* temperature and salinity profiles. The thick tan line represents mixed layer depths calculated from a threshold of $10^{-4}$ $m^2$ $s^{-1}$. (f-i) The same as (b-e), but for station K2. (j-m) The same as (b-e), but for station ALOHA.

Fig. 3. An example of modelled patterns of total inorganic nitrogen (DIN), Chl *a* (Chl), mean size, and ln size variance for four years at stations K2 (a-d) and S1 (e-h).

Fig. 4. (a) Time evolution of log-likelihood of the MHMC chain. (b-i) Time evolution of sum of squared errors (*SSqE*) for DIN, Chl, net primary production (NPP), particulate organic nitrogen (PON), and fractions of size-fractionated Chl *a* concentrations of > 10 *μ*m (P10), 3–10 *μ*m (P03), 1–3 *μ*m (P01), and <1 *μ*m (P_1). (j-q) The same as (b-j), but for station S1.

Fig. 5. Time evolution of fitted model parameters.

Fig. 6. Model fittings to vertical profiles of (a-d) DIN, (e-h) CHL, (i-l) NPP, and (m-p) PON at four seasons at station K2. Black dots represent observational data and red thick solid lines represent the averaged seasonal values predicted by the model. Thin dashed lines represent 95% percentiles of the seasonal data.

Fig. 7. The same as Fig. 6, but for station S1.

Fig. 8. Model fittings for the percentages of the four size fractions of Chl *a* at station K2. (a-d) Percentages of > 10 µm fraction. (e-h) 3-10 µm. (i-l) 1-3 µm. (m-p) <1 µm.

Fig. 9. The same as Fig. 8, but for station S1.

Fig. 10. Modelled seasonal patterns at station K2: (a) DIN, (b) dissolved iron, (c) Chl *a*, (d) phytoplankton mean size, (e) size variance, (f) community-based specific growth rate ($\mu_{com}$), (g)

Chen Bingzhang 2017/9/26 3:04 PM
**Deleted:** wo

Chen Bingzhang 2017/9/26 3:04 PM
**Deleted:** and

Chen Bingzhang 2017/9/26 3:07 PM
**Formatted:** Font:Italic

Chen Bingzhang 2017/9/26 3:10 PM
**Formatted:** Superscript

Chen Bingzhang 2017/9/26 3:11 PM
**Formatted:** Superscript

Chen Bingzhang 2017/9/26 3:11 PM
**Formatted:** Superscript

Chen Bingzhang 2017/9/26 3:05 PM
**Deleted:** d

Chen Bingzhang 2017/8/3 12:05 PM
**Deleted:** TIN

Bingzhang Chen 2017/9/30 3:39 PM
**Deleted:** s

Chen Bingzhang 2017/9/26 3:04 PM
**Formatted:** Font:Italic

Chen Bingzhang 2017/8/3 12:05 PM
**Deleted:** TIN

Chen Bingzhang 2017/8/3 12:05 PM
**Deleted:** TIN

Chen Bingzhang 2017/8/3 12:05 PM
**Deleted:** TIN

Chen Bingzhang 2017/9/26 3:18 PM
**Deleted:** phytoplankton biomass in terms of nitrogen (PHY), (e)

Chen Bingzhang 2017/9/26 3:18 PM
**Deleted:** f

Chen Bingzhang 2017/9/26 3:29 PM
**Deleted:** ln

Chen Bingzhang 2017/9/26 3:29 PM
**Deleted:** s

Chen Bingzhang 2017/9/26 3:18 PM
**Deleted:** g

Chen Bingzhang 2017/9/26 3:19 PM
**Formatted:** Font:Italic

Chen Bingzhang 2017/9/26 3:19 PM
**Formatted:** Font:Italic, Subscript

Chen Bingzhang 2017/9/26 3:24 PM
**Deleted:** h

first derivative of phytoplankton growth rate against ln volume evaluated at mean size, (h) second derivative of phytoplankton growth rate evaluated at mean size, (i) Chlorophyll-to-carbon ratios, and (j) Nitrogen-to-carbon ratios.

Fig. 11. The same as Fig. 10, but for station S1.

Fig. 12. (a) Scatterplots of size variance versus phytoplankton community growth rate ($\mu_{com}$). (b) Contributions of various factors to the dynamics of size variance in surface waters at S1. The term “Competition” equates to $v^2\frac{d^2\mu}{dl^2}$. *MIC* and *MES* grazing equates to $-v^2\frac{d^2g_i}{dl^2}$. “d4$\mu$/dL4” equates to $v^2u\frac{d^4\mu}{dl^4}$. “Trait diffusion” equates to $2u\mu$. All the derivatives are evaluated at the mean size. “Diffusion” means the contribution to the changes of size variance induced by diffusion with the underlying grid. “Net effect” means the sum of the above terms. “Net changes” mean the difference of size variance between adjacent days. (c) The same as (b), but at station K2.

Fig. 13. The same as Fig. 6, but for station ALOHA.

Fig. 14. Schematic diagrams for mixing of two phytoplankton communities with different biomass, mean size, and size variance, each following a lognormal size distribution.

Chen Bingzhang 2017/9/26 3:22 PM
**Deleted:** size

Chen Bingzhang 2017/9/26 3:24 PM
**Deleted:** i

Chen Bingzhang 2017/9/26 3:24 PM
**Deleted:** trait diffusion effects

Chen Bingzhang 2017/9/26 3:41 PM
**Formatted:** Font:Italic

Chen Bingzhang 2017/9/26 3:41 PM
**Formatted:** Font:Italic

Chen Bingzhang 2017/9/26 3:43 PM
**Formatted:** Font:Italic

Chen Bingzhang 2017/9/26 3:52 PM
**Formatted:** Font:Italic

Chen Bingzhang 2017/9/26 4:40 PM
**Deleted:**

Chen Bingzhang 2017/9/26 4:25 PM
**Deleted:**

Chen Bingzhang 2017/9/26 4:25 PM
**Deleted:** 2

Chen Bingzhang 2017/9/26 4:27 PM
**Deleted:** A s

Chen Bingzhang 2017/9/26 4:28 PM
**Deleted:** the transport

Chen Bingzhang 2017/9/26 4:28 PM
**Deleted:**

Chen Bingzhang 2017/9/26 4:28 PM
**Deleted:** mean size of two idealized communities

Chen Bingzhang 2017/9/26 4:29 PM
**Deleted:** having

Chen Bingzhang 2017/9/26 4:27 PM
**Deleted:** The hypothetical biomass, log mean size, and log size variance are 1, 5, 1 for community A, and 0.2, 4, 0.8 for B, respectively.

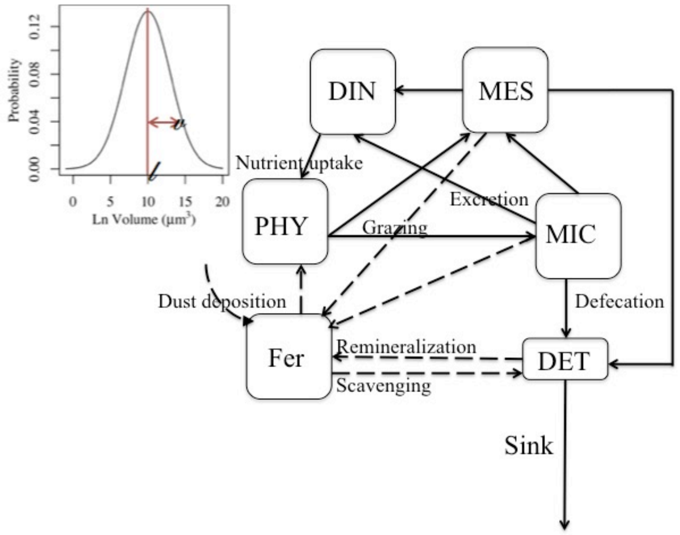

Fig. 1

Bingzhang Chen 2017/9/28 11:32 PM
**Deleted:** ... [228]

Bingzhang Chen 2017/9/30 12:54 PM
**Formatted:** Centered

Bingzhang Chen 2017/9/29 2:50 PM
**Formatted Table**

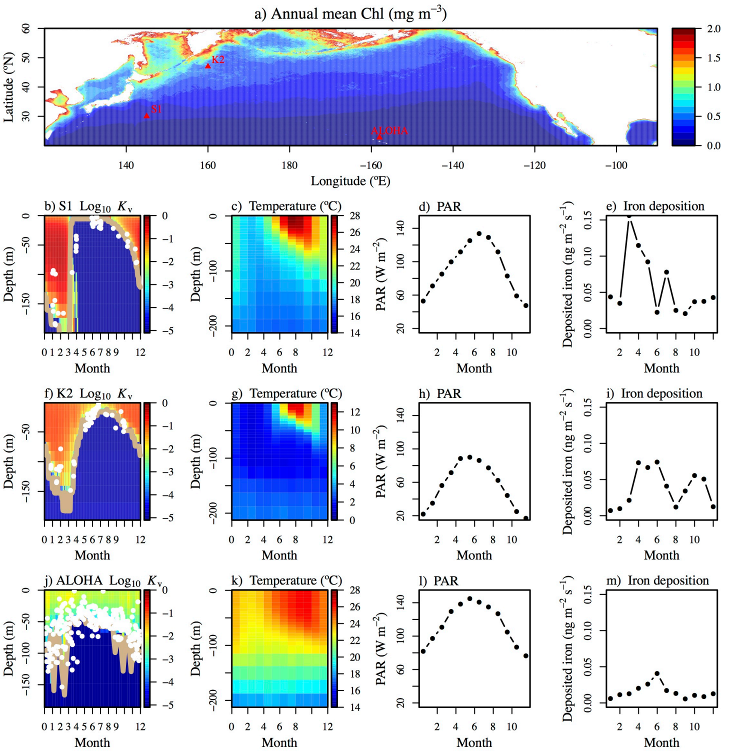

Fig. 2

Chen Bingzhang 2017/9/14 4:42 PM

**Deleted:** *<sp>*

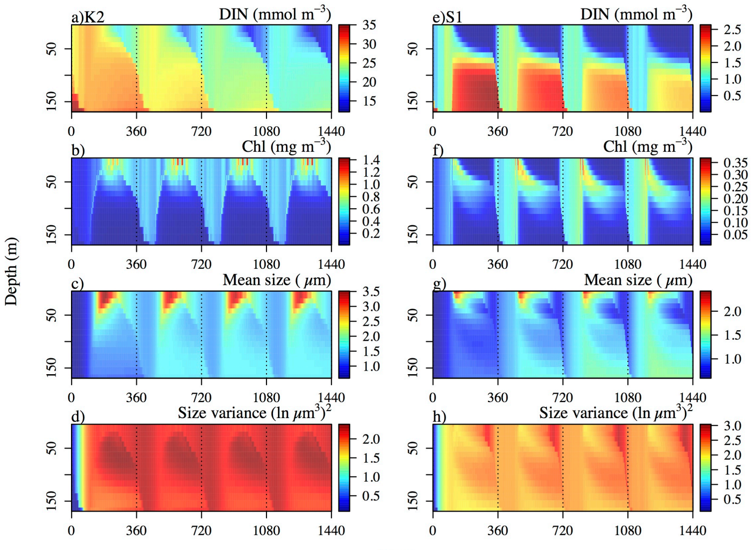

Fig. 3 An example of modelled 4 year patterns at K2 and S1

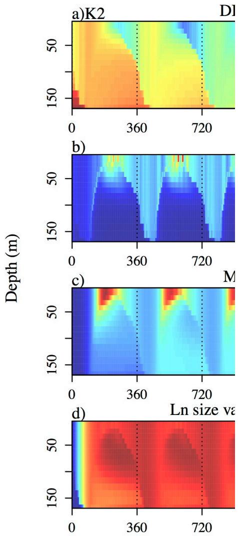

Fig. 3 An example of modell

**Deleted:**

Chen Bingzhang 2017/9/14 4:42 PM

**Deleted:** *<sp>*

Chen Bingzhang 2017/9/14 4:42 PM

**Deleted:** *<sp>*

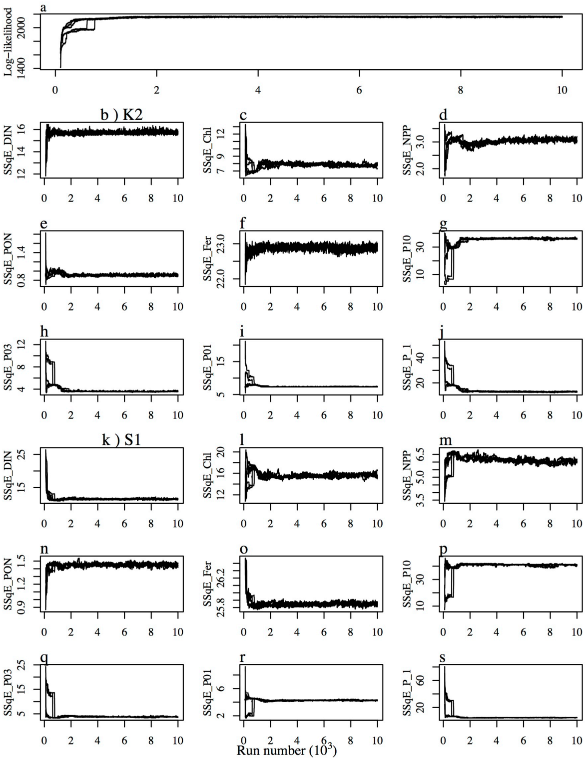

Fig. 4

Chen Bingzhang 2017/9/26 4:40 PM

**Deleted:** *<sp>*

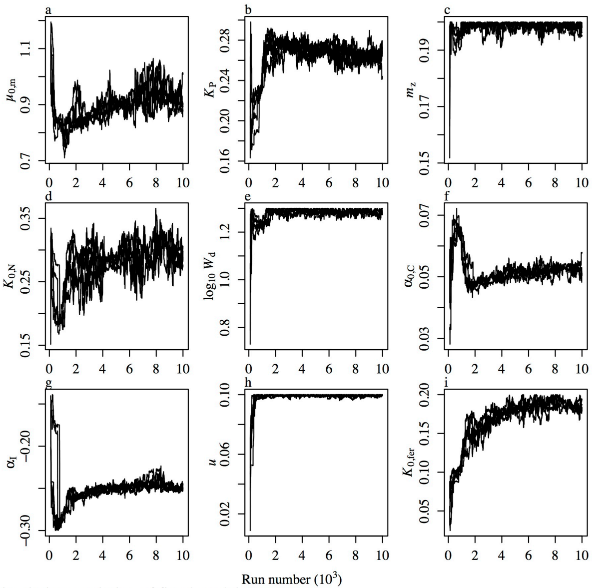

Fig. 5 Time evolution of fitted model parameters.

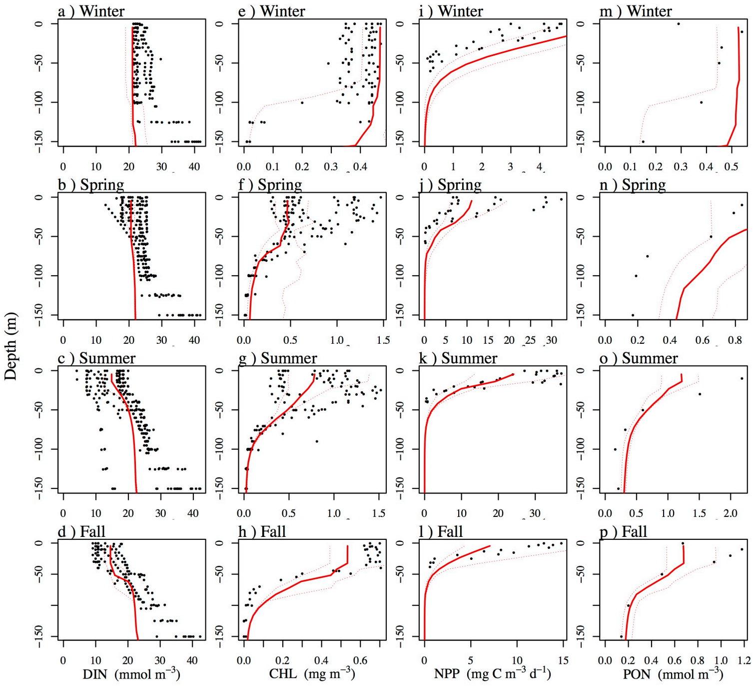

Fig. 6 . Model fittings to vertical profiles of DIN, CHL, NPP, and PON at K2

Chen Bingzhang 2017/9/26 4:40 PM

**Deleted:** <*sp*>

**Bingzhang Chen 2017/9/29 10:58 AM**

**Deleted:** <*sp*>

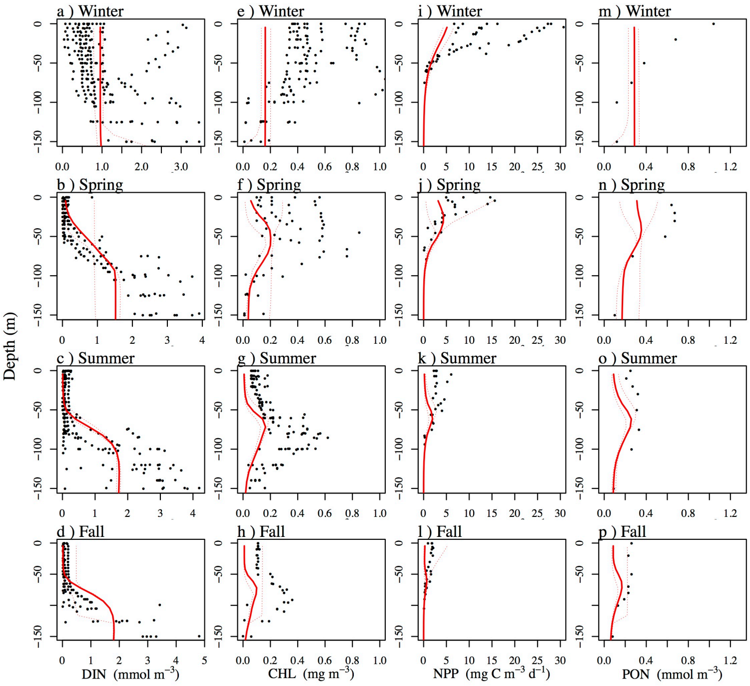

Fig. 7 . Model fittings to vertical profiles of DIN, CHL, NPP, and PON at S1

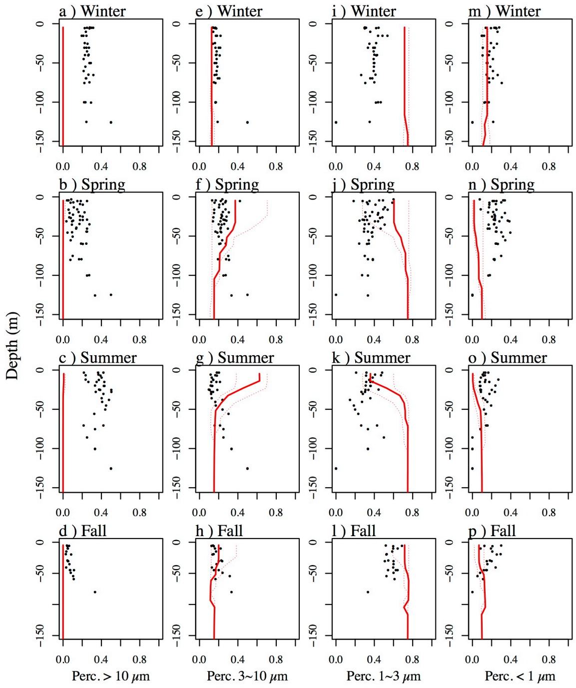

Fig. 8 . Model fittings to vertical profiles of four size fractions at K2

Bingzhang Chen 2017/9/29 10:58 AM
**Deleted:** *<sp>*

Bingzhang Chen 2017/9/29 2:51 PM
**Deleted:** *<sp>* ... [229]

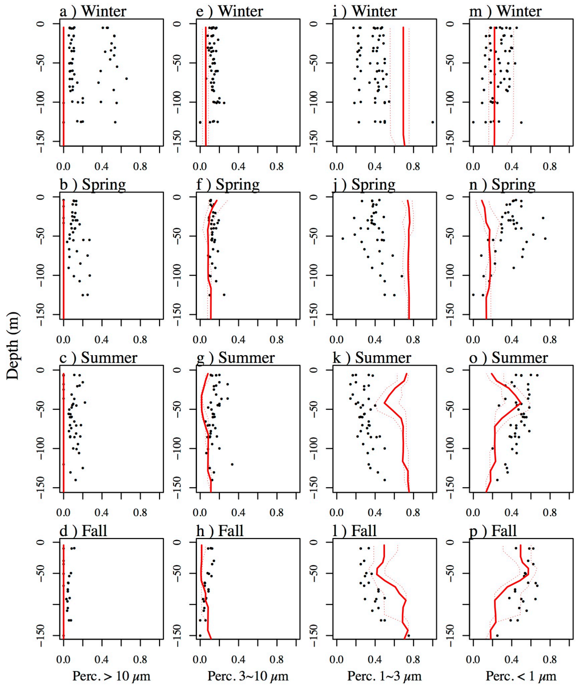

Fig. 9 . Model fittings to vertical profiles of four size fractions at S1

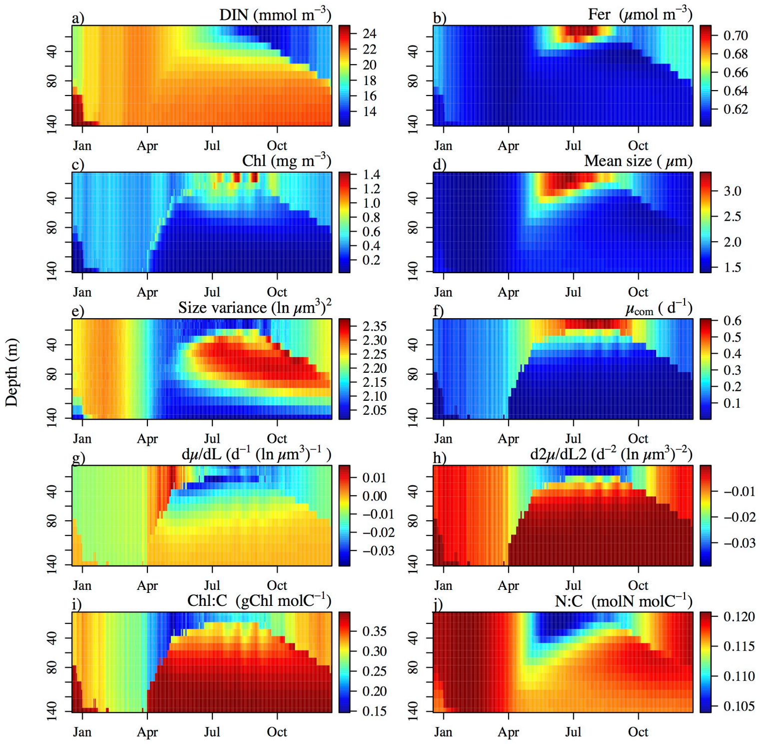

Fig. 10 . Modelled seasonal patterns at K2

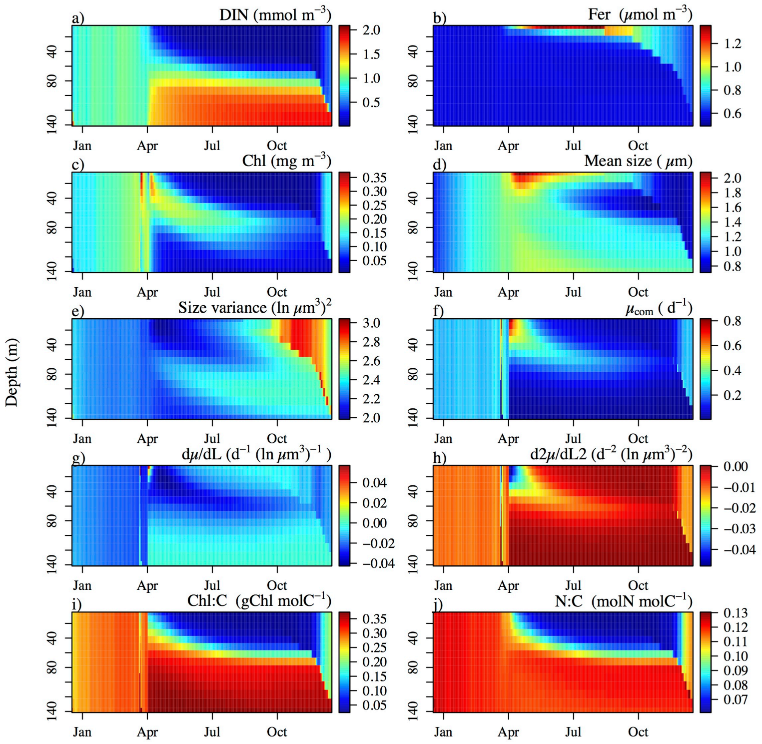

Fig. 11 . Modelled seasonal patterns at S1

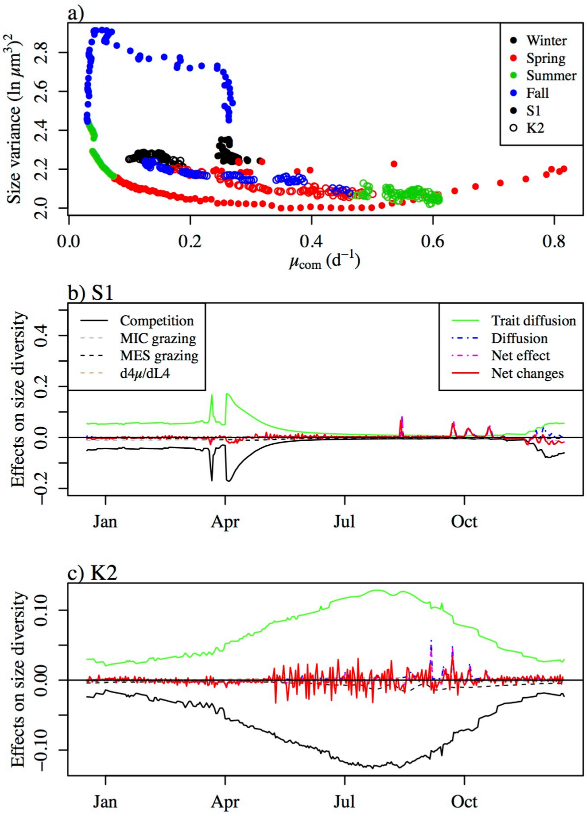

Fig. 12. (a) Scatterplots of size variance versus phytoplankton community growth rate ($\mu_{com}$). (b) Contributions of various factors to the dynamics of size variance in surface waters at S1. The term "Competition" equates to $v^2 \frac{d^2\mu}{dl^2}$. *MIC* and *MES* grazing equates to $-v^2 \frac{d^2 g_i}{dl^2}$. "d4$\mu$/dL4" equates to $v^2 u \frac{d^4\mu}{dl^4}$. "Trait diffusion" equates to $2u\mu$. All the derivatives are evaluated at the mean size. "Diffusion" means the contribution to the changes of size variance induced by diffusion with the underlying grid. "Net effect" means the sum of the above terms. "Net changes" mean the difference of size variance between adjacent days. (c) The same as (b), but at station K2.

Bingzhang Chen 2017/9/29 2:15 PM
**Formatted:** Centered

Bingzhang Chen 2017/9/29 2:15 PM
**Formatted:** Line spacing: single

Chen Bingzhang 2017/10/23 4:52 PM
**Formatted:** Font:10 pt

Chen Bingzhang 2017/10/23 4:52 PM
**Formatted:** Font:10 pt

Chen Bingzhang 2017/10/23 4:52 PM
**Formatted:** Font:10 pt

Chen Bingzhang 2017/10/23 4:52 PM
**Formatted:** Font:10 pt

Chen Bingzhang 2017/10/23 4:52 PM
**Formatted:** Font:10 pt

Chen Bingzhang 2017/10/23 4:52 PM
**Formatted:** Font:10 pt

Chen Bingzhang 2017/10/23 4:52 PM
**Formatted:** Font:10 pt

Chen Bingzhang 2017/10/23 4:52 PM
**Formatted:** Font:10 pt

Chen Bingzhang 2017/10/23 4:52 PM
**Formatted:** Font:10 pt

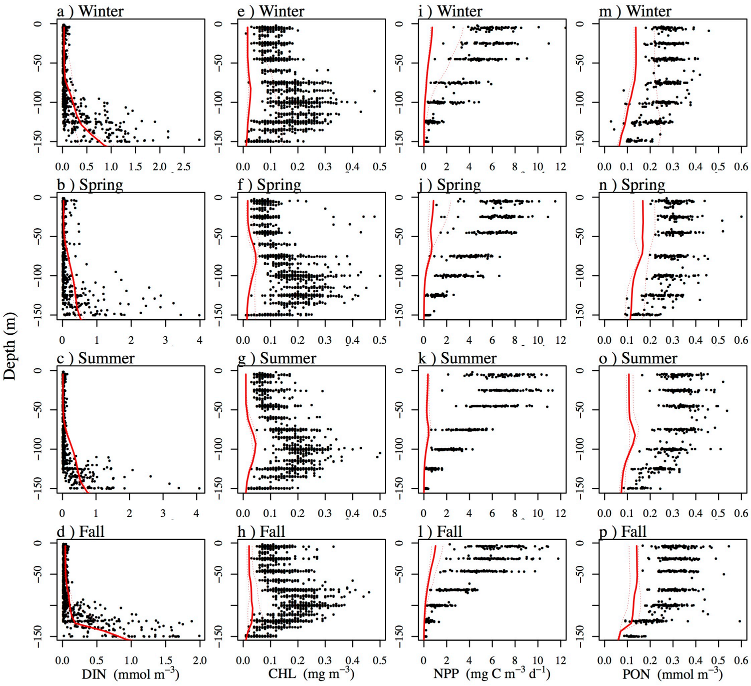

Fig. 13 . Model fittings to vertical profiles of DIN, CHL, NPP, and PON at ALOHA

Bingzhang Chen 2017/9/29 2:51 PM

**Formatted:** Centered

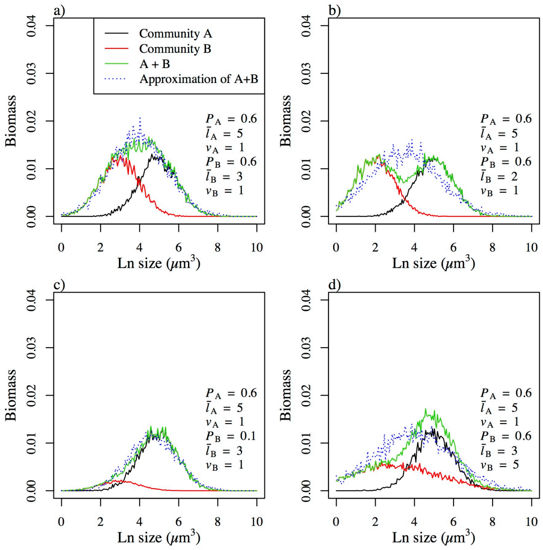

Fig. 14. Schematic diagrams for mixing of two phytoplankton communities with different biomass, mean size, and size variance, each following a lognormal size distribution.

Chen Bingzhang 2017/10/23 4:52 PM
**Deleted:**

**Page 6: [1] Formatted** **Chen Bingzhang** **17/8/5 11:09 PM**

Font:Italic

**Page 6: [2] Deleted** **Bingzhang Chen** **17/9/29 11:11 AM**

The constructed model structure and optimized model parameters are to be used for later application of the “adaptive dynamics” approach in three-dimensional ocean general circulation models (GCMs).

**Page 6: [2] Deleted** **Bingzhang Chen** **17/9/29 11:11 AM**

The constructed model structure and optimized model parameters are to be used for later application of the “adaptive dynamics” approach in three-dimensional ocean general circulation models (GCMs).

**Page 6: [3] Formatted** **Chen Bingzhang** **17/8/7 10:51 AM**

List Paragraph, Numbered + Level: 1 + Numbering Style: 1, 2, 3, … + Start at: 1 + Alignment: Left + Aligned at: 0 cm + Indent at: 0.85 cm

**Page 6: [4] Formatted** **Bingzhang Chen** **17/9/29 11:11 AM**

Font:Italic

**Page 6: [4] Formatted** **Bingzhang Chen** **17/9/29 11:11 AM**

Font:Italic

**Page 6: [5] Formatted** **Chen Bingzhang** **17/8/7 10:51 AM**

Font:Bold, English (US)

**Page 6: [6] Deleted** **Chen Bingzhang** **17/8/3 12:00 PM**

For simplicity, we assume that phytoplankton size is the master trait that determines all physiological functions (Litchman et al., 2007; Finkel et al., 2010; Edwards et al., 2011, 2012, 2015). In addition to phytoplankton total biomass ($\boldsymbol{P}$), we also include phytoplankton mean log size ($\bar{\boldsymbol{l}}$, ln $\mu$m$^3$) and log size variance ($\boldsymbol{v}$, (ln $\mu$m$^3$)$^2$) as independent tracers in the model. We use the product of $\boldsymbol{P}\bar{\boldsymbol{l}}$

**Page 6: [7] Formatted** **Bingzhang Chen** **17/9/29 10:54 AM**

Left

**Page 6: [8] Deleted** **Bingzhang Chen** **17/9/29 10:54 AM**

, respectively, for the tracers of mean and variance involved in diffusion. Note that we prefer $\boldsymbol{P^2}$

**Page 6: [9] Deleted** **Chen Bingzhang** **17/8/3 12:00 PM**

$\boldsymbol{P^2 v}$ slightly improved the model fitting. Because in certain parts of the North Pacific iron instead of nitrogen is the main limiting nutrient for phytoplankton growth (Fujiki et al., 2014), we also include dissolved iron (***fer***) as another independent tracer. Hence the model includes 7 tracers in total (Fig. 1).

**Page 6: [10] Deleted** **Bingzhang Chen** **17/9/30 1:12 PM**

**General d**

**Page 6: [10] Deleted** **Bingzhang Chen** **17/9/30 1:12 PM**

**General d**

**Page 6: [11] Formatted** **Chen Bingzhang** **17/8/3 12:01 PM**

Font:Bold

**Page 6: [12] Formatted** **Chen Bingzhang** **17/10/23 9:28 AM**

Indent: First line: 2.13 ch

**Page 6: [13] Formatted** **Chen Bingzhang** **17/8/3 12:07 PM**

Font:Bold, Italic

**Page 6: [13] Formatted** **Chen Bingzhang** **17/8/3 12:07 PM**

Font:Bold, Italic

**Page 6: [13] Formatted** **Chen Bingzhang** **17/8/3 12:07 PM**

Font:Bold, Italic

**Page 6: [13] Formatted** **Chen Bingzhang** **17/8/3 12:07 PM**

Font:Bold, Italic

**Page 6: [13] Formatted** **Chen Bingzhang** **17/8/3 12:07 PM**

Font:Bold, Italic

**Page 6: [13] Formatted** **Chen Bingzhang** **17/8/3 12:07 PM**

Font:Bold, Italic

**Page 6: [13] Formatted** **Chen Bingzhang** **17/8/3 12:07 PM**

Font:Bold, Italic

**Page 6: [13] Formatted** **Chen Bingzhang** **17/8/3 12:07 PM**

Font:Bold, Italic

**Page 6: [14] Formatted** **Chen Bingzhang** **17/8/3 12:11 PM**

Font:Not Bold

**Page 6: [15] Deleted** **Bingzhang Chen** **17/9/29 11:12 AM**

size (i.e.

**Page 6: [15] Deleted** **Bingzhang Chen** **17/9/29 11:12 AM**

size (i.e.

**Page 6: [15] Deleted** **Bingzhang Chen** **17/9/29 11:12 AM**

size (i.e.

**Page 6: [16] Formatted** **Chen Bingzhang** **17/8/3 2:02 PM**

Font:Bold, English (UK)

**Page 6: [17] Formatted** **S. Lan Smith** **17/10/22 10:31 PM**

Indent: First line: 2.13 ch

**Page 6: [18] Deleted** **Chen Bingzhang** **17/8/3 12:14 PM**

In addition to phytoplankton total biomass ($\boldsymbol{P}$), we also include phytoplankton mean log size ($\bar{\boldsymbol{l}}$, ln $\mu$m$^3$) and log size variance ($\boldsymbol{v}$, (ln $\mu$m$^3$)$^2$) as independent tracers in the model.

**Page 6: [18] Deleted** **Chen Bingzhang** **17/8/3 12:14 PM**

In addition to phytoplankton total biomass (***P***), we also include phytoplankton mean log size ($\boldsymbol{\bar{l}}$, ln $\mu m^3$) and log size variance ($\boldsymbol{v}$, (ln $\mu m^3)^2$) as independent tracers in the model.

**Page 6: [18] Deleted    Chen Bingzhang    17/8/3 12:14 PM**

In addition to phytoplankton total biomass (***P***), we also include phytoplankton mean log size ($\boldsymbol{\bar{l}}$, ln $\mu m^3$) and log size variance ($\boldsymbol{v}$, (ln $\mu m^3)^2$) as independent tracers in the model.

**Page 10: [19] Formatted    Bingzhang Chen    17/9/29 11:20 AM**

Indent: First line: 0 ch

**Page 10: [20] Formatted    Bingzhang Chen    17/9/29 11:21 AM**

Indent: First line: 0 ch

**Page 10: [21] Formatted    Chen Bingzhang    17/8/3 3:20 PM**

Font:Bold, Italic

**Page 10: [22] Formatted    Chen Bingzhang    17/8/3 3:20 PM**

Font:Bold, Italic, Subscript

**Page 10: [23] Formatted    Chen Bingzhang    17/8/3 3:20 PM**

Font:Not Bold

**Page 10: [24] Formatted    Chen Bingzhang    17/8/8 12:08 PM**

Centered

**Page 10: [25] Deleted    Bingzhang Chen    17/9/30 1:15 PM**

The initial condition of inorganic nitrogen was set to the vertical profile of nitrate in January of the World Ocean Atlas (WOA) 2013 monthly climatology. Initial phytoplankton, zooplankton, and detritus biomass wereare all set to 0.1 $\mu$mol L$^{-1}$ in each grid. Initial phytoplankton mean log size ($\bar{l}$) and log size variance ($v$) wereare set to be 1. Initial dissolved iron concentration wais set to the vertical profile of iron in January from a 3D global biogeochemical model output (Aumont et al., 2003). The time step of the model wasis 30 minutes. All the fixed model parameters are shown in Table 1 and the model parameters that are optimized to match observational data are shown in Table 2.

We employed a Dirichlet boundary condition at the bottom for DIN and ***fer*** with the values predefined by the WOA2013 climatology and the model output from Aumont et al. (2003), respectively. For other tracers, we assumed no diffusive flux at the bottom. Detritus wasis allowed to sink out of the system with the loss of nitrogen and iron replenished by diffusion.

**Page 10: [26] Formatted S. Lan Smith 17/10/2 11:34 AM**

Normal, Indent: First line: 2.13 ch, Line spacing: single

**Page 10: [27] Formatted Chen Bingzhang 17/8/3 5:05 PM**

Font:Bold, Italic

**Page 10: [28] Formatted Chen Bingzhang 17/8/3 11:58 AM**

Font:Bold

**Page 10: [29] Formatted Chen Bingzhang 17/8/3 5:00 PM**

Justified, Indent: First line: 2.13 ch

**Page 10: [30] Formatted Chen Bingzhang 17/8/3 5:00 PM**

Font:Italic, Subscript

**Page 10: [31] Deleted Chen Bingzhang 17/8/3 5:00 PM**

$$\frac{dP}{dt} \approx P\left(\mu(l) + \frac{v}{2}\left(\frac{d^2\mu(l)}{dl^2} + u\frac{d^4\mu(l)}{dl^4}\right) - 3u\frac{d^3\mu(l)}{dl^3}\right)\Bigg|_{l=\bar{l}} + \frac{d}{dz}\left(K_v\frac{dP}{dz}\right)$$

**Page 11: [32] Formatted Chen Bingzhang 17/8/22 11:42 PM**

Font:Italic

**Page 11: [32] Formatted Chen Bingzhang 17/8/22 11:42 PM**

Font:Italic

**Page 11: [32] Formatted Chen Bingzhang 17/8/22 11:42 PM**

Font:Italic

**Page 11: [33] Deleted Chen Bingzhang 17/8/3 5:01 PM**

, $K_v$ is the vertical eddy diffusivity (m$^2$ s$^{-1}$)

**Page 11: [33] Deleted Chen Bingzhang 17/8/3 5:01 PM**

, $K_v$ is the vertical eddy diffusivity (m$^2$ s$^{-1}$)

**Page 11: [34] Formatted Chen Bingzhang 17/8/8 2:17 PM**

Superscript

**Page 11: [35] Formatted Chen Bingzhang 17/8/8 2:11 PM**

Indent: First line:  2.36 ch

**Page 11: [36] Deleted** **Chen Bingzhang** **17/8/30 9:45 AM**

**Page 11: [36] Deleted** **Chen Bingzhang** **17/8/30 9:45 AM**

**Page 11: [37] Deleted** **Chen Bingzhang** **17/8/30 9:44 AM**

$P^2$

**Page 11: [37] Deleted** **Chen Bingzhang** **17/8/30 9:44 AM**

$P^2$

**Page 11: [37] Deleted** **Chen Bingzhang** **17/8/30 9:44 AM**

$P^2$

**Page 11: [37] Deleted** **Chen Bingzhang** **17/8/30 9:44 AM**

$P^2$

**Page 11: [37] Deleted** **Chen Bingzhang** **17/8/30 9:44 AM**

$P^2$

**Page 11: [37] Deleted** **Chen Bingzhang** **17/8/30 9:44 AM**

$P^2$

**Page 11: [37] Deleted** **Chen Bingzhang** **17/8/30 9:44 AM**

$P^2$

**Page 11: [37] Deleted** **Chen Bingzhang** **17/8/30 9:44 AM**

$P^2$

**Page 11: [37] Deleted** **Chen Bingzhang** **17/8/30 9:44 AM**

$P^2$

**Page 11: [37] Deleted** **Chen Bingzhang** **17/8/30 9:44 AM**

$P^2$

**Page 11: [38] Formatted** **Chen Bingzhang** **17/8/3 5:02 PM**

Font:Italic

**Page 11: [39] Deleted** **Chen Bingzhang** **17/8/3 5:11 PM**

dissolved inorganic nitrogen ($N$, $\mu$mol L$^{-1}$)

| | | |
|---|---|---|
| **Page 11: [39] Deleted** | **Chen Bingzhang** | **17/8/3 5:11 PM** |

dissolved inorganic nitrogen (*N*, $\mu$mol L$^{-1}$)

| | | |
|---|---|---|
| **Page 11: [40] Formatted** | **Chen Bingzhang** | **17/8/3 5:12 PM** |

Font:Bold, Italic

| | | |
|---|---|---|
| **Page 11: [41] Formatted** | **Bingzhang Chen** | **17/9/28 12:15 PM** |

English (US)

| | | |
|---|---|---|
| **Page 11: [42] Deleted** | **Chen Bingzhang** | **17/8/30 9:57 AM** |

| | | |
|---|---|---|
| **Page 11: [42] Deleted** | **Chen Bingzhang** | **17/8/30 9:57 AM** |

| | | |
|---|---|---|
| **Page 11: [43] Formatted** | **Bingzhang Chen** | **17/9/28 12:15 PM** |

English (US)

| | | |
|---|---|---|
| **Page 11: [44] Formatted** | **Chen Bingzhang** | **17/8/22 11:52 PM** |

Font:Bold, Italic

| | | |
|---|---|---|
| **Page 11: [45] Formatted** | **Bingzhang Chen** | **17/9/29 11:30 AM** |

English (US)

| | | |
|---|---|---|
| **Page 11: [45] Formatted** | **Bingzhang Chen** | **17/9/29 11:30 AM** |

English (US)

| | | |
|---|---|---|
| **Page 11: [45] Formatted** | **Bingzhang Chen** | **17/9/29 11:30 AM** |

English (US)

| | | |
|---|---|---|
| **Page 11: [45] Formatted** | **Bingzhang Chen** | **17/9/29 11:30 AM** |

English (US)

| | | |
|---|---|---|
| **Page 12: [46] Deleted** | **Chen Bingzhang** | **17/8/22 11:53 PM** |

are also able

| | | |
|---|---|---|
| **Page 12: [46] Deleted** | **Chen Bingzhang** | **17/8/22 11:53 PM** |

are also able

| | | |
|---|---|---|
| **Page 12: [46] Deleted** | **Chen Bingzhang** | **17/8/22 11:53 PM** |

are also able

| | | |
|---|---|---|
| **Page 12: [47] Formatted** | **Bingzhang Chen** | **17/9/28 12:15 PM** |

English (US)

**Page 12: [47] Formatted Bingzhang Chen 17/9/28 12:15 PM**

English (US)

**Page 12: [47] Formatted Bingzhang Chen 17/9/28 12:15 PM**

English (US)

**Page 12: [48] Formatted Bingzhang Chen 17/9/29 5:21 PM**

Font:Italic

**Page 12: [48] Formatted Bingzhang Chen 17/9/29 5:21 PM**

Font:Italic

**Page 12: [48] Formatted Bingzhang Chen 17/9/29 5:21 PM**

Font:Italic

**Page 12: [48] Formatted Bingzhang Chen 17/9/29 5:21 PM**

Font:Italic

**Page 12: [49] Formatted Bingzhang Chen 17/9/29 5:32 PM**

Font:Italic

**Page 12: [49] Formatted Bingzhang Chen 17/9/29 5:32 PM**

Font:Italic

**Page 12: [49] Formatted Bingzhang Chen 17/9/29 5:32 PM**

Font:Italic

**Page 12: [49] Formatted Bingzhang Chen 17/9/29 5:32 PM**

Font:Italic

**Page 12: [49] Formatted Bingzhang Chen 17/9/29 5:32 PM**

Font:Italic

**Page 12: [49] Formatted Bingzhang Chen 17/9/29 5:32 PM**

Font:Italic

**Page 12: [49] Formatted Bingzhang Chen 17/9/29 5:32 PM**

Font:Italic

**Page 12: [49] Formatted Bingzhang Chen 17/9/29 5:32 PM**

Font:Italic

**Page 13: [50] Deleted Bingzhang Chen 17/9/30 1:42 PM**

Light levels ($I_z$) at depth $z$ were calculated based on $PAR_0$ and Chl $a$ concentrations following the Beer-Lambert law:

$$I_z = PAR_0 e^{-z\left(K_w + K_{chl} \int_z^0 Chl(x)dx\right)} \tag{12}$$

in which $K_w$ and $K_{chl}$ are the attenuation coefficients for seawater and Chl $a$, respectively. To realistically estimate the average light field that a phytoplankton cell should experience in a mixing water column (Franks, 2015), the ambient light level for phytoplankton within the surface mixed layer (ML) is calculated as the average light throughout the surface mixed layerML, which is defined as the deepest depth with $K_v > 10^{-3}$ m$^2$ s$^{-1}$. This calculation is based on eq. (1) in Franks (2015), which gives that the average time for a phytoplankton cell to move 100 m at the local diffusivity of $10^{-3}$ m$^2$ s$^{-1}$ is roughly half a day. However, to compare with *in situ NPP* estimates that were calculated from incubation bottles without continuous mixing, phytoplankton $\mu$, $\theta$, and $Q_N$ are recalculated from $I_z$ based on the Beer-Lambert law (Eq. 12).

| **Page 13: [51] Formatted** | **Bingzhang Chen** | **17/9/28 12:15 PM** |
|---|---|---|

English (US)

| **Page 13: [52] Deleted** | **Chen Bingzhang** | **17/8/3 11:58 AM** |
|---|---|---|

### 2.2 General description of the 1D model (nutrient, zooplankton (*Z*), detritus (*D*), iron (*fer*), and light)

The 1D model focuses on the upper 250 meters of the ocean. The vertical grid, a total of 30 layers, follows a stretched vertical coordinate with increasing resolution towards the sea surface (surface stretching parameter = 2.0), similar to that used in the Regional Ocean Modelling System (ROMS) (Shchepetkin and McWilliams, 2005). For computational efficiency, the 1D model contains only biological tracers. The physics variables are imported as external data (*see* Sect. 2.3 for details).

For simplicity, phytoplankton cells are assumed not to excrete inorganic nitrogen or to have any natural mortality to be converted into detritus. We assume a generic zooplankton compartment that feeds only on phytoplankton following a Holling Type III functional response without any size-dependent feeding preference:

$$\boldsymbol{Zoo\ ingestion\ per\ capita} = \boldsymbol{g_{max}\frac{P^2}{P^2+K_P^2}} \tag{6}$$

where $g_{max}$ is the maximal zooplankton ingestion rate, $K_P$ is the half-saturation constant for zooplankton grazing.

The total amount of phytoplankton ingested by zooplankton is divided among three fates: zooplankton net growth, excretion into the inorganic nitrogen pool, and defecation of unassimilated food into the detritus pool (Buitenhuis et al., 2010). The mortality rate of zooplankton is set to be proportional to the squares of zooplankton biomass. The dynamics of zooplankton follow:

$$\boldsymbol{\frac{dZ}{dt} = e^{\frac{E_Z}{k}\left(\frac{1}{T_0}-\frac{1}{T}\right)}\left(Zg_{max}\frac{P^2}{P^2+K_P^2}NGE - m_z Z^2\right) + \frac{d}{dz}\left(K_v\frac{dZ}{dz}\right)} \tag{7a}$$

where $E_z$ is the activation energy for heterotrophic processes. $NGE$ is the net growth efficiency of zooplankton. $m_z$ is the zooplankton mortality coefficient. $z$ is water depth (m).

Detritus is converted to inorganic nitrogen at a rate ($R_{dn}$, d$^{-1}$) that has the same temperature sensitivity with zooplankton grazing. Detritus is also assumed to have a constant sinking rate ($W_d$).

$$\frac{dD}{dt} = e^{\frac{E_z}{k}\left(\frac{1}{T_0}-\frac{1}{T}\right)}\left(Zg_{max}\frac{P^2}{P^2+K_P^2}unass + m_z Z^2 - -W_d\frac{dD}{dz} + \frac{d}{dz}\left(K_v\frac{dD}{dz}\right) \quad (7b)$$

The dynamics of inorganic nutrients follow:

$$\frac{dN}{dt} = -P\left(\mu(l) + \frac{v}{2}\left(\frac{d^2\mu(l)}{dl^2} + u\frac{d^4\mu(l)}{dl^4}\right) - 3u\frac{d^3\mu(l)}{dl^3}\right)\Bigg|_{l=\bar{l}} + e^{\frac{E_z}{k}\left(\frac{1}{T_0}-\frac{1}{T}\right)}\left(Zg_{max}\frac{P^2}{P^2+K_P^2}(1 - NGE - unass) + DR_{dn}\right) + \frac{d}{dz}\left(K_v\frac{dN}{dz}\right) \quad (7c)$$

The dynamics of dissolved iron largely follow Aumont et al. (2003), Nikelsen et al. (2015), and the PlankTOM10 model (Buitenhuis et al., 2010):

$$\frac{dfer}{dt} = \left[-P\left(\mu(l) + \frac{v}{2}\left(\frac{d^2\mu(l)}{dl^2} + u\frac{d^4\mu(l)}{dl^4}\right) - 3u\frac{d^3\mu(l)}{dl^3}\right)\Bigg|_{l=\bar{l}} + e^{\frac{E_z}{k}\left(\frac{1}{T_0}-\frac{1}{T}\right)}\left(Zg_{max}\frac{P^2}{P^2+K_P^2}(1 - NGE - unass) + DR_{dn}\right)\right]R_{fer\_N} + \text{dust deposition} - fer_{scav} + \frac{d}{dz}\left(K_v\frac{dfer}{dz}\right) \quad (7d)$$

To translate between nitrogen and iron in particles, a constant *fer*:*N* ratio ($R_{fer\_N}$) of 0.0265 is assumed. Monthly atmospheric dust deposition data are extracted from Tegen and Fung (1995). Following the PlankTOM10 model, iron scavenging rate ($fer_{scav}$) is composed of both background scavenging rate ($k_{scm}$) and particle absorption rate ($k_{sc}$):

$$\boldsymbol{fer_{scav} = k_{scm} + k_{sc} D e^{\frac{E_Z}{k}\left(\frac{1}{T_0}-\frac{1}{T}\right)} \frac{\left(-(1+(l_{fe}-fer)k_{eq})+\sqrt{4ferk_{eq}+(1+(l_{fe}-fer)k_{eq})^2}\right)}{2k_{eq}}}$$

(8a)

where $k_{eq}$ is the equilibrium constant between free iron and ligands and organic complexes:

$$\boldsymbol{k_{eq} = 10^{\left(17.27-\frac{1565.7}{T}\right)}}$$

(8b)

Note that $T$ is in absolute temperature. $l_{fe}$ is the total iron ligand concentration that is assumed constant (0.6 nM).

Light levels ($I_z$) at depth $z$ were calculated based on $PAR_0$ and Chl $a$ concentrations following the Beer-Lambert law:

$$\boldsymbol{I_z = PAR_0 e^{-z\left(K_w + K_{chl}\int_z^0 Chl(x)dx\right)}}$$

(9)

in which $K_w$ and $K_{chl}$ are the attenuation coefficients for seawater and Chl $a$, respectively. To realistically estimate the average light field that a phytoplankton cell should experience in a mixing water column (Franks, 2015), the ambient light level for phytoplankton within the surface mixed layer (ML) is calculated as the average light throughout the surface ML, which is defined as the deepest depth with $K_v > 10^{-3}$ m$^2$ s$^{-1}$. This calculation is based on eq. (1) in Franks (2015), which gives that the average time for a phytoplankton cell to move 100 m at the local diffusivity of $10^{-3}$ m$^2$ s$^{-1}$ is roughly half a day. However, to compare with *in situ NPP* estimates that were calculated from incubation bottles without continuous mixing, phytoplankton $\mu$, $\theta$, and $Q_N$ are recalculated from $I_z$ based on the Beer-Lambert law.

The initial condition of inorganic nitrogen is set to the vertical profile of nitrate in January of the World Ocean Atlas (WOA) 2013 monthly climatology. Initial phytoplankton, zooplankton, and detritus biomass are all set to 0.1 $\mu$mol L$^{-1}$ in each grid. Initial phytoplankton mean log size ($\bar{\boldsymbol{l}}$) and log size variance ($v$) are set to be 1. Initial dissolved iron concentration is set to the vertical profile of iron in January from a 3D global biogeochemical model output (Aumont et al., 2003). The time step of the model is 10 minutes. All the fixed model parameters are shown in Table 1 and the model parameters that are optimized to match observational data are shown in Table 2.

**Page 13: [53] Formatted Chen Bingzhang 17/8/8 12:11 PM**

Normal

**Page 13: [54] Formatted Chen Bingzhang 17/8/22 11:12 PM**

Font:Bold, Italic

**Page 13: [55] Formatted Chen Bingzhang 17/8/8 1:44 PM**

Normal, Right

**Page 13: [56] Formatted Chen Bingzhang 17/8/8 1:45 PM**

Normal

**Page 13: [57] Formatted Chen Bingzhang 17/8/8 2:44 PM**

Font:Italic

**Page 13: [57] Formatted Chen Bingzhang 17/8/8 2:44 PM**

Font:Italic

**Page 13: [57] Formatted Chen Bingzhang 17/8/8 2:44 PM**

Font:Italic

**Page 13: [57] Formatted Chen Bingzhang 17/8/8 2:44 PM**

Font:Italic

**Page 13: [57] Formatted Chen Bingzhang 17/8/8 2:44 PM**

Font:Italic

**Page 13: [57] Formatted Chen Bingzhang 17/8/8 2:44 PM**

Font:Italic

**Page 13: [57] Formatted Chen Bingzhang 17/8/8 2:44 PM**

Font:Italic

**Page 13: [57] Formatted Chen Bingzhang 17/8/8 2:44 PM**

Font:Italic

**Page 13: [57] Formatted Chen Bingzhang 17/8/8 2:44 PM**

Font:Italic

**Page 13: [58] Formatted Bingzhang Chen 17/9/28 12:15 PM**

English (US)

**Page 13: [59] Formatted** **Chen Bingzhang** **17/8/23 12:05 AM**

Font:Italic

**Page 13: [60] Formatted** **Bingzhang Chen** **17/9/28 12:15 PM**

English (US)

**Page 13: [60] Formatted** **Bingzhang Chen** **17/9/28 12:15 PM**

English (US)

**Page 13: [61] Formatted** **Chen Bingzhang** **17/8/23 12:06 AM**

Font:Italic

**Page 13: [62] Formatted** **Bingzhang Chen** **17/9/28 12:15 PM**

Font:Italic, English (US)

**Page 13: [62] Formatted** **Bingzhang Chen** **17/9/28 12:15 PM**

Font:Italic, English (US)

**Page 13: [62] Formatted** **Bingzhang Chen** **17/9/28 12:15 PM**

Font:Italic, English (US)

**Page 13: [63] Formatted** **Chen Bingzhang** **17/8/8 2:05 PM**

Normal, Right

**Page 13: [64] Formatted** **Chen Bingzhang** **17/8/8 2:07 PM**

Normal

**Page 13: [65] Formatted** **Chen Bingzhang** **17/8/8 2:34 PM**

Font:Italic

**Page 13: [65] Formatted** **Chen Bingzhang** **17/8/8 2:34 PM**

Font:Italic

**Page 13: [65] Formatted** **Chen Bingzhang** **17/8/8 2:34 PM**

Font:Italic

**Page 13: [66] Formatted** **Chen Bingzhang** **17/8/8 2:45 PM**

Normal, Right

**Page 13: [67] Formatted** **Chen Bingzhang** **17/8/8 2:07 PM**

Normal

**Page 13: [68] Formatted** **Chen Bingzhang** **17/8/8 2:46 PM**

Font:Italic

| **Page 13: [68] Formatted** | **Chen Bingzhang** | **17/8/8 2:46 PM** |
|---|---|---|

Font:Italic

| **Page 13: [68] Formatted** | **Chen Bingzhang** | **17/8/8 2:46 PM** |
|---|---|---|

Font:Italic

| **Page 13: [69] Formatted** | **Chen Bingzhang** | **17/8/8 2:49 PM** |
|---|---|---|

Normal, Right

| **Page 13: [70] Formatted** | **Chen Bingzhang** | **17/8/8 2:50 PM** |
|---|---|---|

Normal

| **Page 13: [71] Formatted** | **Bingzhang Chen** | **17/9/28 12:16 PM** |
|---|---|---|

English (US)

| **Page 13: [72] Formatted** | **Chen Bingzhang** | **17/10/23 9:25 AM** |
|---|---|---|

Normal, Centered

| **Page 13: [73] Formatted** | **Chen Bingzhang** | **17/8/8 2:50 PM** |
|---|---|---|

Normal

| **Page 13: [74] Formatted** | **Chen Bingzhang** | **17/8/23 12:25 AM** |
|---|---|---|

Normal, Centered

| **Page 13: [75] Formatted** | **Chen Bingzhang** | **17/8/8 2:50 PM** |
|---|---|---|

Normal

| **Page 13: [76] Formatted** | **Chen Bingzhang** | **17/8/8 2:55 PM** |
|---|---|---|

Font:Italic

| **Page 13: [76] Formatted** | **Chen Bingzhang** | **17/8/8 2:55 PM** |
|---|---|---|

Font:Italic

| **Page 13: [77] Formatted** | **Chen Bingzhang** | **17/8/23 12:12 AM** |
|---|---|---|

Normal, Right

| **Page 13: [78] Formatted** | **Chen Bingzhang** | **17/8/23 12:12 AM** |
|---|---|---|

Font:Bold

| **Page 13: [79] Formatted** | **Chen Bingzhang** | **17/8/8 5:33 PM** |
|---|---|---|

Normal

| **Page 13: [80] Formatted** | **Chen Bingzhang** | **17/8/8 5:38 PM** |
|---|---|---|

Normal, Right

**Page 15: [81] Deleted S. Lan Smith 17/10/22 10:35 PM**

is used to generate a new set of parameters based on current position of the parameters.

**Page 16: [82] Deleted S. Lan Smith 17/10/22 10:40 PM**

, developed by

**Page 16: [82] Deleted S. Lan Smith 17/10/22 10:40 PM**

, developed by

**Page 16: [82] Deleted S. Lan Smith 17/10/22 10:40 PM**

, developed by

**Page 16: [82] Deleted S. Lan Smith 17/10/22 10:40 PM**

, developed by

**Page 16: [82] Deleted S. Lan Smith 17/10/22 10:40 PM**

, developed by

**Page 16: [83] Deleted S. Lan Smith 17/10/22 10:44 PM**

usually the main cause for the

**Page 16: [83] Deleted S. Lan Smith 17/10/22 10:44 PM**

usually the main cause for the

**Page 16: [83] Deleted S. Lan Smith 17/10/22 10:44 PM**

usually the main cause for the

**Page 16: [83] Deleted S. Lan Smith 17/10/22 10:44 PM**

usually the main cause for the

**Page 16: [83] Deleted S. Lan Smith 17/10/22 10:44 PM**

usually the main cause for the

**Page 16: [83] Deleted S. Lan Smith 17/10/22 10:44 PM**

usually the main cause for the

**Page 16: [83] Deleted S. Lan Smith 17/10/22 10:44 PM**

usually the main cause for the

**Page 16: [84] Deleted S. Lan Smith 17/10/22 10:46 PM**

DRAM

**Page 16: [84] Deleted S. Lan Smith 17/10/22 10:46 PM**

DRAM

**Page 16: [84] Deleted** **S. Lan Smith** **17/10/22 10:46 PM**

DRAM

**Page 16: [84] Deleted** **S. Lan Smith** **17/10/22 10:46 PM**

DRAM

**Page 16: [85] Deleted** **S. Lan Smith** **17/10/22 10:48 PM**

workflow of the

**Page 16: [85] Deleted** **S. Lan Smith** **17/10/22 10:48 PM**

workflow of the

**Page 16: [85] Deleted** **S. Lan Smith** **17/10/22 10:48 PM**

workflow of the

**Page 16: [86] Deleted** **S. Lan Smith** **17/10/22 10:49 PM**

. The initial $P_{cvm}$ is constructed to have

1)

**Page 16: [86] Deleted** **S. Lan Smith** **17/10/22 10:49 PM**

. The initial $P_{cvm}$ is constructed to have

2)

**Page 16: [86] Deleted** **S. Lan Smith** **17/10/22 10:49 PM**

. The initial $P_{cvm}$ is constructed to have

3)

**Page 16: [86] Deleted** **S. Lan Smith** **17/10/22 10:49 PM**

. The initial $P_{cvm}$ is constructed to have

4)

**Page 16: [86] Deleted** **S. Lan Smith** **17/10/22 10:49 PM**

. The initial $P_{cvm}$ is constructed to have

5)

**Page 17: [87] Formatted** **Chen Bingzhang** **17/8/27 10:00 PM**

Font:Italic

**Page 17: [87] Formatted** **Chen Bingzhang** **17/8/27 10:00 PM**

Font:Italic

**Page 17: [87] Formatted** **Chen Bingzhang** **17/8/27 10:00 PM**

Font:Italic

**Page 17: [87] Formatted** **Chen Bingzhang** **17/8/27 10:00 PM**

Font:Italic

**Page 17: [88] Formatted** **Chen Bingzhang** **17/8/27 10:00 PM**

Subscript

**Page 17: [88] Formatted Chen Bingzhang 17/8/27 10:00 PM**

Subscript

**Page 17: [89] Formatted Chen Bingzhang 17/8/27 10:03 PM**

Font:Italic

**Page 17: [90] Formatted Chen Bingzhang 17/8/27 10:07 PM**

Font:Not Italic

**Page 17: [90] Formatted Chen Bingzhang 17/8/27 10:07 PM**

Font:Not Italic

**Page 17: [91] Formatted Chen Bingzhang 17/8/27 11:10 PM**

Font:Italic

**Page 17: [91] Formatted Chen Bingzhang 17/8/27 11:10 PM**

Font:Italic

**Page 17: [91] Formatted Chen Bingzhang 17/8/27 11:10 PM**

Font:Italic

**Page 17: [91] Formatted Chen Bingzhang 17/8/27 11:10 PM**

Font:Italic

**Page 17: [91] Formatted Chen Bingzhang 17/8/27 11:10 PM**

Font:Italic

**Page 17: [91] Formatted Chen Bingzhang 17/8/27 11:10 PM**

Font:Italic

**Page 17: [91] Formatted Chen Bingzhang 17/8/27 11:10 PM**

Font:Italic

**Page 17: [91] Formatted Chen Bingzhang 17/8/27 11:10 PM**

Font:Italic

**Page 17: [92] Formatted Chen Bingzhang 17/8/27 9:42 PM**

List Paragraph, Indent: Left: 0 cm, Hanging: 4.26 ch, Numbered + Level: 1 + Numbering Style: 1, 2, 3, … + Start at: 1 + Alignment: Left + Aligned at: 0.75 cm + Indent at: 1.98 cm

**Page 17: [93] Formatted Bingzhang Chen 17/9/28 12:15 PM**

English (US)

**Page 17: [94] Formatted** **Chen Bingzhang** **17/8/27 11:15 PM**

English (US)

**Page 17: [95] Formatted** **Chen Bingzhang** **17/8/27 11:15 PM**

Indent: First line: 1.77 ch

**Page 17: [96] Deleted** **S. Lan Smith** **17/10/22 10:52 PM**

um

**Page 17: [96] Deleted** **S. Lan Smith** **17/10/22 10:52 PM**

um

**Page 17: [97] Formatted** **Bingzhang Chen** **17/9/28 12:15 PM**

English (US)

**Page 17: [98] Formatted** **Chen Bingzhang** **17/8/27 11:17 PM**

Font:Italic

**Page 17: [99] Formatted** **Bingzhang Chen** **17/9/28 12:15 PM**

English (US)

**Page 17: [100] Formatted** **Bingzhang Chen** **17/9/28 12:15 PM**

English (US)

**Page 17: [101] Formatted** **Bingzhang Chen** **17/9/28 12:15 PM**

English (US)

**Page 17: [101] Formatted** **Bingzhang Chen** **17/9/28 12:15 PM**

English (US)

**Page 17: [102] Deleted** **Chen Bingzhang** **17/8/23 7:05 AM**

The adaptive component uses information from previous model runs to approximate the distribution of parameter values as a multivariate Gaussian, which it periodically updates as more simulations are conducted. Based on this, the algorithm alters the magnitude and direction of proposed ‘jumps’ in parameter space (i.e., the proposal covariance matrix ($P_{cvm}$)) in order to more efficiently explore the parameter space. Specifically, the $P_{cvm}$ is tuned based on the covariance matrix ($C_{vm}$) of the already accepted parameter sets after a fixed number of iterations following Gelman et al. (2014) (i.e. $P_{cvm} = C_{vm} \bullet 2.4^2/d$, where $d$ is the dimension of the target parameter vector).

With the delayed rejection MCMC, when a newly proposed set of parameters is rejected, $P_{cvm}$ is temporarily downscaled (to 1% of the original $P_{cvm}$ in our case) and a second set of parameters is proposed based on the rejected parameters and the downscaled $P_{cvm}$. DRAM has the advantage of speeding up the mixing properties of MHMC and has been shown to better explore the parameter space than some other algorithms such as the families of Simulated Annealing possibly due to the use of two-stage proposal covariance matrices (Villagran et al., 2008). Compared with the widely used ensemble Kalman filter, DRAM is perhaps more suitable for the nonlinear ecosystems (Annan and Hargreaves, 2007).

**Page 18: [103] Deleted** **Chen Bingzhang** **17/8/27 11:31 PM**

$p$

**Page 18: [103] Deleted** **Chen Bingzhang** **17/8/27 11:31 PM**

$p$

**Page 18: [103] Deleted** **Chen Bingzhang** **17/8/27 11:31 PM**

$p$

**Page 18: [104] Deleted** **Chen Bingzhang** **17/10/23 9:33 AM**

y

**Page 18: [104] Deleted** **Chen Bingzhang** **17/10/23 9:33 AM**

y

**Page 18: [105] Deleted** **S. Lan Smith** **17/10/22 10:58 PM**

a

**Page 18: [105] Deleted** **S. Lan Smith** **17/10/22 10:58 PM**

a

**Page 18: [106] Formatted** **Bingzhang Chen** **17/9/28 12:15 PM**

English (US)

**Page 18: [106] Formatted** **Bingzhang Chen** **17/9/28 12:15 PM**

English (US)

**Page 18: [107] Deleted** **Chen Bingzhang** **17/10/23 9:35 AM**

are

**Page 18: [107] Deleted** **Chen Bingzhang** **17/10/23 9:35 AM**

are

**Page 18: [108] Deleted** **Chen Bingzhang** **17/8/27 11:36 PM**

$p$

**Page 18: [108] Deleted** **Chen Bingzhang** **17/8/27 11:36 PM**

$p$

**Page 18: [109] Formatted** **Bingzhang Chen** **17/9/28 12:15 PM**

English (US)

**Page 18: [109] Formatted** **Bingzhang Chen** **17/9/28 12:15 PM**

English (US)

**Page 18: [109] Formatted** **Bingzhang Chen** **17/9/28 12:15 PM**

English (US)

**Page 18: [109] Formatted** **Bingzhang Chen** **17/9/28 12:15 PM**

English (US)

**Page 18: [110] Formatted** **Chen Bingzhang** **17/9/14 4:45 PM**

Font:Italic

**Page 18: [110] Formatted** **Chen Bingzhang** **17/9/14 4:45 PM**

Font:Italic

**Page 18: [110] Formatted** **Chen Bingzhang** **17/9/14 4:45 PM**

Font:Italic

**Page 18: [110] Formatted** **Chen Bingzhang** **17/9/14 4:45 PM**

Font:Italic

**Page 20: [111] Deleted** **Chen Bingzhang** **17/9/14 4:13 PM**

,

**Page 20: [111] Deleted** **Chen Bingzhang** **17/9/14 4:13 PM**

,

**Page 20: [111] Deleted** **Chen Bingzhang** **17/9/14 4:13 PM**

,

**Page 20: [111] Deleted** **Chen Bingzhang** **17/9/14 4:13 PM**

,

**Page 20: [111] Deleted** **Chen Bingzhang** **17/9/14 4:13 PM**

,

**Page 20: [112] Deleted Chen Bingzhang 17/9/20 3:45 PM**

**O**

**Page 20: [112] Deleted Chen Bingzhang 17/9/20 3:45 PM**

**O**

**Page 20: [112] Deleted Chen Bingzhang 17/9/20 3:45 PM**

**O**

**Page 20: [113] Deleted Chen Bingzhang 17/9/14 4:21 PM**

As expected

**Page 20: [113] Deleted Chen Bingzhang 17/9/14 4:21 PM**

As expected

**Page 20: [113] Deleted Chen Bingzhang 17/9/14 4:21 PM**

As expected

**Page 20: [113] Deleted Chen Bingzhang 17/9/14 4:21 PM**

As expected

**Page 20: [113] Deleted Chen Bingzhang 17/9/14 4:21 PM**

As expected

**Page 20: [113] Deleted Chen Bingzhang 17/9/14 4:21 PM**

As expected

**Page 20: [113] Deleted Chen Bingzhang 17/9/14 4:21 PM**

As expected

**Page 20: [113] Deleted Chen Bingzhang 17/9/14 4:21 PM**

As expected

**Page 20: [113] Deleted Chen Bingzhang 17/9/14 4:21 PM**

As expected

**Page 20: [113] Deleted Chen Bingzhang 17/9/14 4:21 PM**

As expected

**Page 20: [114] Formatted Chen Bingzhang 17/9/22 2:23 PM**

Font:Italic

**Page 20: [114] Formatted Chen Bingzhang 17/9/22 2:23 PM**

Font:Italic

**Page 20: [114] Formatted** **Chen Bingzhang** **17/9/22 2:23 PM**

Font:Italic

**Page 20: [114] Formatted** **Chen Bingzhang** **17/9/22 2:23 PM**

Font:Italic

**Page 20: [115] Formatted** **Chen Bingzhang** **17/9/22 2:24 PM**

Font:Italic

**Page 20: [115] Formatted** **Chen Bingzhang** **17/9/22 2:24 PM**

Font:Italic

**Page 20: [115] Formatted** **Chen Bingzhang** **17/9/22 2:24 PM**

Font:Italic

**Page 20: [116] Deleted** **Chen Bingzhang** **17/9/14 4:30 PM**

such as $K_{0,N}$, $W_d$, $\alpha_{0,C}$, and $K_{0,fer}$

**Page 20: [116] Deleted** **Chen Bingzhang** **17/9/14 4:30 PM**

such as $K_{0,N}$, $W_d$, $\alpha_{0,C}$, and $K_{0,fer}$

**Page 20: [117] Formatted** **Chen Bingzhang** **17/9/22 3:18 PM**

Font:Italic

**Page 20: [117] Formatted** **Chen Bingzhang** **17/9/22 3:18 PM**

Font:Italic

**Page 20: [117] Formatted** **Chen Bingzhang** **17/9/22 3:18 PM**

Font:Italic

**Page 21: [118] Formatted** **Bingzhang Chen** **17/9/29 11:50 AM**

Font:12 pt

**Page 21: [118] Formatted** **Bingzhang Chen** **17/9/29 11:50 AM**

Font:12 pt

**Page 21: [119] Formatted** **Chen Bingzhang** **17/9/20 5:30 PM**

Font:12 pt

**Page 21: [119] Formatted** **Chen Bingzhang** **17/9/20 5:30 PM**

Font:12 pt

**Page 21: [120] Formatted** **Bingzhang Chen** **17/9/29 11:50 AM**

Font:12 pt

**Page 21: [120] Formatted** **Bingzhang Chen** **17/9/29 11:50 AM**

Font:12 pt

**Page 21: [121] Deleted** **Chen Bingzhang** **17/8/3 12:05 PM**

TIN

**Page 21: [121] Deleted** **Chen Bingzhang** **17/8/3 12:05 PM**

TIN

**Page 21: [121] Deleted** **Chen Bingzhang** **17/8/3 12:05 PM**

TIN

**Page 21: [121] Deleted** **Chen Bingzhang** **17/8/3 12:05 PM**

TIN

**Page 21: [121] Deleted** **Chen Bingzhang** **17/8/3 12:05 PM**

TIN

**Page 21: [121] Deleted** **Chen Bingzhang** **17/8/3 12:05 PM**

TIN

**Page 21: [121] Deleted** **Chen Bingzhang** **17/8/3 12:05 PM**

TIN

**Page 21: [122] Deleted** **Chen Bingzhang** **17/9/14 5:30 PM**

Although with some deviations, t

**Page 21: [122] Deleted** **Chen Bingzhang** **17/9/14 5:30 PM**

Although with some deviations, t

**Page 21: [122] Deleted** **Chen Bingzhang** **17/9/14 5:30 PM**

Although with some deviations, t

**Page 21: [122] Deleted** **Chen Bingzhang** **17/9/14 5:30 PM**

Although with some deviations, t

**Page 21: [123] Deleted** **Chen Bingzhang** **17/9/16 10:42 PM**

At station S1, the model also reproduced the relatively invariant proportions of size-fractionated Chl with depth during stratified seasons. This is not expected because of a steep vertical gradient of TIN around 100 m, which was expected to enhance the growth of large phytoplankton. The relative constancy of phytoplankton size structure with depth suggests that large phytoplankton are more susceptible to light limitation as previously suggested (Finkel, 2001; Edwards et al., 2015).

**Page 21: [123] Deleted** **Chen Bingzhang** **17/9/16 10:42 PM**

At station S1, the model also reproduced the relatively invariant proportions of size-fractionated Chl with depth during stratified seasons. This is not expected because of a steep vertical gradient of TIN around 100 m, which was expected to enhance the growth of large phytoplankton. The relative constancy of phytoplankton size structure with depth suggests that large phytoplankton are more susceptible to light limitation as previously suggested (Finkel, 2001; Edwards et al., 2015).

**Page 21: [124] Deleted** **Chen Bingzhang** **17/9/16 10:46 PM**

including the overestimation of

**Page 21: [124] Deleted** **Chen Bingzhang** **17/9/16 10:46 PM**

including the overestimation of

**Page 21: [124] Deleted** **Chen Bingzhang** **17/9/16 10:46 PM**

including the overestimation of

**Page 22: [125] Deleted** **Chen Bingzhang** **17/8/3 12:05 PM**

TIN

**Page 22: [125] Deleted** **Chen Bingzhang** **17/8/3 12:05 PM**

TIN

**Page 22: [125] Deleted** **Chen Bingzhang** **17/8/3 12:05 PM**

TIN

**Page 22: [125] Deleted** **Chen Bingzhang** **17/8/3 12:05 PM**

TIN

**Page 22: [125] Deleted** **Chen Bingzhang** **17/8/3 12:05 PM**

TIN

**Page 22: [125] Deleted** **Chen Bingzhang** **17/8/3 12:05 PM**

TIN

**Page 22: [126] Deleted** **Chen Bingzhang** **17/8/3 12:05 PM**

TIN

**Page 22: [126] Deleted** **Chen Bingzhang** **17/8/3 12:05 PM**

TIN

**Page 22: [126] Deleted Chen Bingzhang 17/8/3 12:05 PM**

TIN

**Page 22: [126] Deleted Chen Bingzhang 17/8/3 12:05 PM**

TIN

**Page 22: [127] Deleted Chen Bingzhang 17/9/22 3:40 PM**

around

**Page 22: [127] Deleted Chen Bingzhang 17/9/22 3:40 PM**

around

**Page 22: [127] Deleted Chen Bingzhang 17/9/22 3:40 PM**

around

**Page 22: [127] Deleted Chen Bingzhang 17/9/22 3:40 PM**

around

**Page 22: [127] Deleted Chen Bingzhang 17/9/22 3:40 PM**

around

**Page 22: [128] Deleted Chen Bingzhang 17/9/22 4:01 PM**

M

**Page 22: [128] Deleted Chen Bingzhang 17/9/22 4:01 PM**

M

**Page 22: [128] Deleted Chen Bingzhang 17/9/22 4:01 PM**

M

**Page 22: [128] Deleted Chen Bingzhang 17/9/22 4:01 PM**

M

**Page 22: [128] Deleted Chen Bingzhang 17/9/22 4:01 PM**

M

**Page 24: [129] Deleted Chen Bingzhang 17/9/26 11:59 AM**

. The absolute magnitude of $\frac{d^2\mu(l)}{dl^2}$ positively correlated to $\mu$, indicating that higher growth rates induced greater resource competition. This agrees well with the “dynamic equilibrium theory” proposed by Huston (1979).

The patterns of trait diffusion, calculated as the sum of all components containing $u$ in the right side of Eq. (1c) to sustain diversity, mirrored those of growth rates. From late fall to early spring, because the values of $\frac{d^2\mu(l)}{dl^2}$ were less negative and trait diffusion estimates were also relatively high, phytoplankton size diversity kept increasing. With stratifying water column starting from spring, the values of $\frac{d^2\mu(l)}{dl^2}$ became more negative and trait diffusion became critically important for sustaining diversity in the system by counteracting the effect of competitive exclusion in nutrient depleted waters.

**Page 24: [130] Deleted Chen Bingzhang 17/9/26 4:48 PM**

overweighs other technical advantages such a

**Page 24: [131] Deleted Chen Bingzhang 17/9/26 4:47 PM**

computational efficiency (Acevedo-Trejos et al., 2016)

**Page 25: [132] Deleted Chen Bingzhang 17/9/26 4:51 PM**

equations themselves (Eq. 1) have already provided the genuine insights for

**Page 25: [132] Deleted Chen Bingzhang 17/9/26 4:51 PM**

equations themselves (Eq. 1) have already provided the genuine insights for

**Page 25: [133] Deleted S. Lan Smith 17/10/22 11:06 PM**

for

**Page 25: [133] Deleted S. Lan Smith 17/10/22 11:06 PM**

for

**Page 25: [133] Deleted S. Lan Smith 17/10/22 11:06 PM**

for

**Page 25: [134] Deleted S. Lan Smith 17/10/22 11:07 PM**

can be

**Page 25: [134] Deleted S. Lan Smith 17/10/22 11:07 PM**

can be

**Page 25: [134] Deleted S. Lan Smith 17/10/22 11:07 PM**

can be

**Page 25: [135] Formatted Chen Bingzhang 17/8/7 11:11 AM**

Font:Italic

**Page 25: [135] Formatted** **Chen Bingzhang** **17/8/7 11:11 AM**

Font:Italic

**Page 25: [136] Deleted** **Bingzhang Chen** **17/10/18 11:45 AM**

since

**Page 25: [136] Deleted** **Bingzhang Chen** **17/10/18 11:45 AM**

since

**Page 25: [137] Deleted** **S. Lan Smith** **17/10/22 11:07 PM**

)

**Page 25: [137] Deleted** **S. Lan Smith** **17/10/22 11:07 PM**

)

**Page 25: [137] Deleted** **S. Lan Smith** **17/10/22 11:07 PM**

)

**Page 25: [137] Deleted** **S. Lan Smith** **17/10/22 11:07 PM**

)

**Page 25: [137] Deleted** **S. Lan Smith** **17/10/22 11:07 PM**

)

**Page 25: [137] Deleted** **S. Lan Smith** **17/10/22 11:07 PM**

)

**Page 25: [137] Deleted** **S. Lan Smith** **17/10/22 11:07 PM**

)

**Page 25: [137] Deleted** **S. Lan Smith** **17/10/22 11:07 PM**

)

**Page 25: [137] Deleted** **S. Lan Smith** **17/10/22 11:07 PM**

)

**Page 25: [137] Deleted** **S. Lan Smith** **17/10/22 11:07 PM**

)

**Page 25: [137] Deleted** **S. Lan Smith** **17/10/22 11:07 PM**

)

**Page 25: [137] Deleted** **S. Lan Smith** **17/10/22 11:07 PM**

)

**Page 25: [137] Deleted S. Lan Smith 17/10/22 11:07 PM**

)

**Page 25: [137] Deleted S. Lan Smith 17/10/22 11:07 PM**

)

**Page 25: [137] Deleted S. Lan Smith 17/10/22 11:07 PM**

)

**Page 25: [138] Deleted S. Lan Smith 17/10/22 11:15 PM**

positively

**Page 25: [138] Deleted S. Lan Smith 17/10/22 11:15 PM**

positively

**Page 25: [138] Deleted S. Lan Smith 17/10/22 11:15 PM**

positively

**Page 25: [138] Deleted S. Lan Smith 17/10/22 11:15 PM**

positively

**Page 25: [138] Deleted S. Lan Smith 17/10/22 11:15 PM**

positively

**Page 25: [139] Deleted S. Lan Smith 17/10/22 11:19 PM**

When

**Page 25: [139] Deleted S. Lan Smith 17/10/22 11:19 PM**

When

**Page 25: [139] Deleted S. Lan Smith 17/10/22 11:19 PM**

When

**Page 25: [139] Deleted S. Lan Smith 17/10/22 11:19 PM**

When

**Page 25: [139] Deleted S. Lan Smith 17/10/22 11:19 PM**

When

**Page 25: [140] Deleted S. Lan Smith 17/10/22 11:20 PM**

also gives

**Page 25: [140] Deleted S. Lan Smith 17/10/22 11:20 PM**

also gives

**Page 25: [140] Deleted S. Lan Smith 17/10/22 11:20 PM**

also gives

**Page 25: [140] Deleted S. Lan Smith 17/10/22 11:20 PM**

also gives

**Page 25: [140] Deleted S. Lan Smith 17/10/22 11:20 PM**

also gives

**Page 25: [140] Deleted S. Lan Smith 17/10/22 11:20 PM**

also gives

**Page 25: [140] Deleted S. Lan Smith 17/10/22 11:20 PM**

also gives

**Page 25: [141] Deleted Chen Bingzhang 17/8/7 11:32 AM**

In typical NPZD-type models in which phytoplankton species compete for the same set of nutrients but do not directly confront each other, the parameters representing the direct interactions among species (such as in the Lotka–Volterra equations) are usually not available. Thus, in traditional approaches that model the trajectories of a number of species, the competition is not easily quantifiable and therefore is rarely quantified. The ability to easily quantify competition intensity makes it easy to test ecological theories such as Huston’s “general hypothesis of species diversity” (Huston, 1979).

**Page 25: [142] Formatted Chen Bingzhang 17/9/26 4:58 PM**

Font:Italic

**Page 25: [142] Formatted Chen Bingzhang 17/9/26 4:58 PM**

Font:Italic

**Page 26: [143] Deleted S. Lan Smith 17/10/22 11:24 PM**

also

**Page 26: [143] Deleted S. Lan Smith 17/10/22 11:24 PM**

also

**Page 26: [143] Deleted S. Lan Smith 17/10/22 11:24 PM**

also

**Page 26: [143] Deleted S. Lan Smith 17/10/22 11:24 PM**

also

**Page 26: [143] Deleted S. Lan Smith 17/10/22 11:24 PM**

also

**Page 26: [143] Deleted S. Lan Smith 17/10/22 11:24 PM**

also

**Page 26: [144] Deleted Chen Bingzhang 17/9/27 10:57 PM**

evolutionary theory

**Page 26: [144] Deleted Chen Bingzhang 17/9/27 10:57 PM**

evolutionary theory

**Page 26: [145] Deleted S. Lan Smith 17/10/22 11:28 PM**

since

**Page 26: [145] Deleted S. Lan Smith 17/10/22 11:28 PM**

since

**Page 26: [146] Deleted S. Lan Smith 17/10/22 11:29 PM**

the

**Page 26: [146] Deleted S. Lan Smith 17/10/22 11:29 PM**

the

**Page 26: [146] Deleted S. Lan Smith 17/10/22 11:29 PM**

the

**Page 26: [146] Deleted S. Lan Smith 17/10/22 11:29 PM**

the

**Page 26: [146] Deleted S. Lan Smith 17/10/22 11:29 PM**

the

**Page 26: [146] Deleted S. Lan Smith 17/10/22 11:29 PM**

the

**Page 26: [147] Formatted Bingzhang Chen 17/9/28 3:26 PM**

Font:Italic

**Page 26: [147] Formatted Bingzhang Chen 17/9/28 3:26 PM**

Font:Italic

**Page 26: [147] Formatted Bingzhang Chen 17/9/28 3:26 PM**

Font:Italic

**Page 26: [147] Formatted Bingzhang Chen 17/9/28 3:26 PM**

Font:Italic

**Page 26: [147] Formatted Bingzhang Chen 17/9/28 3:26 PM**

Font:Italic

**Page 26: [147] Formatted Bingzhang Chen 17/9/28 3:26 PM**

Font:Italic

**Page 26: [147] Formatted Bingzhang Chen 17/9/28 3:26 PM**

Font:Italic

**Page 26: [147] Formatted Bingzhang Chen 17/9/28 3:26 PM**

Font:Italic

**Page 26: [147] Formatted Bingzhang Chen 17/9/28 3:26 PM**

Font:Italic

**Page 26: [147] Formatted Bingzhang Chen 17/9/28 3:26 PM**

Font:Italic

**Page 26: [147] Formatted Bingzhang Chen 17/9/28 3:26 PM**

Font:Italic

**Page 26: [147] Formatted Bingzhang Chen 17/9/28 3:26 PM**

Font:Italic

**Page 26: [147] Formatted Bingzhang Chen 17/9/28 3:26 PM**

Font:Italic

**Page 26: [147] Formatted Bingzhang Chen 17/9/28 3:26 PM**

Font:Italic

**Page 26: [147] Formatted Bingzhang Chen 17/9/28 3:26 PM**

Font:Italic

**Page 26: [147] Formatted Bingzhang Chen 17/9/28 3:26 PM**

Font:Italic

**Page 26: [148] Deleted S. Lan Smith 17/10/22 11:30 PM**

the extent that

**Page 26: [148] Deleted S. Lan Smith 17/10/22 11:30 PM**

the extent that

**Page 26: [148] Deleted** **S. Lan Smith** **17/10/22 11:30 PM**

the extent that

**Page 26: [148] Deleted** **S. Lan Smith** **17/10/22 11:30 PM**

the extent that

**Page 27: [149] Deleted** **S. Lan Smith** **17/10/22 11:31 PM**

were

**Page 27: [149] Deleted** **S. Lan Smith** **17/10/22 11:31 PM**

were

**Page 27: [149] Deleted** **S. Lan Smith** **17/10/22 11:31 PM**

were

**Page 27: [149] Deleted** **S. Lan Smith** **17/10/22 11:31 PM**

were

**Page 27: [149] Deleted** **S. Lan Smith** **17/10/22 11:31 PM**

were

**Page 27: [150] Deleted** **S. Lan Smith** **17/10/22 11:32 PM**

acclimatory

**Page 27: [150] Deleted** **S. Lan Smith** **17/10/22 11:32 PM**

acclimatory

**Page 27: [150] Deleted** **S. Lan Smith** **17/10/22 11:32 PM**

acclimatory

**Page 27: [150] Deleted** **S. Lan Smith** **17/10/22 11:32 PM**

acclimatory

**Page 27: [151] Deleted** **Chen Bingzhang** **17/10/23 9:59 AM**

**1.1**

**Page 27: [151] Deleted** **Chen Bingzhang** **17/10/23 9:59 AM**

**1.1**

**Page 27: [151] Deleted** **Chen Bingzhang** **17/10/23 9:59 AM**

**1.1**

**Page 27: [151] Deleted** **Chen Bingzhang** **17/10/23 9:59 AM**

**1.1**

**Page 27: [152] Deleted S. Lan Smith 17/10/22 11:34 PM**

the

**Page 27: [152] Deleted S. Lan Smith 17/10/22 11:34 PM**

the

**Page 27: [152] Deleted S. Lan Smith 17/10/22 11:34 PM**

the

**Page 27: [152] Deleted S. Lan Smith 17/10/22 11:34 PM**

the

**Page 27: [152] Deleted S. Lan Smith 17/10/22 11:34 PM**

the

**Page 27: [152] Deleted S. Lan Smith 17/10/22 11:34 PM**

the

**Page 27: [153] Deleted Chen Bingzhang 17/8/29 5:01 PM**

Compared to previous continuous trait-based models (Terseleer et al., 2014; Acevedo-Trejos et al., 2015, 2016), **CITRATE** 1.0

**Page 27: [153] Deleted Chen Bingzhang 17/8/29 5:01 PM**

Compared to previous continuous trait-based models (Terseleer et al., 2014; Acevedo-Trejos et al., 2015, 2016), **CITRATE** 1.0

**Page 27: [153] Deleted Chen Bingzhang 17/8/29 5:01 PM**

Compared to previous continuous trait-based models (Terseleer et al., 2014; Acevedo-Trejos et al., 2015, 2016), **CITRATE** 1.0

**Page 27: [154] Deleted S. Lan Smith 17/10/22 11:35 PM**

the

**Page 27: [154] Deleted S. Lan Smith 17/10/22 11:35 PM**

the

**Page 27: [154] Deleted S. Lan Smith 17/10/22 11:35 PM**

the

**Page 27: [154] Deleted S. Lan Smith 17/10/22 11:35 PM**

the

**Page 28: [155] Deleted S. Lan Smith 17/10/22 11:36 PM**

a

**Page 28: [155] Deleted S. Lan Smith 17/10/22 11:36 PM**

a

**Page 28: [156] Deleted S. Lan Smith 17/10/22 11:37 PM**

the growth superiority of

**Page 28: [156] Deleted S. Lan Smith 17/10/22 11:37 PM**

the growth superiority of

**Page 28: [157] Deleted Bingzhang Chen 17/9/28 5:07 PM**

oligotrophic

**Page 28: [157] Deleted Bingzhang Chen 17/9/28 5:07 PM**

oligotrophic

**Page 28: [158] Deleted S. Lan Smith 17/10/22 11:38 PM**

.

**Page 28: [158] Deleted S. Lan Smith 17/10/22 11:38 PM**

.

**Page 28: [158] Deleted S. Lan Smith 17/10/22 11:38 PM**

.

**Page 28: [159] Deleted S. Lan Smith 17/10/22 11:40 PM**

opposite

**Page 28: [159] Deleted S. Lan Smith 17/10/22 11:40 PM**

opposite

**Page 28: [159] Deleted S. Lan Smith 17/10/22 11:40 PM**

opposite

**Page 28: [159] Deleted S. Lan Smith 17/10/22 11:40 PM**

opposite

**Page 28: [160] Deleted S. Lan Smith 17/10/22 11:40 PM**

also

**Page 28: [160] Deleted S. Lan Smith 17/10/22 11:40 PM**

also

**Page 28: [160] Deleted S. Lan Smith 17/10/22 11:40 PM**

also

**Page 28: [160] Deleted S. Lan Smith 17/10/22 11:40 PM**

also

**Page 28: [160] Deleted S. Lan Smith 17/10/22 11:40 PM**

also

**Page 28: [160] Deleted S. Lan Smith 17/10/22 11:40 PM**

also

**Page 28: [160] Deleted S. Lan Smith 17/10/22 11:40 PM**

also

**Page 28: [160] Deleted S. Lan Smith 17/10/22 11:40 PM**

also

**Page 28: [160] Deleted S. Lan Smith 17/10/22 11:40 PM**

also

**Page 28: [160] Deleted S. Lan Smith 17/10/22 11:40 PM**

also

**Page 28: [160] Deleted S. Lan Smith 17/10/22 11:40 PM**

also

**Page 28: [160] Deleted S. Lan Smith 17/10/22 11:40 PM**

also

**Page 28: [160] Deleted S. Lan Smith 17/10/22 11:40 PM**

also

**Page 28: [161] Deleted S. Lan Smith 17/10/22 11:43 PM**

will lead to

**Page 28: [161] Deleted S. Lan Smith 17/10/22 11:43 PM**

will lead to

**Page 28: [161] Deleted S. Lan Smith 17/10/22 11:43 PM**

will lead to

**Page 28: [161] Deleted S. Lan Smith 17/10/22 11:43 PM**

will lead to

**Page 28: [162] Deleted Chen Bingzhang 17/8/29 5:06 PM**

Instead, we employ an observation-based unimodal relationship between maximal growth rate and size to give the large phytoplankton the advantage under nutrient-replete conditions (Chen and Liu, 2010, 2011; Marañón et al., 2013), thus allowing a tradeoff between nutrient affinity and maximal growth rate. One reason is that, in the open ocean, such size-dependent feeding preference is either very weak or does not have a robust pattern for the dominant grazers, microzooplankton (Hansen and Hansen, 1994; Chen et al., 2009, 2010). While previous studies usually assume that the specific clearance rates of zooplankton on phytoplankton decrease with increasing phytoplankton size, which is usually based on the copepod data, field dilution experiments often suggest that the grazing rates of microzooplankton are higher on fast-growing diatoms (Latasa et al., 1997; Zhou et al., 2015). Because our model incorporates a generic zooplankton compartment, which should have an adaptive feeding behaviour on phytoplankton (Behrenfeld and Boss, 2014), we feel that it is justifiable not to apply any size-related feeding preference in **CITRATE** 1.0. Thus, phytoplankton mean size and size diversity are controlled only by bottom-up factors, although zooplankton grazing plays an indirect role in affecting nutrient regeneration and phytoplankton mortality. Whether or not size-dependent zooplankton grazing plays an important role in determining patterns of phytoplankton mean size and size diversity (Terseleer et al., 2014) deserves to be further investigated in future work

**Page 28: [163] Formatted Bingzhang Chen 17/9/28 12:16 PM**

English (US)

**Page 28: [163] Formatted Bingzhang Chen 17/9/28 12:16 PM**

English (US)

**Page 30: [164] Deleted Bingzhang Chen 17/9/28 5:34 PM**

certainly

**Page 30: [164] Deleted Bingzhang Chen 17/9/28 5:34 PM**

certainly

**Page 30: [164] Deleted Bingzhang Chen 17/9/28 5:34 PM**

certainly

**Page 30: [165] Formatted Bingzhang Chen 17/9/28 10:31 PM**

Font:Not Bold, Italic

**Page 30: [165] Formatted** **Bingzhang Chen** **17/9/28 10:31 PM**

Font:Not Bold, Italic

**Page 30: [165] Formatted** **Bingzhang Chen** **17/9/28 10:31 PM**

Font:Not Bold, Italic

**Page 30: [166] Deleted** **S. Lan Smith** **17/10/22 11:51 PM**

From t

**Page 30: [166] Deleted** **S. Lan Smith** **17/10/22 11:51 PM**

From t

**Page 30: [166] Deleted** **S. Lan Smith** **17/10/22 11:51 PM**

From t

**Page 30: [166] Deleted** **S. Lan Smith** **17/10/22 11:51 PM**

From t

**Page 30: [166] Deleted** **S. Lan Smith** **17/10/22 11:51 PM**

From t

**Page 30: [166] Deleted** **S. Lan Smith** **17/10/22 11:51 PM**

From t

**Page 30: [166] Deleted** **S. Lan Smith** **17/10/22 11:51 PM**

From t

**Page 30: [166] Deleted** **S. Lan Smith** **17/10/22 11:51 PM**

From t

**Page 30: [166] Deleted** **S. Lan Smith** **17/10/22 11:51 PM**

From t

**Page 30: [166] Deleted** **S. Lan Smith** **17/10/22 11:51 PM**

From t

**Page 30: [166] Deleted** **S. Lan Smith** **17/10/22 11:51 PM**

From t

**Page 30: [167] Deleted** **Bingzhang Chen** **17/9/28 5:35 PM**

$\boldsymbol{v}$) should be similar due to strong mixing, the approximation is not a big concern. The problem mainly lies at the bottom of the mixed layer where there is a sharp gradient of phytoplankton properties particularly biomass (Fig. 12c). We can roughly estimate that, based on the eddy diffusivity (~2 x $10^5$ $m^2$ $s^{-1}$), grid distance (20 m), and the phytoplankton biomass differences (0.2 $\mu$mol N $L^{-1}$), the transported phytoplankton biomass from the upper grid (higher ***P***) to the lower grid (lower ***P***) at one time step (0.5 min) is roughly 0.0002 $\mu$mol N $L^{-1}$, 1% of the ***P*** in the lower grid. Therefore, oOur tentative conclusion is that

**Page 30: [168] Formatted** **Chen Bingzhang** **17/8/7 4:50 PM**

Font:Not Bold

**Page 30: [168] Formatted** **Chen Bingzhang** **17/8/7 4:50 PM**

Font:Not Bold

**Page 30: [168] Formatted** **Chen Bingzhang** **17/8/7 4:50 PM**

Font:Not Bold

**Page 30: [168] Formatted** **Chen Bingzhang** **17/8/7 4:50 PM**

Font:Not Bold

**Page 30: [168] Formatted** **Chen Bingzhang** **17/8/7 4:50 PM**

Font:Not Bold

**Page 30: [168] Formatted** **Chen Bingzhang** **17/8/7 4:50 PM**

Font:Not Bold

**Page 30: [168] Formatted** **Chen Bingzhang** **17/8/7 4:50 PM**

Font:Not Bold

**Page 30: [168] Formatted** **Chen Bingzhang** **17/8/7 4:50 PM**

Font:Not Bold

**Page 30: [168] Formatted** **Chen Bingzhang** **17/8/7 4:50 PM**

Font:Not Bold

**Page 30: [168] Formatted** **Chen Bingzhang** **17/8/7 4:50 PM**

Font:Not Bold

**Page 30: [168] Formatted** **Chen Bingzhang** **17/8/7 4:50 PM**

Font:Not Bold

**Page 30: [168] Formatted** **Chen Bingzhang** **17/8/7 4:50 PM**

Font:Not Bold

**Page 30: [169] Deleted** **Chen Bingzhang** **17/8/8 10:58 AM**

and may potentially be a concern only under the presence of large gradients of phytoplankton biomass or trait moments

**Page 32: [170] Deleted** **S. Lan Smith** **17/10/23 12:00 AM**

Future

➢

**Page 34: [171] Deleted** **Chen Bingzhang** **17/9/20 3:19 PM**

The code for **CITRATE** 1.0 is written in Fortran90 with the Intel Fortran compiler used. The running environment is Linux or Unix. The user is supposed to be familiar with the Fortran language.

For each station, four different physical forcing data including vertical profiles of eddy diffusive coefficients and temperatures, surface PAR and atmospheric dust deposition. We already provided the relevant data for stations S1 and K2. The temporal resolution is one day for the vertical eddy diffusivity and one month for three other types of data.

After downloading the folder *FlexEFT1D*, go to the directory *FlexEFT1D/DRAM_0.9/NPZDcont/BOTH* and type *vi run*. The user can change the value of *Test* inside the bash script *run*. The *Test* value being 0 means a fast run, usually for a formal model run for a large number of iterations. The *Test* value being 1 means running a model for debugging, which is much slower than the fast run. The user can also modify the compiler flags depending on the purpose in the script. Having chosen the right compiler option, type *./run*, the model will compile and an executable file (NPZDCONT) will be generated.

The next step is to type *vi Model.nml*, the file containing two namelists. The namelist *&Model* contains the options for station names, the type of ecological model, the type of nutrient uptake function (1 only for **CITRATE**), and the type for grazing function (four different grazing functions including the three Holling type functions and the Ivlev function). The station name determines the right physics files to be read and the filenames for model output. For now we only allow three possible stations: S1, K2, and HOT. Other station names will generate an error. If the user wants to add more station names, the subroutine *Setup_OBSdata* within *MOD_1D.f90* is the place to be modified. A number of ecological models besides CITRATE have been developed. It is beyond the scope of the present study to describe all of them in detail. Just note that the model lists are in the fortran file bio_MOD.f90 and some other details are in choose_model.f90 and MOD_1D.f90.

The namelist *&MCMCrun* contains the options for defining the total length of the MCMC chain which is at least 2, the number of the ensemble runs, the number of days for each model run, whether the model should start from previous runs (*Readfile* = 1) or start a new run (*Readfile* = 0), and the number of runs in the historical files (*enssig* and *enspar*).

After defining all the model settings, type "./NPZDCONT" and then the model will run and some outputs will be shown on the screen. Type "./NPZDCONT > out" to make the model outputs stored in the "out" file.

For each model run, the model saves the current parameters into the "enspar" file and the current values of $\sigma$ and SSqE into the 'enssig' file. In this way, even if the model crashes, the user can pick up the current parameter position and updated parameter covariance matrix. The model also generates the files of best parameters, best $\sigma$ and SSqE files, best model output files that correspond to observational data, and model output files at daily resolution at each grid after an ensemble run.

**Page 36: [172] Deleted** **Chen Bingzhang** **17/9/13 2:40 PM**

| | | | |
|---|---|---|---|
| $K_p$ | Grazing half-saturation constant of zooplankton | $0.5^e$ | $\mu$M N |

**Page 37: [173] Deleted** **Chen Bingzhang** **17/9/14 4:46 PM**

"burn-in" period

**Page 37: [173] Deleted** **Chen Bingzhang** **17/9/14 4:46 PM**

"burn-in" period

**Page 37: [173] Deleted** **Chen Bingzhang** **17/9/14 4:46 PM**

"burn-in" period

**Page 37: [173] Deleted** **Chen Bingzhang** **17/9/14 4:46 PM**

"burn-in" period

**Page 37: [173] Deleted** **Chen Bingzhang** **17/9/14 4:46 PM**

"burn-in" period

**Page 37: [174] Deleted** **Chen Bingzhang** **17/9/13 3:14 PM**

1

**Page 37: [174] Deleted** **Chen Bingzhang** **17/9/13 3:14 PM**

1

**Page 37: [174] Deleted** **Chen Bingzhang** **17/9/13 3:14 PM**

1

**Page 37: [175] Deleted** **Chen Bingzhang** **17/9/13 3:17 PM**

3.3

**Page 37: [175] Deleted** **Chen Bingzhang** **17/9/13 3:17 PM**

3.3

**Page 37: [176] Deleted** **Chen Bingzhang** **17/9/13 2:36 PM**

| | | | | |
|---|---|---|---|---|
| $Q_{0N}$ | Phytoplankton minimal N:C ratio | 0.076[a] (0.05, 0.13) | 0.093 (0.0007) | mol: mol |
| $g_{max}$ | Maximal zooplankton grazing rate at 15 ºC | 1 (0.5, 2) | 0.90 (0.024) | $d^{-1}$ |

**Page 37: [177] Deleted** **Chen Bingzhang** **17/9/13 3:20 PM**

094

**Page 37: [177] Deleted** **Chen Bingzhang** **17/9/13 3:20 PM**

094

**Page 37: [178] Deleted** **Chen Bingzhang** **17/9/13 3:20 PM**

19

**Page 37: [178] Deleted** **Chen Bingzhang** **17/9/13 3:20 PM**

19

**Page 37: [179] Deleted** **Chen Bingzhang** **17/9/13 3:39 PM**

0.08

**Page 37: [179] Deleted** **Chen Bingzhang** **17/9/13 3:39 PM**

0.08

**Page 37: [180] Deleted** **Chen Bingzhang** **17/9/13 3:20 PM**

0.097

**Page 37: [180] Deleted** **Chen Bingzhang** **17/9/13 3:20 PM**

0.097

**Page 37: [181] Deleted** **Chen Bingzhang** **17/9/13 3:26 PM**

5

**Page 37: [181] Deleted** **Chen Bingzhang** **17/9/13 3:26 PM**

5

**Page 37: [181] Deleted** **Chen Bingzhang** **17/9/13 3:26 PM**

5

**Page 37: [182] Deleted** **Chen Bingzhang** **17/9/13 3:22 PM**

0.89

**Page 37: [182] Deleted** **Chen Bingzhang** **17/9/13 3:22 PM**

0.89

**Page 37: [183] Deleted** **Chen Bingzhang** **17/9/13 2:36 PM**

| | | | | |
|---|---|---|---|---|
| $\alpha_K$ | Size scaling exponent for $K_N$ | $0.27^{e}$ (0.1, 0.3) | 0.24 (0.001) | dimensionle |

**Page 37: [184] Deleted** **Chen Bingzhang** **17/9/13 3:36 PM**

d

**Page 37: [184] Deleted** **Chen Bingzhang** **17/9/13 3:36 PM**

d

**Page 37: [185] Deleted** **Chen Bingzhang** **17/9/14 2:56 PM**

1.34

**Page 37: [185] Deleted** **Chen Bingzhang** **17/9/14 2:56 PM**

1.34

**Page 37: [186] Deleted** **Chen Bingzhang** **17/9/13 2:36 PM**

| | | | | |
|---|---|---|---|---|
| $\alpha_\mu$ | First-order size scaling component for $\mu_\mathrm{m}$ | $0.25^{e}$ (0.1, 0.4) | 0.27 (0.005) | dimensionle |
| $\beta_\mu$ | Second-order size scaling component for $\mu_\mathrm{m}$ | $-0.025^{e}$ (–0.05, 0) | –0.013 (0.0002) | dimensionle |

**Page 37: [187] Deleted** **Chen Bingzhang** **17/9/13 3:36 PM**

f

**Page 37: [187] Deleted** **Chen Bingzhang** **17/9/13 3:36 PM**

f

**Page 37: [188] Deleted** **Chen Bingzhang** **17/9/22 11:42 AM**

058

**Page 37: [188] Deleted	Chen Bingzhang	17/9/22 11:42 AM**

058

**Page 37: [188] Deleted	Chen Bingzhang	17/9/22 11:42 AM**

058

**Page 37: [189] Deleted	Chen Bingzhang	17/9/13 2:36 PM**

| | | | | |
|---|---|---|---|---|
| $\alpha_{fer}$ | Size scaling exponent for $K_{0,fer}$ | $0.27^{c}$ (0.1, 0.3) | 0.30 (0.001) | dimensionle |

**Page 37: [190] Deleted	Chen Bingzhang	17/9/13 3:36 PM**

[g]

**Page 37: [190] Deleted	Chen Bingzhang	17/9/13 3:36 PM**

[g]

**Page 37: [190] Deleted	Chen Bingzhang	17/9/13 3:36 PM**

[g]

**Page 37: [191] Deleted	Chen Bingzhang	17/9/13 3:25 PM**

092

**Page 37: [191] Deleted	Chen Bingzhang	17/9/13 3:25 PM**

092

**Page 37: [191] Deleted	Chen Bingzhang	17/9/13 3:25 PM**

092

**Page 37: [192] Deleted	Chen Bingzhang	17/8/7 2:58 PM**

| | | | | |
|---|---|---|---|---|
| *dustso* | Dust iron solubility | $0.02^{h}$ (0.01, 0.05) | 0.022 (0.0007) | dimensionle |

**Page 37: [193] Formatted	Bingzhang Chen	17/9/28 12:16 PM**

Spanish

**Page 37: [194] Deleted	Chen Bingzhang	17/9/13 3:34 PM**

Marañón et al., (2013); [b]

**Page 37: [194] Deleted	Chen Bingzhang	17/9/13 3:34 PM**

Marañón et al., (2013); [b]

**Page 37: [194] Deleted** **Chen Bingzhang** **17/9/13 3:34 PM**

Marañón et al., (2013); [b]

**Page 37: [194] Deleted** **Chen Bingzhang** **17/9/13 3:34 PM**

Marañón et al., (2013); [b]

**Page 37: [194] Deleted** **Chen Bingzhang** **17/9/13 3:34 PM**

Marañón et al., (2013); [b]

**Page 37: [194] Deleted** **Chen Bingzhang** **17/9/13 3:34 PM**

Marañón et al., (2013); [b]

**Page 37: [194] Deleted** **Chen Bingzhang** **17/9/13 3:34 PM**

Marañón et al., (2013); [b]

**Page 39: [195] Formatted** **Chen Bingzhang** **17/9/20 4:03 PM**

Font:Not Bold

**Page 39: [196] Formatted** **Chen Bingzhang** **17/9/20 4:04 PM**

Line spacing: double

**Page 39: [197] Formatted** **Chen Bingzhang** **17/9/20 4:03 PM**

Font:Not Bold

**Page 39: [198] Formatted** **Bingzhang Chen** **17/9/28 11:18 PM**

Font:10.5 pt

**Page 39: [199] Formatted** **Bingzhang Chen** **17/9/29 12:05 PM**

Space Before: 0 pt

| **Page 39: [200] Formatted Table** | **Bingzhang Chen** | **17/9/29 12:05 PM** |
|---|---|---|

Formatted Table

| **Page 39: [201] Formatted** | **Bingzhang Chen** | **17/9/28 11:18 PM** |
|---|---|---|

Font:10.5 pt

| **Page 39: [202] Formatted** | **Bingzhang Chen** | **17/9/29 12:05 PM** |
|---|---|---|

Space Before: 0 pt

| **Page 39: [203] Formatted** | **Bingzhang Chen** | **17/9/28 11:18 PM** |
|---|---|---|

Font:10.5 pt

| **Page 39: [204] Formatted** | **Bingzhang Chen** | **17/9/29 12:05 PM** |
|---|---|---|

Space Before: 0 pt

| **Page 39: [205] Formatted** | **Bingzhang Chen** | **17/9/29 12:05 PM** |
|---|---|---|

Left, Space Before: 0 pt

| **Page 39: [206] Formatted** | **Bingzhang Chen** | **17/9/28 11:18 PM** |
|---|---|---|

Font:10.5 pt

| **Page 39: [207] Formatted** | **Bingzhang Chen** | **17/9/29 12:05 PM** |
|---|---|---|

Space Before: 0 pt

| **Page 39: [208] Formatted** | **Bingzhang Chen** | **17/9/28 11:18 PM** |
|---|---|---|

Font:10.5 pt

| **Page 39: [209] Formatted** | **Bingzhang Chen** | **17/9/29 12:05 PM** |
|---|---|---|

Space Before: 0 pt

| **Page 39: [210] Formatted** | **Bingzhang Chen** | **17/9/28 11:18 PM** |
|---|---|---|

Font:10.5 pt

| **Page 39: [211] Formatted** | **Bingzhang Chen** | **17/9/29 12:05 PM** |
|---|---|---|

Space Before: 0 pt

| **Page 39: [212] Formatted** | **Bingzhang Chen** | **17/9/28 11:18 PM** |
|---|---|---|

Font:10.5 pt

| **Page 39: [213] Formatted** | **Bingzhang Chen** | **17/9/29 12:05 PM** |
|---|---|---|

Space Before: 0 pt

| **Page 39: [214] Formatted** | **Bingzhang Chen** | **17/9/28 11:18 PM** |
|---|---|---|

Font:10.5 pt

**Page 39: [215] Formatted** **Bingzhang Chen** **17/9/29 12:05 PM**

Space Before: 0 pt

**Page 39: [216] Formatted** **Bingzhang Chen** **17/9/28 11:18 PM**

Font:10.5 pt

**Page 39: [217] Formatted** **Bingzhang Chen** **17/9/29 12:05 PM**

Space Before: 0 pt

**Page 39: [218] Formatted** **Bingzhang Chen** **17/9/28 11:18 PM**

Font:10.5 pt

**Page 39: [219] Formatted** **Bingzhang Chen** **17/9/29 12:05 PM**

Space Before: 0 pt

**Page 39: [220] Formatted** **Bingzhang Chen** **17/9/28 11:18 PM**

Font:10.5 pt

**Page 39: [221] Formatted** **Bingzhang Chen** **17/9/29 12:05 PM**

Space Before: 0 pt

**Page 39: [222] Formatted** **Bingzhang Chen** **17/9/28 11:18 PM**

Font:10.5 pt

**Page 39: [223] Formatted** **Bingzhang Chen** **17/9/29 12:06 PM**

Space Before: 6 pt

**Page 39: [224] Formatted** **Bingzhang Chen** **17/9/29 12:08 PM**

Font:10.5 pt, (Asian) Japanese, (Other) English (US)

**Page 39: [225] Formatted** **Bingzhang Chen** **17/9/28 11:18 PM**

Font:10.5 pt

**Page 39: [226] Formatted** **Bingzhang Chen** **17/9/28 11:18 PM**

Font:10.5 pt

**Page 39: [227] Formatted** **Bingzhang Chen** **17/9/29 12:06 PM**

Space Before: 6 pt

**Page 53: [228] Deleted** **Bingzhang Chen** **17/9/28 11:32 PM**

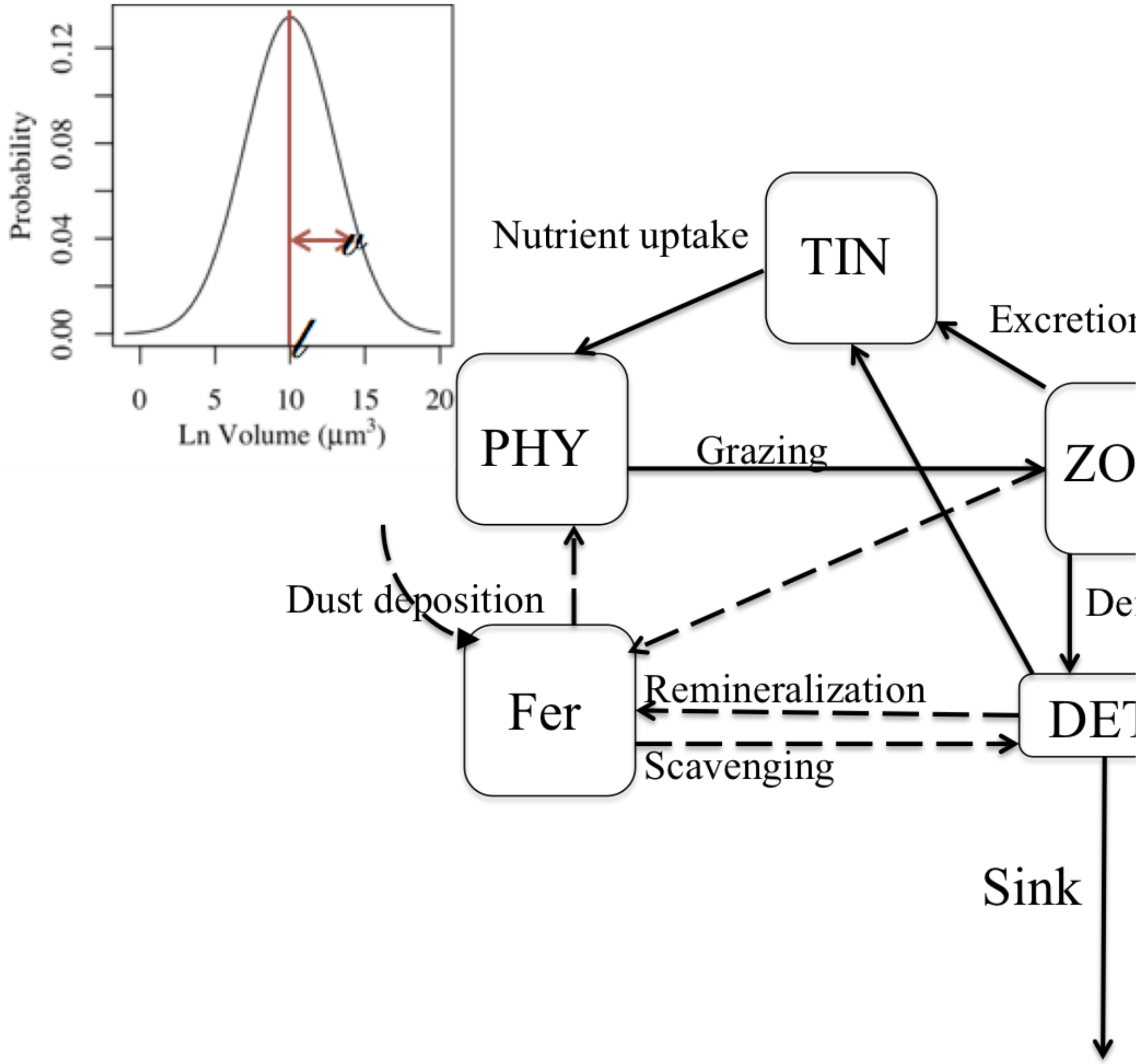

**Page 60: [229] Deleted** **Bingzhang Chen** **17/9/29 2:51 PM**

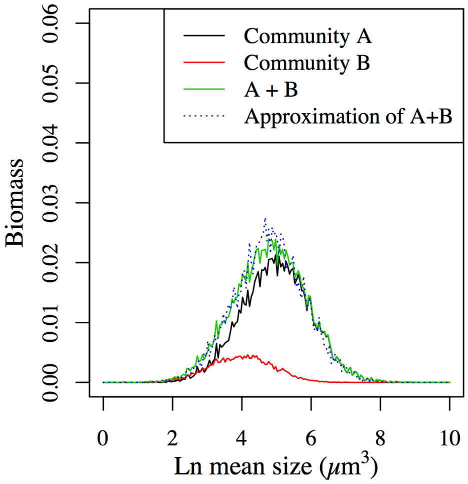
Community A
Community B
A + B
Approximation of A+B
Biomass
0.00
0.01
0.02
0.03
0.04
0.05
0.06
0
2
4
6
8
10
Ln mean size ($\mu m^3$)

Fig. 12